A proposal submitted to the European Space Agency
for the FIRST/Planck Programme

PLANCK
Low Frequency Instrument

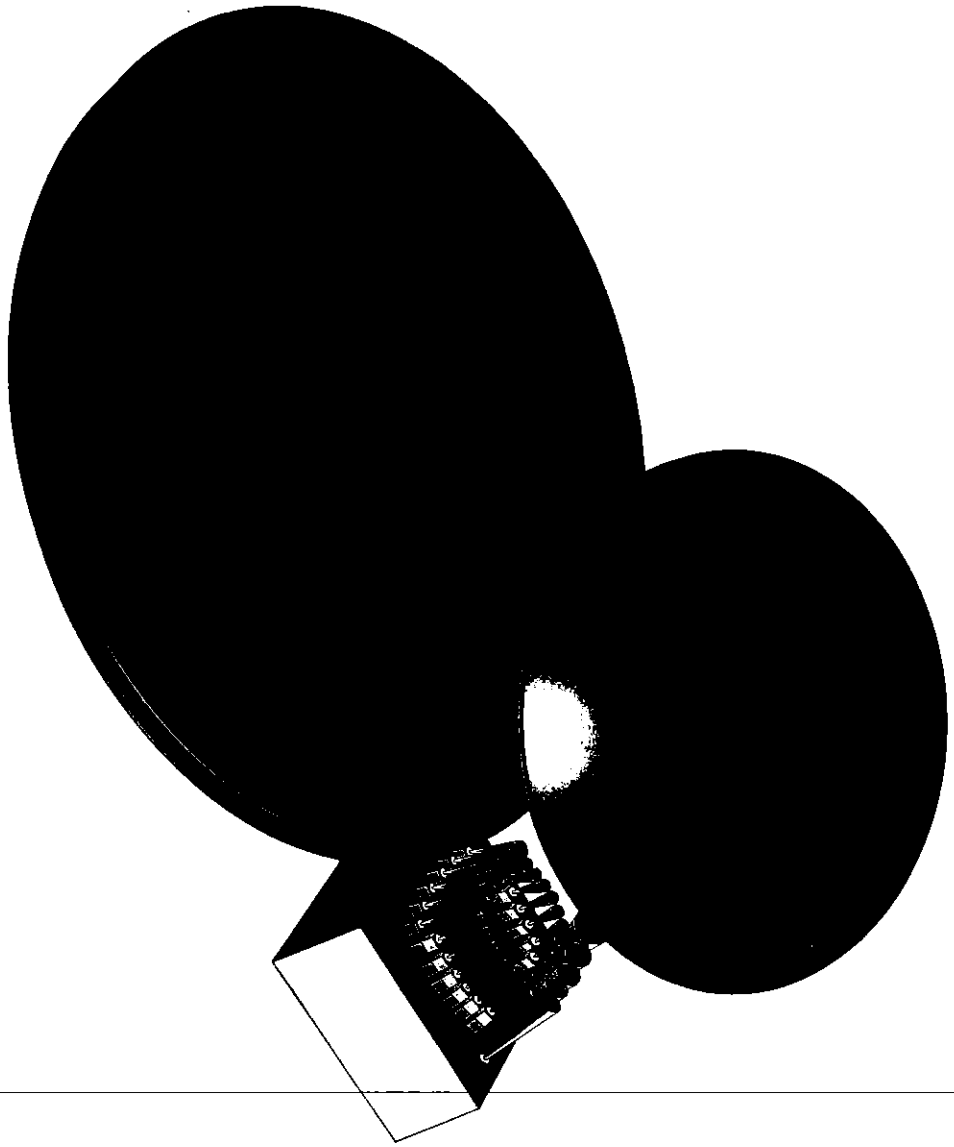

Part I
Scientific and Technical Plan

UCSB

A proposal submitted to the European Space Agency
for the FIRST/Planck Programme

Planck
Low Frequency Instrument

Scientific and Technical Plan

Low Frequency Instrument for Planck
a proposal to the European Space Agency

Part I: Scientific and Technical Plan

PRINCIPAL INVESTIGATOR:
Nazzareno Mandolesi
Consiglio Nazionale delle Ricerche
Istituto TeSRE
Via P. Gobetti 101
I-40129 Bologna Italy
Tel: 39 51 6398682 Fax: 39 51 6398724
e-mail: reno@tesre.bo.cnr.it

SURVEY SCIENTIST:
Charles R. Lawrence
Jet Propulsion Laboratory
4800 Oak Grove Drive
Pasadena CA 91109 USA
Tel: 1 818 354 5307 Fax: 1 818 354 8895
crl@jplsp.jpl.nasa.gov

INSTRUMENT MANAGER:
Marco Bersanelli
Consiglio Nazionale delle Ricerche
Istituto IFCTR
Via Bassini 15
I-20133 Milano Italy
Tel: 39 2 23699308 Fax: 39 2 2362946
marco@ifctr.mi.cnr.it

DATA PROCESSING CENTER MANAGER:
Fabio Pasian
Osservatorio Astronomico di Trieste
Via G.B. Tiepolo 11
I-34131 Trieste Italy
Tel: 39 40 3199221 Fax: 39 40 309418
e-mail: pasian@ts.astro.it

LFI PROJECT MANAGER:
Christopher R. Butler
Agenzia Spaziale Italiana
Viale Regina Margherita 202
I-00198 Roma Italy
Tel: 39 6 8567 1 Fax: 39 6 85370772

CO - INVESTIGATORS:

Kevin Bennett
Space Science Department
Astrophysics Division
P.O.Box 299
NL-2200 AG Noordwijk, The Netherlands
Tel: 31 71 565 3559 Fax: 31 71 565 4690
e-mail: kbennett@astro.estec.esa.nl

Thierry J.-L. Courvoisier
INTEGRAL Science Data Centre
Chemin d'Ecogia 16
CH-1290 VERSOIX Switzerland
Tel: 41 22 950 91 01 Fax: 41 22 950 91 33
e-mail: Thierry.Courvoisier@obs.unige.ch

Luigi Danese
SISSA
via Beirut 2-4
I-34013 Trieste Italy
Tel: 39 40 3787476 Fax: 39 40 3787528
e-mail: danese@sissa.it

Rodney D. Davies
Nuffield Radio Astronomy Laboratories
University of Manchester Jodrell Bank
Macclesfield Cheshire
SK11 9DL United Kingdom
Tel: 44 1477 571321 Fax: 44 1477 571618
e-mail: rdd@jb.man.ac.uk

Richard Davis
Nuffield Radio Astronomy Laboratories
University of Manchester Jodrell Bank
Macclesfield Cheshire
SK11 9DL United Kingdom
Tel: 44 1477 571321 Fax: 44 1477 571618
e-mail: rjd@jb.man.ac.uk

Gianfranco De Zotti
Osservatorio Astronomico di Padova
Vicolo dell'Osservatorio 5
I-35122 Padova Italy
Tel: 39 49 8293444 Fax: 39 49 8759840
e-mail: dezotti@pd.astro.it

Todd Gaier
Jet Propulsion Laboratory
4800 Oak Grove Drive
Pasadena CA 91109 USA
Tel: 1 818 354 4402 Fax: 1 818 354 8895
e-mail: gaier@merlin.jpl.nasa.gov

Krzysztof M. Gorski
Theoretical Astrophysics Center
Juliane Maries Vej 30
2100 Copenhagen 0 Denmark
Tel: 45 35 325898 Fax: 45 35 325910
e-mail: gorski@tac.dk

Erik Kollberg
Microwave Technology
Chalmers University of Technology
S-41296 Göteborg Sweden
Tel: 46 31 7721841 Fax: 46 31 164513
e-mail: kollberg@ep.chalmers.se

Philip M. Lubin
Physics Dept.
University of California Santa Barbara
Santa Barbara, CA 93106 USA
Tel: 1 805 893 8432 Fax: 1 805 893 8597
e-mail: lubin@cfi.ucsb.edu

Enrique Martinez-Gonzalez
Consejo Superior de Investigaciones Cientificas
Instituto de Fisica de Cantabria
Facultad de Ciencias, Avda. de Los Castros s/n
SP-39005 Santander Spain
Tel: 34 42 201468 Fax: 34 42 201459
e-mail: martinez@ifca.unican.es

Hans Ulrik Norgaard-Nielsen
Danish Space Researh Institute
Juliane Maries Vej 30
DK-2100 Copenhagen Denmark
Tel: 45 35 325728 Fax: 45 35 362475
e-mail: hunn@dsri.dk

Rafael Rebolo
Instituto de Astrofisica de Canarias
c/ Via Lactea
La Laguna Tenerife Spain
Tel: 34 22 605262 Fax: 34 22 605210
e-mail: rrl@ll.iac.es

George Smoot
University of California, Berkeley
MS 50205 LNBL
Cyclotron Rd. Berkeley CA 94720 USA
Tel: 1 510 486 5505 Fax: 1 510 486 7149
e-mail: smoot@celest.lbl.gov

Jan Erik Solheim
Department of Physics
University of Tromsø
N-9037 Tromsø Norway
Tel: 47 77 64 51 91 Fax: 47 77 64 55 95
e-mail: janerik@phys.uit.no

Luigi Spinoglio
Consiglio Nazionale delle Ricerche
Istituto IFSI
Via del Fosso del Cavaliere s/n
I-00133 Roma Italy
Tel: 39 649934395 Fax: 39 64993 4383
e-mail: luigi@ifsi.rm.cnr.it

Gianni Tofani
Consiglio Nazionale delle Ricerche
Istituto CAISMI
Largo E. Fermi 5
I-50125 Firenze Italy
Tel: 39 55 2752217 Fax: 39 55 2752 287
e-mail tofani@arcetri.astro.it

Jussi Tuovinen
Millimetre Wave Laboratory of Finland
Otakaari 7 B, Espoo P.O. Box 1202
FIN-02044 VTT Finland
Tel: 358 9 4566508 Fax: 358 9 4567013
e-mail: Jussi.Tuovinen@vtt.fi

Nicola Vittorio
Università di Roma, Tor Vergata
Via della ricerca scientifica
00133 Roma Italy
Tel: 39 6 72594421 Fax: 39 6 2023507
e-mail: vittorio@roma2.infn.it

Lawrence A. Wade
Jet Propulsion Laboratory
4800 Oak Grove Drive
Pasadena CA 91109 USA
Tel: 1 818 354 2272 Fax: 1 818 354 4878
e-mail: lawrence.a.wade@jpl.nasa.gov

Simon White
Max-Planck-Institut für Astrophysik
Karl-Schwarzschild-Str. 1
D-85740 Garching bei München Germany
Tel: 49 89 3299 3211 Fax: 49 89 3299 3235
e-mail: swhite@mpa-garching.mpg.de

Contents

Executive summary x

1 Scientific Objectives and Capabilities 1
1.1 Introduction . . . 1
1.2 Planck Main Science: CMB Anisotropies . . . 2
1.2.1 The Angular Power Spectrum . . . 2
1.2.2 Cosmological Parameters . . . 5
1.2.3 Polarisation . . . 7
1.3 Foregrounds and LFI Science . . . 8
1.3.1 Studies of the Galaxy . . . 8
1.3.2 Extragalactic Sources . . . 10
1.3.3 Clusters of galaxies . . . 12
1.4 The Planck concept and the LFI . . . 12
1.4.1 Sky coverage and orbit . . . 12
1.4.2 Control of systematic effects . . . 14
1.5 LFI Scientific Capabilities . . . 15
1.5.1 Distribution and Amplitude of Foreground Fluctuations . . . 16
1.5.2 Foreground versus CMB Power Spectra . . . 19
1.5.3 Methods for Foreground Separation . . . 20
1.5.4 Extracting Cosmological Parameters from the C_ℓ's . . . 21
1.6 Summary of the Scientific Case . . . 23

2 Technical Description 25
2.1 Introduction & Overview . . . 25
2.1.1 Physical configuration, functional description, and thermal design . . . 26
2.1.2 Radiometer design and systematics . . . 27
2.1.3 LFI performance . . . 32
2.1.4 Operating modes . . . 32
2.2 The LFI Front End Unit . . . 32
2.2.1 Feed horns and OMTs . . . 33
2.2.2 Hybrids, phase switches and amplifiers . . . 34
2.3 Waveguide and Coax Sections . . . 37
2.4 The Back End Unit . . . 39
2.4.1 Back end modules . . . 39
2.4.2 Data acquisition electronics . . . 39
2.5 Radiometer Electronics Box Assembly and Software . . . 40
2.5.1 Signal processing unit . . . 40
2.5.2 The Data processing unit . . . 41
2.5.3 Power supply unit . . . 41
2.5.4 On-board software . . . 41
2.5.5 Harness and grounding . . . 42
2.5.6 Redundancy . . . 42
2.6 The Sorption Cooler . . . 42
2.6.1 Sorption compressor and its operation . . . 42
2.6.2 Sorption cooler electronics . . . 43
2.6.3 Development . . . 44
2.7 Risk Assessment and Heritage . . . 45

3 Information management and data processing plans 47
3.1 Introduction . . . 47
3.2 Data Processing Tasks . . . 47
3.2.1 Level 1 (Telemetry Processing) . . . 48
3.2.2 Level 2 (Data Reduction and Calibration) . . . 49
3.2.3 Level 3 (Component Separation and Optimisation) . . . 51
3.2.4 Level 4 (Generation of final products) . . . 52
3.3 Organisation of the pipeline . . . 53
3.3.1 Data Flow . . . 54
3.3.2 Management of Overall DPC Structure . . . 55
3.4 Integrated Data and Information System (IDIS) . . . 55
3.4.1 IDIS Philosophy . . . 56
3.4.2 Development . . . 58
3.4.3 IDIS Development Organisation . . . 59
3.5 LFI-specific implementation . . . 59
3.5.1 DPC Development . . . 59
3.5.2 DPC operations and interaction with spacecraft operations . . . 61
3.5.3 Post-operations / archive phase . . . 61
3.5.4 Quality Assurance procedures . . . 62
3.5.5 Organization structure . . . 62
3.5.6 Staffing required . . . 63
3.5.7 Local implementations . . . 64

4 Testing and Calibration 68
4.1 Testing . . . 68
4.1.1 Front end unit . . . 68
4.1.2 Back end unit . . . 69
4.1.3 Horns, OMTs, waveguides . . . 70
4.1.4 Radiometer Tests . . . 70
4.1.5 Radiometer electronics box assembly . . . 71
4.1.6 Sorption cooler system . . . 71
4.2 Calibration . . . 71
4.2.1 Ground calibration . . . 71
4.2.2 On-orbit calibration . . . 71
4.3 Test and Calibration Facilities . . . 72

5 System Level Assembly, Integration and Verification (AIV) 73
5.1 LFI Baseline configuration . . . 73
5.1.1 Design and development criteria . . . 73
5.1.2 Model philosophy . . . 73
5.1.3 Verification method . . . 75
5.1.4 Integration and verification flow . . . 75
5.1.5 Documentation tree . . . 76
5.2 Higher level AI&V . . . 76
5.2.1 Rationale for the modular approach . . . 76
5.2.2 LFI-HFI integration . . . 76
5.2.3 Electronic Ground Support Equipment . . . 77

6 Flight Operations **79**
6.1 Planck-LFI survey . . . 79
6.2 Nominal operations . . . 79
6.2.1 ON mode . . . 80
6.2.2 OFF mode . . . 80
6.2.3 Stand-by, Sleep, Test modes . . . 80
6.3 Telemetry and data compression . . . 80
6.4 Calibration . . . 81
6.5 Diagnostic modes . . . 81
6.6 Fail-safe configurations . . . 81
6.6.1 Fail-safe mode 1 . . . 82
6.6.2 Fail-safe mode 2 . . . 82
6.7 Transfer phase . . . 82

7 Qualification and Experience of the PI Team **83**

8 Organisation and Management of the LFI Consortium **91**
8.1 Introduction . . . 91
8.1.1 Project Organisation . . . 91
8.1.2 Work Breakdown Structure . . . 92
8.2 LFI external relationships . . . 96
8.2.1 Relationship with ESA . . . 96
8.2.2 Relationships with the HFI and TP teams . . . 96
8.2.3 Relationships with funding agencies . . . 97
8.2.4 Relationships with the external scientific community . . . 97
8.2.5 Relationship to the wider external community . . . 97
8.3 Schedule . . . 97

References **i**

Acronyms **v**

A Proposed Integration Approach **A.1**
A.1 Steps 1 and 2 . . . A.1
A.2 LFI/HFI frontend integration procedure . . . A.3
A.3 Example Planck Payload Module Assembly Procedure . . . A.3

B LFI Associates and Key Personnel **B.1**
Associate . . . B.1
Key personnel . . . B.4

List of Figures

1.1 Planck vs. COBE angular resolution . . . 3
1.2 Angular power spectrum for the standard CDM model . . . 4
1.3 Angular power spectrum and cosmological parameters . . . 6
1.4 Temperature versus polarisation anisotropy for standard CDM . . . 8
1.5 Polarisation maps at Planck resolution . . . 9
1.6 Galactic foregrounds . . . 10
1.7 Simulation of the LFI full sky observations . . . 16
1.8 Angular power spectra of Galactic and extragalactic foregrounds . . . 18
1.9 Temperature fluctuations as a function of frequency . . . 19
1.10 Reconstructed angular power spectrum . . . 20

2.1 Block diagram of the Low Frequency Instument . . . 26
2.2 Beam pattern of representative LFI channel . . . 28
2.3 Sidelobes contamination fron galactic emission . . . 29
2.4 Prototype 44 GHz radiometer . . . 30
2.5 Suppression of fluctuations due to spacecraft spin . . . 31
2.6 The LFI Front End Unit . . . 33
2.7 Concept of the 4 K reference load . . . 35
2.8 Physical layout of a MMIC amplifier block . . . 36
2.9 Photograph and measured state-of-the-art performance at Jodrell Bank of a 30 GHz MIC prototype Planck amplifier. . . . 37
2.10 Photographs and measured performance of a W-band MMIC amplifier . . . 38
2.11 Schematic of the Radiometer Electronics Box Assembly. . . . 40
2.12 Prototype compressor element for Planck . . . 44
2.13 Photograph of the BEAST 25 K hydrogen sorption cooler . . . 45

3.1 Data flow among Planck DPC sites . . . 54
3.2 Commonalities between LFI and HFI DPCs . . . 55
3.3 IDIS structure . . . 56
3.4 IDIS management structure . . . 58
3.5 Inter-relations among LFI Working Groups . . . 60
3.6 Organisation of the work for the LFI DPC . . . 63

4.1 Test flow of the Low Frequency Instrument. . . . 69

5.1 Block diagram of the LFI instrument . . . 74
5.2 AI&V flow chart for both LFI models (EQM and FM) . . . 75
5.3 Experiment Check-out Equipment . . . 78

8.1 LFI organisation . . . 92
8.2 LFI Work Breakdown Structure: top levels . . . 92
8.3 General management WBS . . . 93
8.4 LFI Instrument development WBS . . . 94
8.5 LFI DPC development and operations WBS . . . 95
8.6 LFI external relationships . . . 96
8.7 Top level LFI schedule . . . 99

A.1 LFI Radiometer Array Assembly . . . 2
A.2 Views of the LFI/HFI Array Assembly . . . 3

A.3 LFI/HFI Array Assembly orientation 4
A.4 Exploded view of Planck assembly 5
A.5 Integrated strawman 5
A.6 Perspective view of the integrated strawman concept 6
A.7 Schematic of the thermal interfaces to the FPU 7
A.8 Thermal interfaces to the Planck coolers 8

List of Tables

1.1 Expected Numbers Of Individually Detectable Sources At $|b| > 20°$ 11
1.2 Potential Instrument Summary 13
1.3 Uncertainties IN Extracted Cosmological Parameters 22

2.1 Summary of LFI Performance Goals 32
2.2 Mechanical Characteristics of the LFI Feedhorns 34
2.3 Electrical Characteristics of the LFI Feedhorns and OMTs 34
2.4 Performance of the LFI Front-end Amplifiers 37
2.5 Backend Characteristics 39
2.6 Cooling Loads and Sorption Cooler Power 43
2.7 LFI Equipment List 46

4.1 LFI Subassemblies 68
4.2 Performance Tests 69
4.3 LFI Instrument Performance/Calibration Test Matrix 70

8.1 Working Groups and Chairpersons 92

Executive Summary

The main scientific goal of the Planck Low Frequency Instrument (LFI) is to measure the Cosmic Microwave Background (CMB) anisotropies at high angular resolution, with an accuracy set by astrophysical limits. The LFI will produce full sky maps at 30, 44, 70 and 100 GHz, with angular resolution of $33'$, $23'$, $14'$ and $10'$, respectively, and with an average sensitivity per resolution element $\Delta T/T \simeq (2 \div 4) \times 10^{-6}$. These unprecedented angular resolution and sensitivity will uncover the wealth of cosmological information encoded in the anisotropy pattern at degree and sub-degree angular scales. This will answer a number of truly fundamental questions about our Universe: How fast is the Universe expanding? What is the ultimate fate of the Universe? What are its material constituents (baryons, dark matter, ...)? Where did the initial perturbations come from? When did the first structures form in the Universe? What is the nature of particle physics at energies $\simeq 10^{16}$ GeV?

The Planck LFI represents the third generation of mm-wave instruments designed for space observations of CMB anisotropies, following the COBE Differential Microwave Radiometer (DMR) and the Microwave Anisotropy Probe (MAP). The DMR, launched in 1989, detected structure in the CMB angular distribution at angular scales $> 7°$. The LFI will produce images of the sky at four frequencies between 30 and 100 GHz, with an unprecedented combination of sky coverage, calibration accuracy, freedom from systematic errors, stability and sensitivity (including polarized components). The LFI will have a better angular resolution than MAP and a sensitivity from 2 to 3 times better. Thus, the LFI data products will be far superior to those of all ongoing and planned experiments. The LFI is designed and optimized to measure CMB anisotropies to the fundamental accuracy limits imposed by cosmic variance and astrophysical foregrounds. In the LFI frequency range the contaminating effect of the galactic emission, dominating the astrophysical foreground noise on scale $\geq 30'$, is minimum at around 60 GHz; while the confusion noise due to extragalactic sources, dominating on smaller angular scales, is minimum in the range 100–200 GHz, where it is primarily due to radio sources. The 70 and 100 GHz channels are therefore optimal to get the cleanest possible view of primordial CMB fluctuations, over the full range of angular scales. In both channels the astrophysical foreground noise is expected to be well below the cosmological signal for all observed angular scales. At 100 GHz then the LFI will accurately measure the power spectrum of CMB anisotropies up to multipoles $\ell \simeq 1500$ with an accuracy of the order of, or better, than 1%. Little cosmological information is left at angular scales smaller than 10 arcminutes, if standard inflationary models hold; in fact anisotropies at such scales are quasi-exponentially erased by photon diffusion.

The LFI measurements will determine of the primary cosmological parameters (Hubble constant, deceleration parameter, curvature of space, baryon density, dark matter densities including neutrinos, amplitude and spectral index of the primordial scalar density perturbations, and the gravity wave content of the Universe) to an accuracy of a few percent. The LFI data can test models for the origin of primordial perturbations, i.e. whether they are due to topological defects or to quantum fluctuations, and to constrain the global properties of the Universe (topology, rotation, shear, etc.). Polarization measurements, which will be possible with an accuracy of a few μK towards the ecliptic caps, will independently confirm these findings and help in breaking any degeneracies in the determination of cosmological parameters.

The LFI will also detect the Sunyaev-Zeldovich effect towards a few hundred of clusters of galaxies, allowing an independent determination of the Hubble constant and providing information on the intercluster medium complementary to those from X-rays. The LFI four-frequency all-sky surveys will also be unique in providing complete samples comprising from several hundred to a few thousands extragalactic sources, selected in an essentially unexplored frequency range. New classes of sources may be revealed in these data. The familiar "flat-"spectrum radiosources (compact radiogalaxies, radio loud QSOs, BL Lacs, blazars), should show spectral features in this frequency range, carrying essential information on their physical properties. Such surveys will be particularly valuable to investigate sources with strongly

inverted spectra, such as GHz peaked sources which may be the youngest stages of radiosource evolution and may thus provide insight into their genesis.

Moreover, the LFI maps will provide a rich database for studies of Galactic evolution, the interstellar medium, and discrete Galactic sources, including supernova remnants, Sagittarius A, and sources self-absorbed up to high frequencies such as some symbiotic stars and planetary nebulae.

The combination of data from its two instruments, LFI and HFI (High Frequency Instrument), give to the Planck Surveyor the imaging power, the redundancy and the control of systematic effects and foreground emissions needed to achieve the extraordinarily exciting scientific goals of this mission in a broad spectral range, from 30 to 857 GHz. This, in turn, is crucial for improving the accuracy in the determination of the cosmological parameters. On more general grounds, LFI and HFI will deal primarily with different astrophysical processes (radio and dust emission, respectively). Both processes coexist in real astrophysical sources. The LFI data are crucial to separate the cosmic signal from the contaminating effect of extragalactic radio sources which dominate the foreground fluctuations on small angular scales in the cosmologically cleanest frequency range, at least up to 200 GHz. On the other hand, the HFI maps will be useful to subtract the Galactic dust emission which is important on intermediate to large angular scales down to 100 GHz. Also, the full set of Planck data will be essential to address a number of important astrophysical problems such as to elucidate physical and evolutionary connections between nuclear activity (responsible for the radio emission) and processes governing the abundance and the properties of the interstellar material (responsible for the sub-mm dust emission).

In conclusion, the combination of LFI and HFI renders Planck Surveyor the definitive mission for imaging the primordial CMB anisotropies, as well as an outstanding astropysical full sky survey.

The success of the mission thus relies heavily on the combination of measurements from both instruments to obtain a single final set of data, derived optimally from all products of the two Data Processing Centers (DPCs). This can be achieved efficiently by sharing with the HFI DPC the approach to data reduction and scientific pipeline processing while maintaining adequate redundancy and cross checking. The two DPCs are organised in a geographically distributed fashion, to take maximum advantage of the expertise available in the Consortia. To cope with the possible disadvantages of distributed DPCs, an Integrated Data and Information System (IDIS) will be developed to allow proper intra-Consortium and inter-Consortia information exchange. IDIS is deemed to be essential for the proper data and information management in a large Consortium involving several Co-Investigators, Associates, engineers, technical and scientific staff located throughout countries in both Europe and North America. The IDIS will be developed as a joint effort involving both Consortia and the Telescope Provider.

The geographical distribution of the DPC is organised in four Levels, communicating with each other through the IDIS. Level 1 processing will transform raw data into organised data timelines. It is carried out by a data center shared by the two instrument Consortia. This choice leads to optimisation of costs, and allows quicker reaction and immediate cross-checking between telemetry from the two instruments. Level 2 will utilise the raw time series from Level 1 to reconstruct sets of calibrated data. Level 3 will transform, by means of pipeline processing, the frequency maps produced by both instruments into preliminary maps. Operations related to Levels 2 (only on LFI data) and 3 of the pipeline will be carried out by the main LFI DPC Center. This approach guarantees that specific instrument competence on LFI is available during the daily checking and reporting of instrument performance, and during the process of data calibration. At the same time, the scientific competence available at the DPC can be used for part of the component separation and inter-frequency cross-checks using data from both instruments. Thus, a proper level of interaction with the corresponding Level 3 of the HFI DPC can be achieved. Finally, to help homogenise the work of the two DPCs, a separate group common to the two instrument Consortia will carry out tasks related to Level 4 (reception, archiving, and preparation of all material needed for public release).

Data processing activities in the LFI Consortium have been planned so as to allow a robust, well-defined architecture of the data pipeline and its associated tools as well as to encourage scientific creativity, when facing unpredictable findings in the real data. This is achieved by an organization scheme which includes an implementation team integrating prototype software provided by a Simulations Working Group (WG) into the pipeline to be run at the DPC.

The Simulations WG, receiving input from Working Groups dealing with hardware components (Ra-

diometers, Electronics, Thermal WGs), as well as with the scientific aspects of the mission (Theory and Foregrounds WGs) develops simulations which represent an ideal sky in the various frequency bands covered by LFI, introducing realistic degradations due to the instrument performance. Simulated time-ordered data are thus produced. The Simulations WG will also develop prototype Data Reduction Software. Science analysis software will also be developed freely by scientists participating in the LFI Consortium, in order to test the most effective ways of extracting science from calibrated data. This software will also be provided to the LFI DPC as prototypes for the Science Pipeline Software.

An integration team (the DPC Team) will engineer the prototype Data Reduction and Science Pipeline software into production software. Efforts will be also specifically concentrated on operational aspects, such as the possibility of correct recovery in the case of hardware failures, or on the concept of providing proper backup to operational hardware.

The instrument proposed for Planck-LFI is likely the most powerful microwave radiometer ever conceived. It consists of a compact, 56-channel multifrequency array of cryogenically cooled receivers with ultra-low-noise amplifiers based on indium phosphide (InP) high-electron-mobility transistors (HEMTs).

Major breakthroughs in transistor amplifier technology achieved in the last few years make the LFI a very timely project. Outstanding performance and reliability of cryogenically cooled InP HEMTs have been recently demonstrated. These devices ensure not only the minimum noise contribution from the receiver but also minimum heat dissipation.

The LFI instrument design proposed here takes advantage of this progress, and it differs in two important respects from that developed during the COBRAS/SAMBA Phase A Study. First, InP, rather than gallium arsenide (GaAs) HEMTs are used; and, second, the radiometers are split into two sub-assemblies connected by waveguides or coaxial cables, one located at the telescope focus, the other on the Planck equipment platform. These changes result in increased performance and reliability for the Planck payload, and allow dramatic reduction (from 5.8 W to <0.6 W) of the power dissipated by the LFI in the focal assembly. The large power dissipation of the LFI focal assembly in the Phase A design was the principal driver of the COBRAS/SAMBA thermal design; the reduction in the new design enables a third important improvement, namely, the LFI focal assembly is actively cooled to 20 K.

The LFI amplifiers at 30 and 44 GHz will use discrete InP HEMTs incorporated into a microwave integrated circuit (MIC). At these frequencies the parasitics and uncertainties introduced by the bond wires in a MIC amplifier are controllable, particularly given the relatively low number of channels (total of 10) at these frequencies, and the additional tuning flexibility facilitates optimization for low noise. Cryogenic MIC amplifiers have demonstrated noise temperatures of 9 K at 30 GHz and 12 K at 44 GHz, with 20% bandwidth. At 70 and 100 GHz there will be 12 and 34 channels, respectively. Amplifiers at these frequencies will use MMICs (monolothic microwave integrated circuits), which incorporate all circuit elements and the HEMT transistors on a single InP chip. The amplifiers can thus be mass-produced in a controlled process, a real advantage given the large number of amplifers. Thousands of wafers of InP MMIC circuits are currently produced industrially. Cryogenic MMIC amplifiers have been demonstrated at 75–115 GHz which exhibit $\leq$50 K noise from 90–105 GHz. The LFI will thus fully exploit both MIC and MMIC technologies at their best.

Cooling to 20 K of the LFI is achieved with a vibrationless hydrogen sorption cooler. In addition to meeting temperature and capacity requirements, the sorption cooler has major advantages for Planck: it is highly efficient; there are no cold moving parts, no vibration, and very low EMI; and integration with the instruments and spacecraft is simple, since the only part of the cooler in the focal assembly is a J-T valve and associated tubing while the compressor and control electronics are located remotely on the spacecraft. The sorption cooler also provides 18 K precooling to the HFI helium J-T cooler. The new thermal design allows efficient radiative cooling of the Planck payload (with the elimination of the 50–80 K and 20 K Stirling coolers used by the HFI in the Phase A design) and a much better optimized design of the combined LFI and HFI front end assemblies in the focal plane.

To meet the challenging performance goals of the LFI requires not only great sensitivity and angular resolution, but also stringent control of systematic errors. Because of the way Planck scans the sky, the raw instrumental sensitivity near the ecliptic poles will be at μK level. Almost certainly near the poles the true sensitivity of both the LFI and the HFI will be determined not by raw instrumental sensitivity,

but rather by systematics. There are many possible sources of systematic errors, including Galactic and extragalactic foregrounds, sidelobe pickup of the Galaxy, Sun, Earth, and Moon, distorted beam shapes, beam smearing due to the spacecraft spin, temperature variations of the telescope and instruments, non-white noise in the instruments, spacecraft pointing errors and nutation, the effect of changing magnetic fields on sensitive components, as well as problems such as ground loops, EMC, and EMI that can be evaluated before launch. Many of these sources of error have been studied in some detail, with the goal of understanding the magnitude of the error and estimating to what extent it can be removed. The results are extremely encouraging. No insuperable obstacles to the achievement of spectacular sensitivity by Planck have been found. Nevertheless, caution is required. The effects have been studied one at a time, and removing them if they are large is often extremely demanding computationally. Moreover, no realistic simulations have been done of the effects in combination (e.g., removing the effects of Galactic foregrounds observed with distorted beams smeared by spacecraft motion, with contamination from far sidelobes). The LFI philosophy, therefore, is to reduce the magnitude of potential systematic errors as much as possible within cost and resource constraints by careful design of the hardware, rather than to rely on removing them in software. In particular, a scan strategy with the spin axis always kept in anti-Sun direction greatly reduces the risk of thermal effects which may reflect directly on the instrument stability. Full sky coverage can be maintained with a 90° angle between the spin axis and the telescope pointing direction.

The overall LFI mass is 110 Kg mass, the power is 450 W (including the sorption cooler and related electronics). The data rate can be kept within the 20 kb per second allocated to LFI with modest on-board data compression, provided that a pointing accuracy better than $1'$ over a few minutes is performed by the spacecraft.

The LFI will be implemented by the LFI Consortium, which is based on the coordinated effort of scientific institutes, individual investigators, and industries from many countries.

To enable successful implementation of the LFI, we have defined clear lines of responsibility and authority, a Work Breakdown Structure (WBS) with clear work-package and interface definitions, and detailed schedules of the deliverables and receivables.

The Project Organisation reflects the key roles played by the Co-I's, senior scientists or managers who take responsibilities for substantive contributions to the LFI, either scientific or technical. The PI has overall responsibility for the LFI, and acts as the unique official interface between the LFI Consortium and the Planck ESA Project. A Planck LFI Project Office, lead by the Project Manager, will support the PI in the general management of the project, and support the Instrument Manager and the DPC Manager in the management of their activities. The Survey Scientist (SS), reporting directly to the PI, provides scientific and technical support to the Consortium and to the Science Team (ST). The Instrument and DPC Managers, in their managerial roles, report to the PI. The Funding Committee (FC) composed of the PI and one Co-I from each country with a substantial financial commitment to the LFI (see the Funding Proposal), will ensure that institutes, groups and industries from their respective countries keep organisational committments and make funding and manpower available as required.

The scientific and technical activities of the Consortium are organised through a number of Working Groups advisory to the PI. Each WG is chaired by a Co-I and is supported by a number of Associates who provide significant expertise but are not expected to take functional responsibilities.

There are two formal lines of communication between the ESA Planck Project Office and the Planck LFI Consortium. One is through the PI, the other through the ESA Planck Science Team, where the LFI is represented by the PI, the Instrument Manager, the DPC Manager, and the Survey Scientist. Other contacts, mainly during the design phase, occur via various groups or committees which include ESA and HFI experts as needed.

The LFI, the HFI and the Telescope Provider (TP) have already established or will soon establish integrated teams to address all common areas. For the scientific programme it is the intention of the three teams to set up a "Common Scientific Committee", composed of a number (TBD) of Co-I's chosen to give a balanced representation of the teams as well as of the various national contributions to the Planck Project.

The majority of the CMB scientific community is already significantly involved in the Planck Project.

In any case Planck data can be accessed by the external scientific community. For example, the LFI Consortium will consider proposals for Associateship from those scientists willing to contribute significantly to the scientific and/or technical aspects of the Project. Associates can participate in the "data exploitation by Planck scientists", as defined in the Planck Science Management Plan (SMP). The LFI Team will provide support to the community for accessing and exploiting the Planck archive.

The Planck mission, and in particular its cosmological goals, are already generating substantial public interest. The LFI Consortium is strongly committed to promoting public awareness of the mission as it proceeds, and intends to make full use of ESA support in such activities as detailed in ESA's recent document, "Publicity Agreement for Scientists involved in ESA Science Projects".

The estimated overall cost is aligned with budgets for other instruments of similar complexity. Committments to meet the obligations taken within the LFI Consortium have been received by all participating Institutions. Applications for funding to the relevant Agencies have been or will be submitted. An appropriate level of funding to initiate Consortium activities have already been granted in a number of cases. NASA has approved and funded adequately the participation of the US Team.

Chapter 1

Scientific Objectives and Capabilities

1.1 Introduction

The major scientific advance attributed to the discovery of the Cosmic Microwave Background (CMB) was the confirmation of the hot big-bang model. In this model the Universe was once hot and dense, and has been expanding and adiabatically cooling ever since. When the Universe was $\sim 10^5$ years old, its temperature was around 3000 K ($kT \sim 0.25$ eV): protons were able to capture electrons to form neutral hydrogen. Before this time the Universe was opaque to radiation: the mean free path of photons was so short that they behaved as a fluid, strongly coupled to the protons and electrons. This thermodynamic transition at $T = 3000$ K (called recombination) suddenly reduced the opacity for Thomson scattering, setting the photons free, and the majority of them have interacted only gravitationally with the matter since that time. The sphere surrounding us at redshift $z \simeq 1000$, which represents the position at which the photons seen today last interacted directly with the matter, is called the last scattering surface.

Soon after the CMB discovery, it was realized that the presence of density fluctuations at the last scattering epoch would necessarily induce angular anisotropy in the CMB intensity. In the standard gravitational instability picture, density fluctuations are usually assumed to be an isotropic and homogeneous stochastic process, described by a power spectrum that was initially a power law in wavenumber k: $P(k) = Ak^n$. Observations of CMB anisotropy are able on the one hand to demonstrate the existence of density inhomogeneities at early times, and on the other hand to provide a direct measurement of the amplitude and shape of their power spectrum.

On large angular scales CMB anisotropies arise from density fluctuations much larger than λ_H, the (comoving) horizon scale at last scattering. They are caused by photons climbing out of the potential wells produced by density inhomogeneities on this surface. A monochromatic fluctuation of comoving wavelength λ ($\equiv 2\pi/k$) generates a potential fluctuation $\delta\phi \propto \lambda^{(1-n)/2}$ and thus a temperature fluctuation $\Delta T/T \propto \theta^{(1-n)/2}$, where θ is the angle subtended by λ at last scattering. This is the so-called Sachs-Wolfe (1967) effect, and is the main source of anisotropy on scales larger than $\theta_H \simeq 2^\circ\Omega^{1/2}$, the angle subtended by λ_H at last scattering.

The first detection of these CMB temperature anisotropies (Smoot *et al.* 1992) was the great success of NASA's COsmic Background Explorer (COBE, launched in 1989), touching off a media storm which reached the front page of virtually every major newspaper around the globe. The anisotropies seen by COBE at an angular resolution of 7° FWHM have been interpreted as Sachs-Wolfe anisotropies, and are consistent with a scale-invariant primordial power spectrum (*i.e.* $n = 1$), placing constraints on n at about the 30% level (Gorski *et al.* 1996).

In the aftermath of the COBE success, there was an enormous increase in both the theoretical and experimental effort in this field. Two things quickly became apparent. First, current technology is capable of reaching sensitivities 100 times better than that of COBE. Second, COBE left completely untouched a wealth of cosmological information encoded in the pattern of CMB anisotropies at degree and sub-degree angular scales. We can safely say that a definitive measurement of CMB anisotropies is still the most important unrealized goal in observational cosmology.

Although a great deal of progress has been made and will continue to be made with ground-based and balloon-borne experiments, there is no doubt that an all-sky map, free from the problems induced by the Earth's atmosphere and other terrestrial foregrounds, will provide vastly more scientific return. With the post-COBE detection of anisotropy on a variety of angular scales, the rapid technological progress, and the intense theoretical activity of the last 6 years, the case for high resolution CMB satellite missions has strengthened. Detailed, high resolution ($\lesssim 10'$) measurements will reveal the full structure of the background radiation and will answer a number of truly fundamental questions about our Universe: How fast is the Universe expanding? What is the ultimate fate of the Universe? What are its material constituents (baryons, dark matter, ...)? Where did the initial perturbations come from? When did the

first structures form in the Universe? What is the nature of particle physics at energies $\simeq 10^{16}$ GeV?

In recognition of the importance of these CMB goals, NASA selected the Microwave Anisotropy Probe (MAP; for more information see the MAP homepage at http://map.gsfc.nasa.gov) as a Mid-Ex mission to be launched in 2000. The rapid schedule and the financial bounds of the Mid-Ex program placed seriuos limits on MAP's design. This leaves the way clear for a definitive *third* generation space CMB mission, with high sensitivity at all relevant angular scales and over the entire relevant wavelength range.

As extensively discussed in the Phase A report, the Low Frequency Instrument (LFI) and the High Frequency Instrument (HFI) on board of the ESA M3 Planck Surveyor mission will produce carefully made, calibrated maps of the whole sky with unprecedented sensitivity and angular resolution (down to $\sim 5'$) over a broad frequency range (from 30 to 857 GHz), resulting in data products which are far superior to those of all ongoing and planned experiments. Planck will measure and accurately characterize small fluctuations in the CMB temperature, which are only about one part in 10^5 of the CMB temperature, and in addition it may be able to measure CMB polarisation, which is expected at the 10^{-6} level. These measurements should reveal the primordial structure that grew to form galaxies and will test ideas about the properties and evolution of our Universe and the structures within it. By mapping CMB anisotropies precisely, the Planck Surveyor satellite will provide decisive and extraordinarily exciting measurements of the geometry, constitution, and early history of the Universe.

The Planck/LFI will play a key role in the Planck Surveyor mission for the following reasons:

- Its 70 and 100 GHz channels are optimal to get the cleanest possible view of primordial CMB fluctuations: Galactic emission, dominating the astrophysical foreground noise on scale $\geq 30'$, is minimum around 60 GHz; the confusion noise due to extragalactic sources, dominating on smaller angular scales, is minimum in the range 100–200 GHz, where it is primarily due to radio sources. A combination of data from all LFI channels will allow an accurate subtraction of contaminating foreground signals; the removal of Galactic dust emission will be further improved using HFI maps.
- At 100 GHz the LFI reaches an angular resolution of $10'$, allowing to determine the power spectrum of CMB anisotropies up to multipoles $\ell \simeq 1000$. In the standard Cold Dark Matter model, anisotropies on smaller scales are quasi-exponentially erased by photon diffusion: little cosmological information remains there.
- Polarisation measurements, which will be possible with an accuracy of few μK towards the ecliptic caps, will provide independent estimates of cosmological parameters and will help in breaking any degeneracies in the determination of cosmological parameters.
- The LFI data are *essential* to accurately subtract the radio source contribution to fluctuations, which are the main astrophysical limitation for CMB anisotropy measurements also in the HFI 143 and 217 GHz channels.
- The high sensitivity, accurately calibrated maps of the Galactic synchrotron and free-free will constitute a unique tool for investigating the distribution of: i) the interstellar magnetic field; ii) relativistic electrons; iii) the ionized components of the interstellar medium.
- The multifrequency LFI all-sky surveys will be unique in providing complete samples of bright extragalactic sources with strongly inverted spectra.

1.2 Planck Main Science: CMB Anisotropies

1.2.1 The Angular Power Spectrum

Although it is hard to show in its full extent the quality of the Planck maps, we want to give a visual impression of the crucial role that high resolution observations play in CMB anisotropy studies. In Figure 1.1 we show a full sky map of the expected CMB anisotropy, with COBE-size and Planck-size pixels. Of course a definitive probe of the pattern of CMB anisotropy requires an angular resolution better than that set by the relevant physical effects. The superior resolution of Planck meets this requirement, as we now show through a brief description of the models which produce CMB anisotropy patterns like those shown in Figure 1.1.

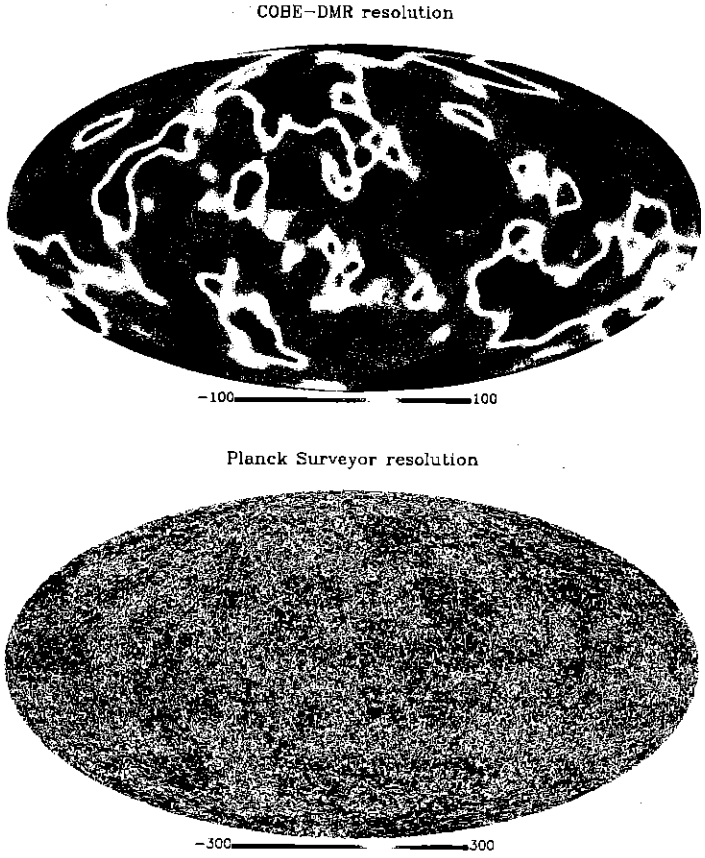

Figure 1.1: Planck vs. COBE angular resolution. The same pattern of the CMB anisotropy is observed at the COBE/DMR (upper panel) and Planck (lower panel) resolution. This simulation uses the standard Cold Dark Matter model.

It is useful to expand the CMB anisotropy on the celestial sphere in a spherical-harmonic series

$$\frac{\Delta T(\theta,\phi)}{T} = \sum_{\ell m} a_{\ell m} Y_{\ell m}(\theta,\phi)\,, \tag{1.1}$$

and to work in terms of the 'multipole moments' $a_{\ell m}$. Theories predict only the statistical properties of the $a_{\ell m}$: they should have zero mean, $\langle a_{lm}\rangle = 0$, and non-zero variance $C_\ell \equiv \langle |a_{\ell m}|^2\rangle$ (the angle brackets indicate an average over all observers in the Universe; the absence of a preferred direction implies that $\langle |a_{lm}|^2\rangle$ should be independent of m). The set of C_ℓ is known as the angular power spectrum and is the key theoretical prediction for any given model. If the CMB temperature fluctuations are gaussian, as suggested by inflation models, then the angular power spectrum completely defines their statistical properties.

The multipole ℓ is essentially the Fourier conjugate of the angle θ: $\ell \simeq 180^\circ/\theta(\mathrm{deg})$. One degree subtends a (comoving) length on the surface of last scattering that corresponds to about $100\,\mathrm{h}^{-1}$Mpc (h is the Hubble constant, H_0, in units of $100\,\mathrm{km\,s^{-1}\,Mpc^{-1}}$, and 1 Mpc is approximately 3 million light-years). Therefore, the ℓ-th multipole is basically determined by density fluctuations on a length scale, $\lambda \approx 2\pi r_0/\ell$, with $r_0 = 2c/(H_0\Omega_0)$: thus, $\lambda \approx 40,000\mathrm{h}^{-1}\mathrm{Mpc}/(\Omega_0\ell)$

In Figure 1.2 we plot the angular power spectrum for the standard Cold Dark Matter (CDM) model, with scale invariant initial conditions (heavy continuous black line). In the low ℓ limit, $\ell(\ell+1)C_\ell$ is

approximately constant, because of scale-invariant potential perturbations on the last scattering surface, out of which the photons must climb (the Sachs-Wolfe effect). To understand the oscillatory structure of the angular power spectrum at $\ell \gtrsim 100$ (corresponding to angles $\lesssim 2°$), consider the Universe just before it cooled enough to allow protons to capture electrons. At these early times, the photons and the proton-electron plasma behaved as a single "baryon-photon fluid". In the presence of a gravitational potential, forced acoustic oscillations in the fluid arise, described by a driven harmonic oscillator equation. The driving force is given by gravity, the inertia by the baryons and the restoring force (pressure) by the photons (Sunyaev & Zel'dovich 1970; Hu, Sugiyama, & Silk 1997).

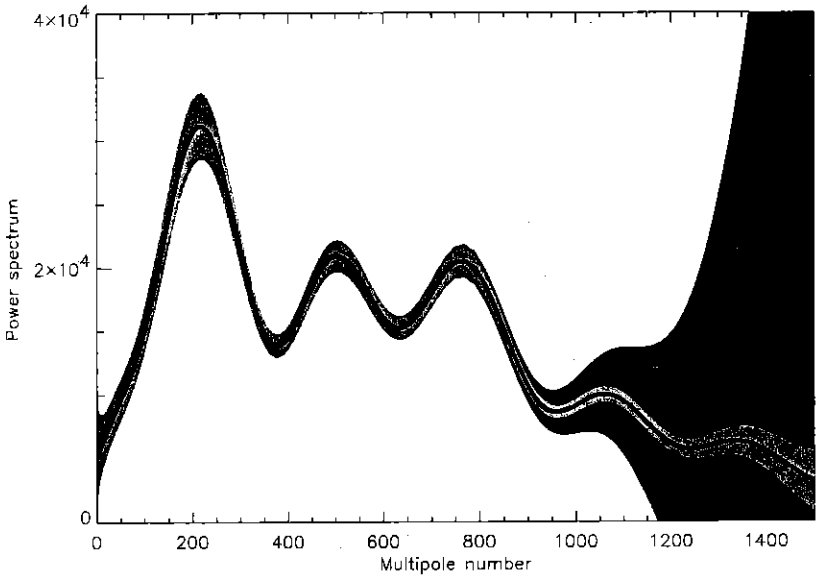

Figure 1.2: Angular power spectrum, $\ell(\ell+1)C_\ell$, for the standard Cold Dark Matter model, with scale invariant initial conditions (heavy continuous black line). The coloured bands indicate the estimated uncertainties in the C_ℓ amplitude due to cosmic variance, instrumental noise and angular resolution. Green and blue bands refer to the MAP and Planck/LFI experiments, respectively.

Since recombination is nearly instantaneous, the CMB provides a snapshot of these acoustic oscillations, with different wavelength modes being caught in different phases of oscillation. The energy density, or brightness, fluctuations in the photons (coming from density and velocity components of the harmonic oscillator) are seen by later observers as temperature anisotropies. The first peak in the angular power spectrum corresponds to a perturbation that became maximally overdense just when the Universe recombined, i.e. 1/4 of an oscillation. Similarly the third, fifth etc. peaks represent scales that have undergone an extra integral number of oscillations by this time. The even peaks are maximally underdense modes, which also give rise to power peaks (power is temperature difference *squared*), though of generally smaller amplitude since the rebound must fight against gravity. The troughs, which do not extend all the way to zero, are velocity maxima, which are $\pi/2$ out of phase with the density maxima.

In the short but finite time taken for the Universe to recombine the photons can diffuse a certain distance. Anisotropies on scales smaller than this 'mean free path' will be erased by diffusion, leading to the quasi-exponential damping (Silk 1968; Hu & White 1997) seen in the spectrum at large ℓ's. This becomes quite effective at $\ell \gtrsim 1000$, corresponding to angular scales $\lesssim 10'$. Little cosmological information thus remains in the CMB at smaller scales, at least for the standard Cold Dark Matter models.

We must also consider the importance of sky coverage: the estimate of the power spectrum has a sampling variance which is ultimately limited by the fact that there is no more sky once you have

mapped all of it. This 'cosmic variance' (Abbott & Wise 1984) sets the ultimate limit on the accuracy of estimates of the power spectrum, and drives the simple science requirement of as much high-quality sky coverage as possible. The fractional error on the C_ℓ's can be written as follows, summing in quadrature the cosmic and instrumental noise variances (Knox 1995):

$$\frac{\delta C_\ell}{C_\ell} = \frac{4\pi}{A}\sqrt{\frac{2}{2\ell+1}}\left[1+\frac{A\sigma^2}{NC_\ell W_\ell}\right]. \tag{1.2}$$

Here A is the surveyed area of the sky, σ is the *rms* pixel noise, N is the number of pixels in the sky map and $W_\ell = \exp[-\ell^2\sigma_B^2]$ the window function describing the region of ℓ-space observable with a beam of FWHM equal to $2\sqrt{2\ln 2}\sigma_B$. In Figure 1.2 we also show the expected uncertainties in the angular power spectrum when the noise variances for MAP and Planck/LFI are taken into account. Clearly the angular resolution and sensitivity of Planck are fully adequate to sample all the interesting features expected in the angular power spectrum of the primary CMB anisotropy.

1.2.2 Cosmological Parameters

The detailed shapes, heights and locations of peaks and troughs in the angular power spectrum are predicted by all models which, like CDM, are based on the inflationary scenario. Furthermore they depend critically on the chosen cosmological parameters (Jungman *et al.* 1996; Hu *et al.* 1995). Let us focus on two illustrative examples which show the dependence of the angular power spectrum on the total and baryonic density parameters (Ω_0 and Ω_b, respectively).

The linear scale associated with the harmonic series of peaks in C_ℓ is the (comoving) horizon size at last scattering: $\lambda_H = 2c/(\Omega_0^{1/2}H_0)(1+z)^{-1/2}$. Since the recombination process depends primarily on temperature, it occurs reliably at $z \simeq 1000$, quite independently of the cosmological model (*i.e.* of Ω_0 and H_0). However, the *angular* scale associated with this linear scale depends on the distance to the last scattering surface and hence on the geometry of the Universe (the comoving angular diameter distance): $\lambda_H = r_0\theta_H$, which yields $\theta_H = 2^\circ\Omega_0^{1/2}$. This means that the overall angular scale of the anisotropy spectrum, in particular the separation of the peaks, is a sensitive probe of the spatial curvature of the universe. Moreover, in open models the potential fluctuations are not constant in time since the epoch corresponding to $z \sim \Omega_0^{-1}$, after which the expansion rate is determined only by the curvature term. This time variation in the gravitational potential imprints further temperature fluctuations on the CMB: when a photon passes through a potential well, the blueshift it acquires falling in will not be exactly canceled by the redshift later acquired climbing out (this is an example of the so-called integrated Sachs-Wolfe effect). As a consequence, in open cosmologies, the amplitudes of low order multipoles gets boosted [see Fig. 1.3 (upper panel)].

The amplitude of the peaks clearly depends on the ratio of the inertia to the restoring force, or on the baryon to photon ratio. A larger baryon to photon ratio will increase the compressions (which produce the even peaks in C_ℓ for inflationary models) and decrease the rarefactions [odd peaks for inflationary models; see Figure 1.3 (lower panel)]. The amplitude of the fluctuations will also depend on the driving force, or the gravitational potential. The size of the potential in turn depends on how close the last scattering event was to the epoch when the density of matter started to exceed the density of radiation [this epoch, called the equality epoch, occurred at a redshift $z_{\rm eq} \simeq 40,000\Omega_0h^2/(1+0.23N_\nu)$, where N_ν is the number of massless neutrino families], since potentials inside the horizon decay in a radiation dominated era but not in a fully matter dominated one. This introduces an additional dependence on Ω_0h^2: there is more power on degree-scales for models with lower matter content. Here is a summary of how other parameters affect the angular power spectrum:

- *Hubble constant*: lowering h, while keeping Ω_bh^2 fixed at the nucleosynthesis value, delays the epoch of matter radiation equality, boosts the peaks and, because of the different expansion rate, slightly changes their location in ℓ-space.
- *Cosmological constant*: increasing the cosmological constant, Λ, while keeping the space flat, again delays matter radiation equality and boosts the peaks. Low ℓ multipoles are affected by the inte-

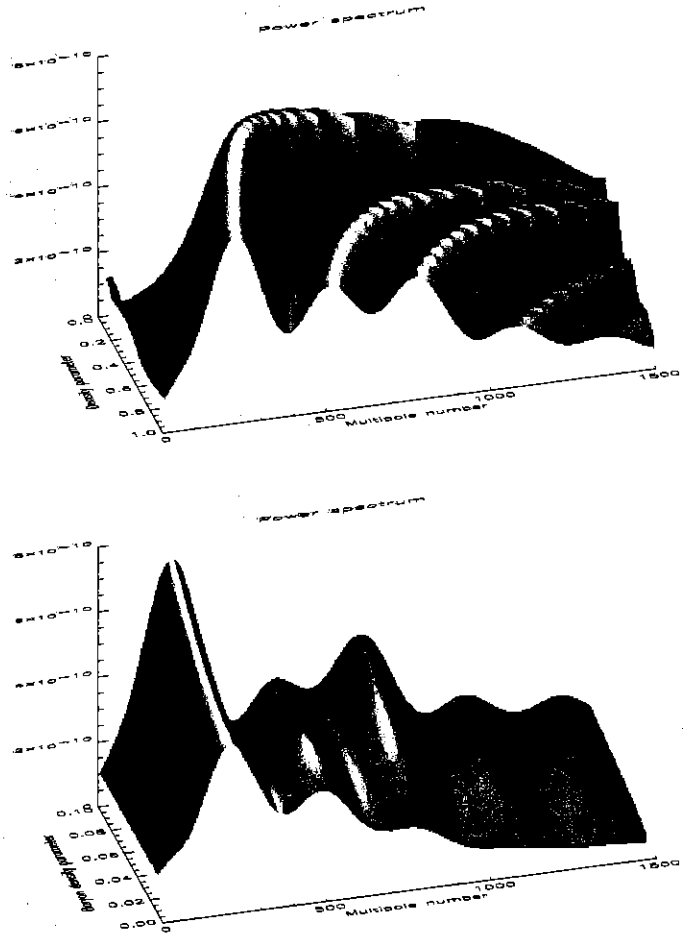

Figure 1.3: The angular power spectrum, $\ell(\ell+1)C_\ell$, of the CMB anisotropy in Cold Dark Matter scenarios is shown as a function of the multipole number ℓ and Ω_0 (upper panel), and Ω_b (lower panel).

grated Sachs-Wolfe effect. Again, because of the different expansion rate, there is a change in the location of peaks.

- *Spectral index*: increasing n will raise the angular spectrum at large ℓ's with respect to the low ℓ's. Planck angular resolution and sensitivity will allow an estimate of n with very high precision, providing constraints on different inflationary models and, hence, on fundamental physics at energies $\gtrsim 10^{16}$ GeV.

- *Reionization*: reionization of the intergalactic medium at $z << 1000$ suppresses the power at $\ell \gtrsim 100$. Evidence for early reionization would set important constraints on theories of galaxy formation and on the epoch at which the first structures formed.

- *Nature of dark matter*: if the critical density is provided by a mixture of cold ($\Omega_{\rm CDM} \gtrsim 0.7$) and hot ($\Omega_\nu \lesssim 0.3$) dark matter, as suggested by some theorists to reconcile the COBE/DMR results with recent observations of large scale structure (e.g. Primack 1996), the angular power spectrum shows systematic differences (at the level of $\sim 10\%$) compared with the $\Omega_{\rm CDM} = 1$ case. These differences, primarly due to a change in the equation of state in the Universe at the recombination

epoch, can be detected by an experiment with Planck 's sensitivity and resolution, thus providing important constraints on particle physics models.

- *Gravitational wave background*: gravitational waves (tensor modes) in addition to the more usual density perturbations (scalar modes) generate additional CMB anisotropies, but only at large angular scales. Inflationary models predict that the ratio of tensor to scalar contribution to the quadrupole anisotropy ($r = C_2^{(T)}/C_2^{(S)}$) is related to the spectral index of primordial tensor fluctuations, n_t. The Planck sensitivity and angular resolution allow a very clean test of inflationary models, since the angular power spectra due to tensor and scalar modes vary with multipoles in a very different way.

Planck/LFI will be able to measure $\simeq 1000$ multipole moments, C_ℓ. So there is potential, as extensively discussed in the Phase A report, for obtaining most of these important cosmological parameters at the few percent level, and several of them to previously undreamt levels of precision. Surprises are always possible when new windows on the Universe are opened up. If the Universe is *not* at all like we expect it to be, then the Planck Surveyor data will be exactly what is required to make further progress. It may be that the statistics of the fluctuations are significantly non-Gaussian, or that the power spectrum is of an entirely unexpected form. In any case, the data from Planck will revolutionize our understanding of the Universe.

1.2.3 Polarisation

In the Phase A study design the LFI detects two orthogonal polarisations at all frequencies, but with modest sensitivity, while the HFI does not detect polarisation at all, even though the temperature sensitivity is excellent. The revised package provides good sensitivity for the LFI as well as the addition of polarisation sensitivity in the HFI at 143, 217, and 545 GHz, and enhanced polarisation capability for LFI. An assessment of the actual sensitivity of Planck/LFI to CMB polarisation will depend on the optimization of the detector design, to be carried out during the instrument development phase (see § 2.1.3), and will require a careful analysis of and further data on the effect of polarized components of foregound emissions. The significant experimental challenge lies in the very small level of the cosmological polarisation signal, requiring both great sensitivity, to obtain a useful signal-to-noise ratio, and broad frequency coverage, to detect the signal in the presence of polarized foreground emission. Planck is the only currently planned platform with these capabilities.

Theoretically, the degree of linear polarisation is directly related to the quadrupole anisotropy in the photons when they last scatter (Kaiser 1983; Kamionkowski *et al.* 1996; Seljak & Zaldarriaga 1997). While the exact scale dependence of polarisation depends on the mechanism for producing the anisotropy, several general properties arise. The polarisation peaks at angular scales smaller than the horizon at last scattering, since the processes that produce it are causal (see Fig. 1.4). Furthermore, the polarized fraction of the temperature anisotropy is small, since only those photons that last scattered in an optically thin region could have possessed a quadrupole anisotropy (multiple scattering causes photon trajectories to mix and hence erases anisotropy). This fraction depends on the duration of last scattering: for the standard thermal history, it is 5-10% on a characteristic scale of tens of arcminutes, slightly smaller than the scale where the temperature power spectrum peaks.

Why should we be concerned with the polarisation of the CMB? The prediction of polarisation comes simply from the well known physics of Thomson scattering and the assumption that the temperature anisotropies we observe are the result of fluctuations at last scattering. The verification of the (partial) polarisation of the CMB on small scales would thus represent a fundamental check on our basic assumptions about the behavior of fluctuations in the universe, in much the same way that the redshift dependence of the CMB temperature is a test of our assumptions about the background cosmology.

Furthermore, observations of polarisation provide an important tool for reconstructing the model of the fluctuations from the observed power spectrum (as distinct from fitting an *a priori* model prediction to the observations). Polarisation probes the epoch of last scattering directly, unlike the temperature fluctuations which may evolve between last scattering and the present. This localization in time is a very

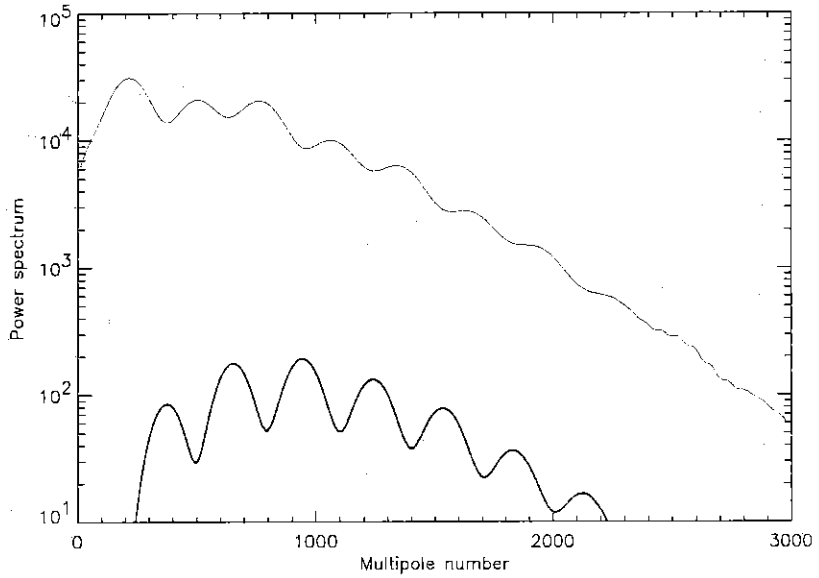

Figure 1.4: Temperature (blue line) versus polarisation (red line) anisotropy for standard Cold Dark Matter model with scale–invariant initial conditions. Only scalar fluctuations are considered.

powerful tool for reconstructing the sources of anisotropy. Moreover, different sources of temperature anisotropies (scalar, vector and tensor) give different patterns in the polarisation, both in its intrinsic structure and in its correlation with the temperature fluctuations themselves (see Fig. 1.5). Thus by including polarisation information, one can cleanly distinguish the physical processes which determine the temperature power spectrum and hence constrain the cosmological model. Hence polarisation may provide direct evidence that gravity waves are the source of some of the anisotropies, which would lead to a much more powerful probe of inflation than is possible using density perturbation information alone.

Finally, the polarisation power spectrum provides information complementary to the temperature power spectrum even for ordinary (scalar or density) perturbations. This can be of use in breaking degeneracies in the determination of the cosmological parameters, thus constraining them even more accurately (Zaldarriaga, Spergel & Seljak 1997).

1.3 Foregrounds and LFI Science

The LFI is designed and optimized to measure primary anisotropies in the CMB; however, the images that it will produce at 30, 44, 70 and 100 GHz will have an unprecedented combination of sky coverage, calibration accuracy, freedom from systematic errors, stability, and sensitivity (including to polarized radiation). As a result, the LFI data will also be a unique resource for studying the astrophysics of the Galaxy, of extragalactic point sources and of clusters of galaxies through the Sunyaev-Zeldovich effect. Here we briefly summarize the science that can be addressed exploiting the LFI data; methods for separating the primary CMB anisotropies from different foregrounds will be discussed in § 1.5.4.

1.3.1 Studies of the Galaxy

The LFI maps of the Galactic foregrounds (synchrotron, free-free and dust emission) will have a measurement accuracy comparable to that achieved on the CMB, with orders of magnitude lower noise than any current data, and 3-4 times better sensitivity than MAP. Figure 1.6 shows, as a function of frequency, the approximate intensity of these Galactic foregrounds, relative to the CMB at high Galactic latitudes.

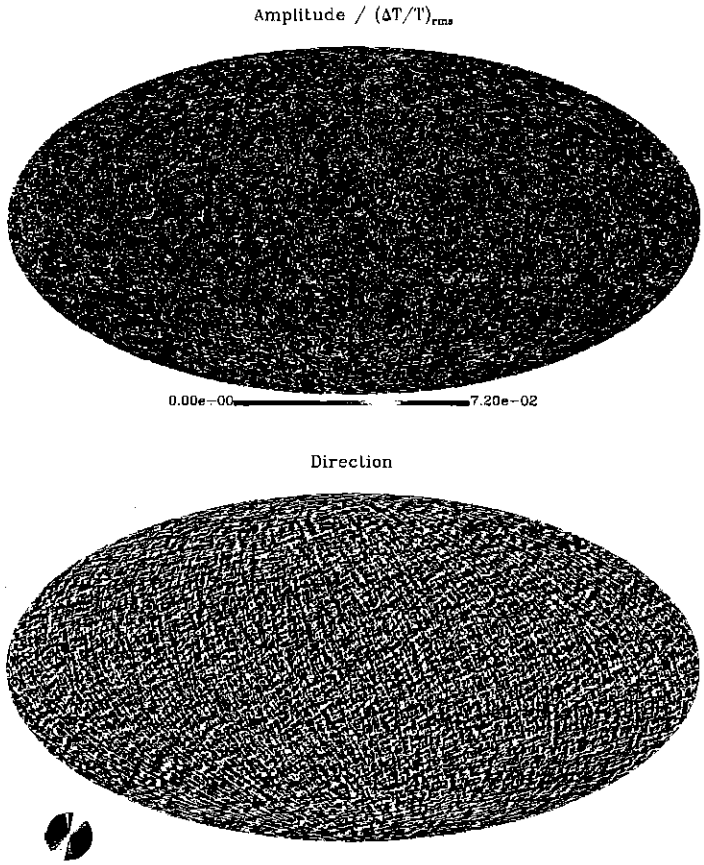

Figure 1.5: Polarisation maps at Planck resolution. Polarisation is in general a "spin 2" field on the sky. Here we present one standard CDM simulation here by showing amplitude (relative to the rms temperature fluctuations; upper panel) and direction (lower panel) of the polarisation "vector". The polarisation directions are associated with colors by the small circle at the lower left corner of the figure.

Polarisation measurements will be very useful in singling out the synchrotron emission whose percentage polarisation can be expected at a level of 30-50% at the frequencies sampled by Planck/LFI, where Faraday depolarisation will be minimal. Maps of the synchrotron emission of the Galaxy will give information about: i) the structure of the magnetic field; ii) the spatial and energy distribution of relativistic electrons; iii) the variations of electron density, of electron energy and of magnetic field induced by supernova shocks and winds from OB stars. The maps will explore correlations between magnetic fields and the matter distribution more systematically and often on much smaller scales than ground-based surveys.

Free-free emission from ionized gas in the Galaxy is not easily identified at radio frequencies, except near the Galactic plane. It may, however, be the dominant foreground at 30–80 GHz. The multifrequency all-sky Planck/LFI maps, coupled with X-ray maps and Hα surveys, will therefore be a very valuable tool for investigating the structure, distribution and physical conditions in the hot regions of the interstellar medium.

Galactic dust emission is expected to be important, or even dominant, at 100 GHz, and to fade rapidly at lower frequencies. Planck/LFI measurements will contribute to investigate the distribution and nature of cold dust in the Galaxy. The simultaneous study of dust and free-free emission will be very useful to investigate the relationships between different phases (HI and HII gas) of the interstellar medium.

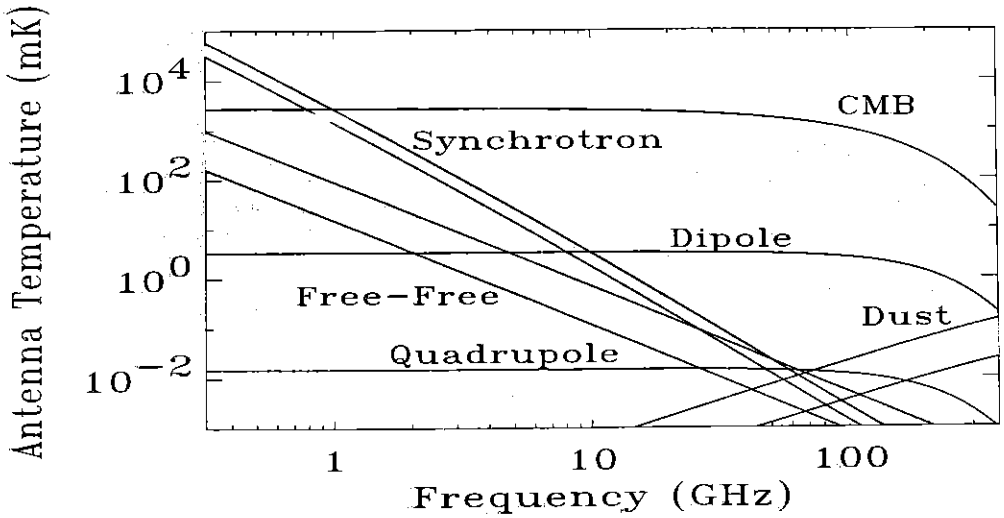

Figure 1.6: Frequency dependence and approximate relative strength of Galactic synchrotron, free-free, and dust emission compared with that of the cosmic microwave background and its features.

Draine and Lazarian (1997) have recently proposed that spinning dust grains can produce a significant signal peaking at a few 10's of GHz. While there is no compelling evidence to support this hypothesis, it is still a lesson that surprising new sources of emission or unexpected variations in Galactic emission may be awaiting us. The need to be sensitive to such unexpected foregrounds is a primary motivation for Planck's broad spectral coverage.

Planck measurements will also detect and provide spectral information on the brightest discrete Galactic radio sources, including a relatively large complete sample of supernova remnants and the puzzling source Sagittarius A. These data will be unique in allowing a search for extremely compact bremsstrahlung or synchrotron sources, self-absorbed up to tens of GHz and therefore unobservable in existing surveys.

1.3.2 Extragalactic Sources

Although Planck's instruments have sensitivities near fundamental physical limits, the small size of the telescope means that the overall sensitivity of Planck to compact sources is poor compared to ground based instruments such as the Effelsberg and Green Bank 100m telescopes, the VLA, and the Millimeter Arrays being planned for the next decade, as well as to space-based missions such as FIRST. Nevertheless, because Planck will observe the entire sky, it will be able to detect a large number of compact sources, as estimated in Table 1.1 (see Toffolatti *et al.* 1997 for a detailed description of the adopted models). Furthermore, the absolute calibration of the Planck data will be determined to great accuracy from the motion of the Earth around the Sun. Since the beam area of a given telescope scales a ν^{-2}, large area radio continuum surveys above 30 GHz are not feasible from the ground. As a result, the LFI surveys will provide unique information on the frequency range they explore; the data sets they will produce will be important in several areas of extragalactic radio astronomy, particularly since Planck covers just the frequency range where the shape of the spectral energy distribution of Active Galactic Nuclei is least well known.

The LFI is expected to detect mostly "flat-"spectrum radiosources (compact radiogalaxies, radio loud QSOs, BL Lacs, blazars), in a frequency region where spectral features carrying essential information

TABLE 1.1

EXPECTED NUMBERS OF INDIVIDUALLY DETECTABLE SOURCES AT $|b| > 20°$.

$\nu_{\rm eff}$ (GHz)	$\lambda_{\rm eff}$ (mm)	beam (arcmin)	$\sigma_{\rm noise}$ (mJy)	$\sigma_{\rm Gal}$ (mJy)	$\sigma_{\rm conf}$ (mJy)	$\sigma^{(1)}_{\rm CMB}$ (mJy)	$S^{(2)}_{\rm lim}$ (mJy)	$N(>S_{\rm lim})_{\rm radio}$ (8 sr)	$N(>S_{\rm lim})_{\rm FIR}$ (8 sr)
30	10.0	33	13	100	37	78	650	300-800	0-2
44	6.8	23	19	45	17	80	480	450-1600	3-10
70	4.3	14	25	15	8	61	330	600-2500	6-18
100	3.0	10	27	7	6	64	350	500-2800	4-12
100	3.0	10.6	13	7	6	64	330	500-2800	4-12
143	2.1	7.4	12	6	4	56	290	330-3600	5-15
217	1.38	4.9	14	5	6	31	180	350-4000	120-200
353	0.85	4.5	24	18	18	16	200	300-2500	2000-3500
545	0.55	4.5	44	62	45	3	450	40-250	6000-10000
857	0.35	4.5	36	120	70	-	700	10-50	17000-25000

(1) Flux density fluctuations of the cosmic microwave background corresponding to $\Delta T/T = 10^{-5}$.
(2) Adopted detection limit for discrete sources, equal to $5 \times (\sigma^2_{\rm noise} + \sigma^2_{\rm conf} + \sigma^2_{\rm Galaxy} + \sigma^2_{CMB})^{1/2}$. A rough estimate of anisotropies, $\sigma_{\rm Galaxy}$, due to the Galactic emission at high Galactic latitudes ($|b| > 20°$), has been obtained following Danese *et al.* (1996) and Bersanelli *et al.* (1996; Figure 2.3, 3.4 and Appendix A.1), and taking into account the angular dependence of galactic dust fluctuations as determined by Gautier *et al.* (1992). $\sigma_{\rm conf}$ is the amplitude of fluctuations due extragalactic sources fainter than $S_{\rm lim}$.

on physical conditions of sources show up. These features include: spectral breaks related to the "synchrotron age" of the source; spectral steepenings corresponding to the transition between optically thick and optically thin synchrotron emission; spectral turnovers due to self absorption of extremely compact "flaring" components (Brown *et al.* 1989).

The predictions given in Table 1.1 do not include sources with strongly inverted spectra, peaking at mm wavelengths. These would either be missing from, or be strongly under-represented in low frequency surveys. The recent study of GHz Peaked Spectrum radio sources (GPS) by O'Dea and Baum (1997) has revealed a flat distribution of peak frequencies extending out to 15 GHz in the rest frame. This suggests the existence of an hitherto unknown population of sources with a spectral peak at high frequency (see also Lasenby 1996). It is very hard to guess how common such sources may be. Snellen (1997) exploited the sample of de Vries *et al.* (1997) to estimate a count of $(22 \pm 10)\,{\rm Jy}^{-3/2}\,{\rm sr}^{-1}$ for sources having peak frequencies between 1 and 8 GHz and peak flux densities between 2 and 6 Jy. He also found that counts of GPS sources are only slowly decreasing with increasing peak frequency in that range. If indeed the distribution of peak frequencies extends smoothly up to several tens of GHz, it is conceivable that scores to hundreds of GPS sources will be detected by Planck/LFI. Thus, although these rare sources will not be a threat for studies of CMB anisotropies, we may expect that the LFI channels will provide crucial information about their properties. GPS sources are important because they may be the youngest stages of radio source evolution (Fanti *et al.* 1995; Readhead *et al.* 1996) and may thus provide insight into the genesis and evolution of radio sources; alternatively, they may be sources which are kept very compact by unusual conditions (high density and/or turbulence) in the interstellar medium of the host galaxy (van Breugel *et al.* 1984).

Planck/LFI may also allow the study of another very interesting class of radio sources, characterized by advection-dominated emission. These have an inverted spectrum with spectral index $\alpha \sim -0.4$ up to a frequency of 100–200 GHz, followed by fast convergence (Narayan & Yi 1995; Fabian & Rees 1995; Di Matteo & Fabian 1997). Based on the analysis by Franceschini *et al.* (1997b), we would expect a few

tens of sources of this kind to be detected by Planck/LFI.

1.3.3 Clusters of galaxies

The Sunyaev-Zel'dovich (1970; hereafter SZ) effect is the result of the Compton scattering of the CMB radiation by non-relativistic electron gas, either in the intergalactic space proper, or within clusters of galaxies (see Rephaeli 1995 for a recent review). This "thermal" effect, arising from the thermal motions of the electrons, results in a systematic shift of photons from the Rayleigh-Jeans to the Wien side of the spectrum. With respect to the incident radiation field, the change of the CMB intensity across a cluster can be viewed as a net flux emanating from the cluster. The flux is negative below the crossover frequency, $\nu_0 = 217\,\mathrm{GHz}$, and positive above this characteristic frequency.

While the main emphasis so far has been on the measurement of the SZ effect in individual clusters, the ability to observe a large number of clusters in a satellite survey at millimetric wavelengths enhances interest in cluster number counts using the SZ signal. A full calculation of the SZ counts, and hence of the expected CMB anisotropy introduced by clusters, must include: a cosmological model, which defines the cosmic volume, V, dependence on redshift; a model for structure formation (*i.e.* a properly normalized power spectrum of matter density fluctuations), which defines the cluster mass function, $N(M,z)$; a self-consistent modeling of intracluster gas properties (e.g. amount and spatial distribution) as a function of the cluster total mass and cosmological epoch, which determines the cluster flux. Thus, the predicted number counts are:

$$N(>\overline{\Delta F_\nu}) = \int \frac{dV}{dz} dz \int_{\overline{M}} dM N(M,z)\,, \tag{1.3}$$

The lower bound of the inner integral is the mass of a cluster whose SZ flux (averaged over the receiver pass-band and measured by an antenna of given angular resolution) is $\overline{\Delta F_\nu}$.

Because of its angular resolution and sensitivity, Planck will observe a large number of clusters at millimetric wavelengths. While the model dependence of the number and amplitude of cluster SZ signals makes predictions of the cluster foreground contamination difficult, Planck observations provide a splendid opportunity to get information on the intracluster medium complementary to the X-ray observations. In fact, the SZ surface brightness is proportional to n_e, while the X-ray surface brightness is proportional to n_e^2. Thus, SZ measurements are much better suited than X-ray observations to probe the less dense regions, further away from the cluster core.

The comparison of SZ and X-ray measurements will yield an independent measure of the Hubble constant (Cavaliere, Danese, de Zotti, 1977, 1979; Gunn 1978; Birkinshaw *et al.* 1994; Myers *et al.* 1997). On the other hand, if we make use of the cosmological parameter estimation derived from the C_ℓ's, Planck detection of several hundred individual clusters will certainly result in an enhanced knowledge of the population of clusters and of the properties of their hot gas.

1.4 The Planck concept and the LFI

A definitive CMB anisotropy measurement requires both extremely good sensitivity and rejection of systematic effects. The design of the experiment is driven by these two requirements. The detectors are cooled to low temperatures to achieve the best possible sensitivity. Avoidance and removal of systematic effects influence every aspect of the mission. An observation scheme that controls and tests systematic effects is imperative. Each pixel on the sky will be measured repeatedly by several different detectors at each of several frequencies on many different time scales. This process allows full characterization and subtraction of any instrumental offsets and drifts and provides for separation of astrophysical foregrounds.

1.4.1 Sky coverage and orbit

The baseline mission allows for 15 months of routine scientific operations, which begin 3–4 months after launch. The entire sky can be imaged twice in this period. However, in anticipation of a possible extension

TABLE 1.2

POTENTIAL INSTRUMENT SUMMARY

Characteristic	LFI				HFI					
Detector technology	HEMT arrays				Bolometer arrays					
Detector temperature	20 K				0.1–0.15 K					
Center frequency [GHz]	30	44	70	100	100	143	217	353	545	857
Number of detectors	4	6	12	34	4	12	12	6	6	6
Angular resolution, FWHM [′]	33	23	14	10	10.7	8.0	5.5	5.5	5.5	5.5
Bandwidth $[\Delta\nu/\nu]$	0.20	0.20	0.20	0.20	0.25	0.25	0.25	0.25	0.25	0.25
$10^6\Delta T/T$	1.6	2.4	3.6	4.3	1.8	2.1	4.6	15	144	4630
Both polarisations	yes	yes	yes	yes	no	yes	yes	no	yes	no

of the mission, spacecraft and instrument consumables are designed to allow an extention of the nominal lifetime.

The nominal Planck mission uses a spinning spacecraft located near the Earth-Sun Lagrange point L_2, with the spin axis oriented in the anti-Sun direction and the boresight of a single telescope at approximately right angle to the spin axis. LFI and HFI share a common optical system and observing strategy. The LFI is based on indium phosphide, High Electron Mobility Transistor (HEMT) amplifiers, cooled to about 20 K. The individual beams of a shared focal plane array of LFI and HFI detectors sweep out nearly great circles passing close to the ecliptic poles. The spin axis is precessed in small steps to maintain the Sun-pointing aspect. The output of the detectors is sampled rapidly (more than 4 times per resolution element). Coadding observations builds up an image of the whole sky steadily over 6 months as the Earth and the spacecraft orbit the Sun. Since each circle is scanned many times in succession, instrumental drifts or offsets on timescales long compared to the spin period are easily removed. In the case of beams at exactly right angles to the spin axis, the north and south ecliptic pole regions tie any given great circle to all others; otherwise the circles are tied together at their crossing points.

In the current baseline design the angle α between the optical axis of the telescope and the spacecraft spin axis is 85°. The advantage of angles less than 90° is that scan circles intersect at many points on the sky, which seems to have some advantages for tying together the various scans and removing the effect of $1/f$ noise. Nevertheless, the LFI Consortium prefers an angle $\alpha = 90°$ with the spin axis on the ecliptic plane, for the following reasons:

- Thermal stability is greatest if the spin axis is always pointed in the anti-Sun direction. At present, without a detailed design for the spacecraft and the entire flight system, it is impossible to analyse the dynamic thermal effects of steering the spin axis around.

- The LFI array is about 6° across. Even if the optical axis is perpendicular to the spin axis a large number of intersections exists. Our simulations show that even with worst-case levels of $1/f$ noise, striping in the images can be efficiently removed.

- Flight operations are simpler if the spin axis is not steered around.

- Most importantly, the build-up of integration time at the poles is maximized for a 90° angle. For example, the noise level in the polar cap with a 90° angle will be more than a factor of two lower than in the polar "ring" obtained with an 85° angle. For detection of polarisation this factor could be crucial, and a 6° patch is large enough to determine the most important aspect of polarisation and a definitive test of inflation.

1.4.2 Control of systematic effects

Thermal and Enviromental Control – Thermal stability to quite high precision is necessary to reach the required scientific goals. The pointing strategy reduces the effects of solar radiation variation to a minimum. The geometry of the spacecraft is such that the payload will remain in the shadow of the sun-shade for angles between the spin-axis and the Sun-Earth-Planck directions up to 15°. The closer the spin-axis remains to the Sun-Planck direction, the smaller are any temperature variations induced by departure from perfect cyclindrical symmetry. Thermal control is such a critical issue that thermal design is the primary mission design driver. Thermal design aims at producing both low temperatures for sensitivity and thermal stability for reducing drifts. The payload has large radiating surfaces, thermal isolation, and active control elements specifically designed for keeping very stable and low temperatures for the detectors and ancillary components, such as the active electronics, power supplies and optics.

Stray Radiation Rejection – The reduction of variations in the solar radiation is also strongly linked to the requirement to control stray radiation from reaching the detectors. The stringent limits on stray radiation rejection (either directly or through diffraction and scattering) are the primary driver for the orbit selection. A relatively tight spacecraft orbit around L_2 puts the Sun, Earth, and Moon in a location where the Sun-shade blocks all of them from directly illuminating the instruments. A tight Lissajous orbit around L_2 can avoid eclipses and keep the telemetry and command antennas pointed away from the payload thereby minimizing the potential effects of RF interference.

Beam Patterns and Distortion – The knowledge of the beam pattern is essential both for control and calculation of the sidelobes and stray light rejection, and also for calibration of the data and reconstruction of the observations into maps and angular power spectra. Although the choice of a far-Earth orbit, such as L_2, greatly reduces the requirement on sidelobe rejection level, very stringent limits must be met. The total rejection of the Sun must be at the 10^{-9} level, at about the 10^{-7} level for the Earth, and at the $\sim 10^{-6}$ level for the Galactic plane. The spillover is controlled by under-illuminating the mirrors, and by employing a suitable optical design. The telescope size and design also determines the level of beam distortion for off-axis feeds. A major issue for LFI will be whether the beams are sufficiently symmetric that they yield the expected angular resolution (see Table 1.2) and can be properly co-added by the map-making algorithm. Since the Phase A study a new layout of the focal surface has been decided, which is now assumed as a baseline. For the new configuration, in which the LFI feeds are all $\sim 3°$ from the optical axis, the TICRA Phase A telescope does not have satisfactory off-axis performances for LFI. The signal observed by the receivers is defined by the optical response of the instrument, which is expressed mathematically as a convolution of the beam pattern over the microwave sky. A detailed analysis of the Phase A telescope with the new focal plane arrangement shows that the effective angular resolution that the LFI would achieve at 100 GHz is not the 10′ specified in the Phase A study, but rather between 13′ and 14′, depending on feed position, with significant distortions of the beam patterns that would not only reduce the effective angular resolution, but also complicate the combination of different beams and the data analysis considerably. Current mechanical-structural studies of the Planck payload have demonstrated the feasibility of accomodating a telescope with the sizes necessary to fully achieve the main scientific goals described in § 1.2.

1/f noise and striping – Drifts and offsets varying on time scales larger than the spin rate (1 min) can be efficiently removed and suppressed by using the spacecraft spin modulation. However, the effects of instrumental drifts on timescales less than the spin period cannot be completely suppressed by using the spacecraft spin modulation. If not fully removed these drifts will add excess noise that is correlated, thus producing artifacts in the data which would appear as striping in the reconstructed maps. The instrumental drifts are measured to have a $1/f$ spectrum, dominated by transistor gain fluctuations in the receivers. The LFI radiometer design (a pseudo-correlation receiver with a reference load at a temperature of 4 K) has been chosen specifically to minimize the effect of $1/f$ gain fluctuations. Nontheless, residual striping may be present, and we have studied algorithms to reduce their effect. By simulating LFI observations of CMB anisotropies including the white and $1/f$ noise typical of the LFI InP HEMTs (Seiffert *et al.* 1996; Gaier *et al.* 1996b), we have generated maps which include the striping effect. To reduce the effects of long term drifts we developed a destriping code based on the global minimizations of the differences between the temperatures measured at the same sky positions in different scan circles.

The efficiency of the destriping technique has been quantified by using estimators such as χ^2 or the rms temperature of the stripes, and by studying the impact of the $1/f$ noise on the CMB power spectrum reconstruction. We have considered different observational strategies, with angles $70° \leq \alpha \leq 90°$, with different repointing schemes (e.g., moving the spin axis always on the ecliptic plane or by allowing for oscillations over the ecliptic, neglecting thermal drifts), and for on-axis and off-axis beams. Although assuming spin axis oscillations and/or $\alpha < 90°$ yields somewhat better results, even for $\alpha = 90°$ and no oscillations, the residual noise degradation is at the few μK level for a single receiver.

Calibration – Proper reconstruction, inter-comparison and interpretation of the Planck maps requires accurate calibration, i.e. conversion of the signal strength from raw telemetry data into physical units. It is necessary to measure the calibration for each LFI detector accurately and frequently throughout the mission. The primary calibration of the LFI detectors will be based on observations of stable astronomical sources of known, adequate intensity wich naturally fall in the field of view of the LFI during the mission. The fundamental gain calibration source will be the CMB dipole. The amplitude of the dipole is known to 1%, and the LFI will be able to use it to obtain a calibration to that accuracy on a time base of a few hours. The CMB dipole is very good as a gain calibrator since it has exactly the spectrum of the desired cosmological signal and is sufficiently diffuse as not to depend on the detailed beam size and shape. A particularly accurate absolute calibration of the detected signal is achieved on long (> 6 months) time scales by using the $\approx 270\mu$K modulation of the CMB dipole due to the ~ 30 km s^{-1} motion of the satellite around the Sun. In this way it is possible to obtain an independent absolute calibration with accuracy $< 0.2\%$ (Bersanelli *et al.* 1997). Additional calibration will come from observing external planets. After correction for slowly varying seasonal effects, they provide a highly stable signal with adequate levels (0.1 to 100 mK in the LFI beams). The planet observations provide a check of the CMB dipole gain calibration procedures but are sensitive to the beam and so provide a means to measure the beam size and shape in substantial detail.

1.5 LFI Scientific Capabilities

As briefly outlined in § 1.4, each of the Planck detector observes (almost) the same great circle on the sky, for two hours between each 5′ step. This great circle will be sampled, at a given frequency, more than four times per resolution element. So, the very first result of the Planck observations will be time ordered data (TOD): each receiver will measure n temperature values $y_1, ..., y_n$. At 100 GHz, where the FWHM is 10′, we have $n = 8640$ (the points observed in one minute) $\times 120$ (the number of minutes spent on the same great circle) $\times 4320$ (the number of spin axis different pointings in one year). Averaging the data every two hours (*i.e.* for each great circle) still yields $n \gtrsim 10^7$ at the Planck/LFI frequencies.

Generating a full sky map requires the evaluation of m pixel temperatures, $x_1, ...x_m$. For Planck/LFI $m = 168,000$ and $1.512 \cdot 10^6$ at 30 and 100 GHz, respectively, if the pixel sizes equal the beam width FWHM. So, passing from TOD to maps allows a data compression by roughly a factor of 50 (20) at 30 (100) GHz. As the main science goal of Planck is to estimate cosmological parameters, it is important to apply map-making algorithms that are lossless: the same information in principle obtainable directly from the TOD has to be obtained also from the maps. It is reasonable to assume that the TOD depends linearly on the map: $\vec{y} = A\vec{x} + \vec{B}$, where the $n \times m$ matrix A_{ij} allows a correspondence between the direction observed at time t_i and the pixel j of the map, and $\vec{B}$ is the instrumental noise. Making a map implies inverting the previous relation to find $\vec{x}$, the best estimate of $\vec{x}$, such that $\vec{x} = W\vec{y}$. Different map-making algorithms, corresponding to different choices for W have been recently discussed by Tegmark(1997), showing that both the COBE method (Method 3 in his Table 1) and assorted variants of Wiener filtering are optimal in the sense that they are lossless, even in the case of non gaussian CMB fluctuations. Wright *et al.* (1996) and Wright (1996) have shown that the COBE method allows one to make maps even when millions of pixels are involved, as in the Planck case. Moreover, this method is independent of cosmological model assumptions. So the map making problem appears to be completely under control, since both optimal and feasible algorithms are already available.

1.5.1 Distribution and Amplitude of Foreground Fluctuations

The Planck maps obtained in this way at different frequencies contain CMB fluctuations as well as fluctuations due to foregrounds and instrumental noise. In order to separate the foregrounds from primordial CMB anisotropies, one can take advantage of their different frequency dependence and angular morphology; discrete sources can in principle be distinguished also on the basis of their quite different angular size. Unfortunately, there is currently no emission component for which both angular distribution and frequency dependence are well determined (Kogut 1996 and references therein). An important question in the present context is: "What is the level of angular fluctuations introduced by foregrounds in the Planck maps?". Or, "What is the angular power spectrum of the foregrounds, particularly at intermediate and high galactic latitudes?".

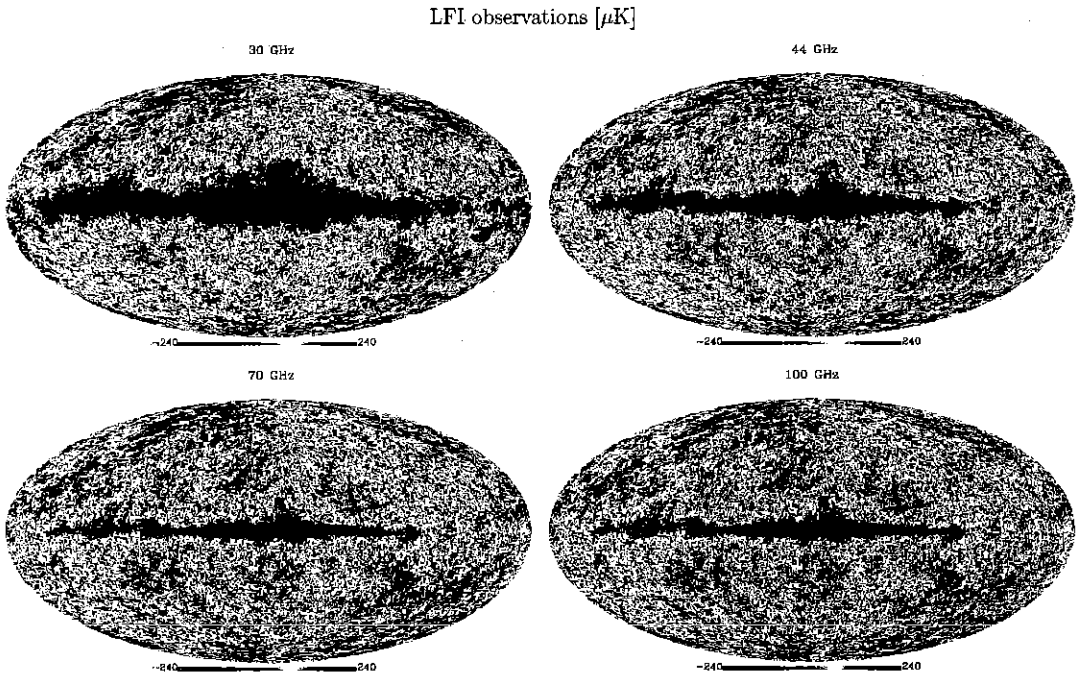

Figure 1.7: Simulation of LFI full sky observations. Each map contains the contribution of synchrotron radiation, dust and free-free emission, and CMB primordial fluctuations (without the dipole). Synchrotron radiation is extrapolated from 408 MHz observations (Haslam *et al.* 1982) assuming a spectral index varying as ν^{-3}, the dust contribution is obtained from DIRBE/IRAS merged maps at 100 μm (Schlegel *et al.* 1997) assuming a temperature $T = 20\,\mathrm{K}$ and an emissivity $\propto \nu^{1.5}$, whereas the free-free emission is assumed to have the same spatial template as dust with a brightness temperature spectral index of 2.15 ($T_{\mathrm{br}} \propto \nu^{-2.15}$). The CMB fluctuations are obtained for a standard COBE-normalized CDM model. The indicated temperatures are fluctuations around an average computed out of the Galactic plane ($b > 30°$).

Galactic synchrotron emission

Maps of the Galactic synchrotron emission can be obtained, and its spectral index can be readily determined, at frequencies ≤ 1 GHz where the observational baselevel uncertainty is much less than the signal. The well-known survey by Haslam *et al.* (1982) at 408 MHz is the only all-sky map available. Large-area surveys with careful attention to baselines and calibration have also been made at 1420 MHz (Reich & Reich 1986) and most recently at 2326 MHz (Jonas, Baart & Nicolson 1998).

The mean temperature brightness spectral index between 38 and 1420 MHz is $\beta \simeq 2.7$ with variations of at least 0.3 (Lawson *et al.* 1987). The de-striped 408 and 1420 MHz maps gave temperature spectral indices of 2.8 to 3.2 in the northern galactic pole regions (Davies, Watson, Gutierrez 1996).

Evidences of a mean spectral index $\beta \simeq 3$ at higher frequencies have been reported by Melhuish *et al.* (1997), Hancock *et al.* (1997), and Platania *et al.* (1997). The analysis of COBE/DMR maps by Kogut *et al.* (1996) has found no significant correlations with Haslam *et al.* (1982) 408 MHz maps, indicating that measurements of large angular scale anisotropy at COBE/DMR frequencies (which are close to Planck/LFI frequencies) are weakly affected by fluctuations of the Galactic synchrotron emission.

As for the angular distribution, Lasenby (1996) has used the 408 and 1420 MHz surveys to estimate the angular power spectrum of the high latitude region surveyed in the Tenerife experiments and found it to be of rather low amplitude and with an angular spectral index $\gamma \lesssim 2$ ($C_\ell \propto \ell^{-\gamma}$) for $\ell \leq 300$. A steeper mean power spectrum ($\propto \ell^{-3}$) was estimated by Tegmark & Efstathiou (1996). This indicates that the contamination by Galactic synchrotron emission will not get any worse, compared to the CMB anisotropy levels, for higher resolution measurements. In any case, the high (30–50%) polarisation of the Galactic synchrotron emission at the LFI frequencies will greatly help in identifying this emission component.

It thus appears (see Fig. 1.8) that a very detailed modelling of the Galactic synchrotron emission in the Planck bands is not crucial for cosmological studies.

Galactic free-free emission

For free-free emission the problem is opposite to that of synchrotron: the spectral behaviour is well determined but the spatial distribution is poorly mapped at high Galactic latitudes. We must therefore rely on tracers of the ionized interstellar medium. Most of the available information at intermediate and high latitudes comes from Hα surveys. The distribution of Hα regions may be modelled (Reynolds 1992) as a layer parallel to the Galactic plane with a half-thickness intensity of 1.2 Rayleigh (R)[1]. The rms variation in this Hα emission is about 0.6 R on degree scales. An analysis of the four-year COBE/DMR sky maps at different frequencies aimed at isolating emission with a free-free emission spectrum ($\beta = 2.15$) yielded results consistent with the Hα large scale model with a free-free half height amplitude of $10 \pm 4\,\mu$K and an rms free-free signal on a 7° scale of $\Delta T_{\rm ff} = 7 \pm 2\,\mu$K (Kogut 1996).

Kogut *et al.* (1996) have compared the COBE/DMR maps with the DIRBE maps and found a correlation between the free-free and dust emission. They concluded that, with their resolution of 7°, the angular spectral index is $\gamma = 3.0$, a well-determined value for dust and HI on degree scales. This was confirmed to some extent by de Oliveira-Costa *et al.* (1997) for the North Celestial Pole (NCP) region in a correlation of Saskatoon data with the IRAS & DIRBE map.

Leitch *et al.* (1997), looking near the NCP, found emission with an approximately $\beta = 2$ spectral index some 5-10 times higher than the free free level found for the NCP based upon an extrapolation in angular power spectra from Kogut *et al.* (1996) or from the Hα emission. Moreover their estimates are above those deduced from the Tenerife experiments. Their discussion, however, leaves out the possibility that they see flat-spectrum synchrotron associated with a supernova remnant.

The Hα images of the NCP area made by Gaustad *et al.* (1996) have been analyzed by Veeraraghavan & Davies (1997) to provide an estimate of the spatial power spectrum on scales of 10′ to a few degrees. After subtracting the geocoronal emission, they found a power law index of 2.3 ± 0.1 over this angular

[1] $1R \equiv 10^6/4\pi$ photons cm^{-2} sr^{-1} s^{-1} $= 2.42 \times 10^{-7}$ erg cm^{-2} sr^{-1} s^{-1} at a wavelength $\lambda_{H\alpha} = 6563$ Angstroms. In the context of the present discussion 1R will give a brightness temperature of about $10\,\mu$K at 45 GHz.

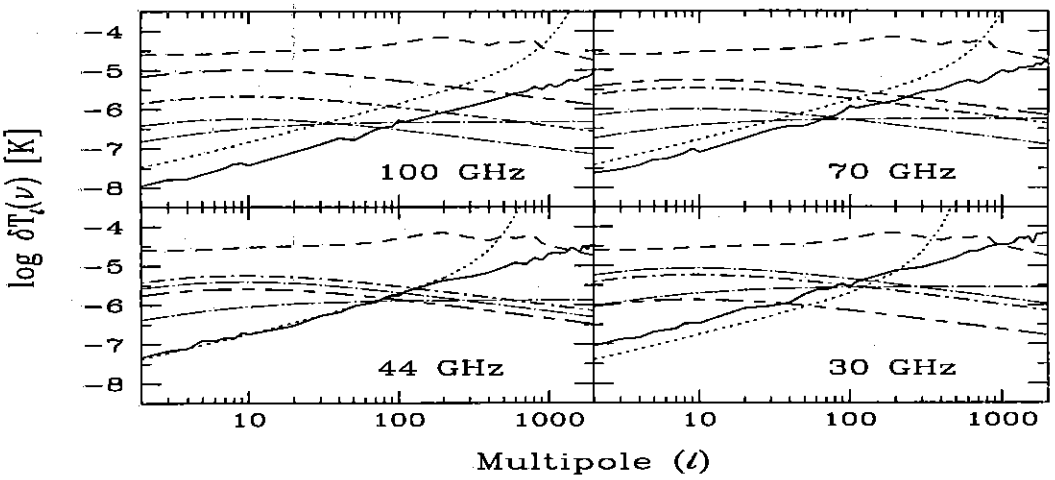

Figure 1.8: Angular power spectra of the different components contributing to fluctuations at the 4 LFI frequencies. The power spectrum of CMB fluctuations predicted by the standard CDM model ($\Omega = 1$, $H_0 = 50\,\mathrm{km\,s^{-1}\,Mpc^{-1}}$, $\Omega_b = 0.05$), shown by the heavy solid line, is compared with contributions from dust (long+short dashes), free-free (dots+short dashes), and synchrotron emission (dots+long dashes) in the Galaxy, at $|b| > 30°$, as well as with fluctuations due to extragalactic sources (roughly diagonal solid lines). For synchrotron emission we have plotted both the power spectrum adopted by Tegmark & Efstathiou (1996) and that observed in the Tenerife patch (Lasenby 1996). The latter is significantly lower than the former in the range of scales where it has been actually measured, but has flatter shape so that it becomes relatively more important on small angular scales. On the other hand, the power spectrum will fall off on scales smaller than the coherence length of emitting blobs; it is thus very likely that the Galactic contributions are overestimated at large ℓ-values. The couples of lines corresponding to extragalactic sources assume that sources brighter than 1 Jy (upper line) or 100 mJy can be subtracted out. The effect of source clustering is neglected The dotted lines show the unsmoothed noise contribution of the instruments.

range, with an rms amplitude much lower than expected from the extrapolation of Kogut *et al.* (1996) results on all angular scales, in spite of the significantly flatter power spectrum.

Thus, although Galactic free-free emission is, at the moment, the most difficult foreground to control and bright regions may be present even at high galactic latitudes, it appears to be generally weak and unlikely to be a major problem for the Planck/LFI experiment.

Galactic dust

At high Galactic latitudes dust emission is weak at the Planck/LFI frequencies so that it is difficult to determine its spectrum. Broadly speaking, it is expected to dominate the high latitude Galactic fluctuations above $\simeq$ 70–100 GHz and to sink down rapidly at lower frequencies (but see Draine & Lazarian 1997). Kogut (1996) reports an rms antenna temperature fluctuation on a 7° scale, due to dust, of $\Delta T_\mathrm{d} = 2.7 \pm 1.3\ \mu$K at 53 GHz, estimated by cross-correlating the COBE DMR 4-year maps with the DIRBE map at 140 μm for $|b| > 20°$. Emission at this level is well below the expected amplitude of primordial anisotropies of the CMB. However, individual patches may have dust emission significantly larger than the high galactic latitude average.

The analysis of dust contamination is further complicated by the highly non-Gaussian nature of its Galactic distribution. The new Berkeley-Durham dust map (Schlegel *et al.* 1997) shows that its power spectrum is not well described by a global ℓ^{-3} power law everywhere at high Galactic latitude, as has

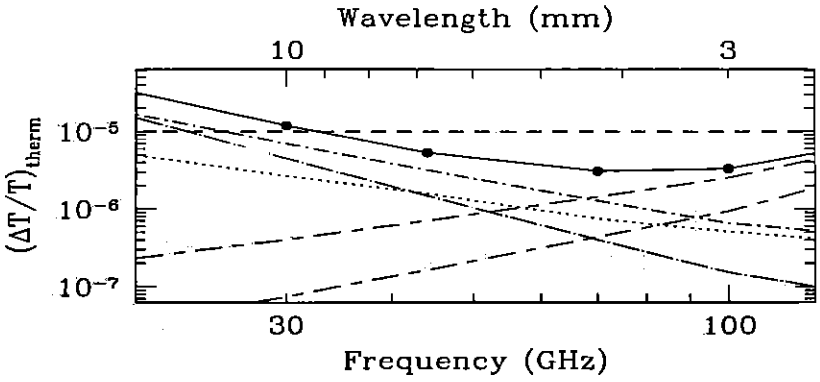

Figure 1.9: Temperature fluctuations as a function of frequency for an angular scale of 30′. The horizontal dashed line shows the expected level of primordial CMB anisotropies. Average contributions from Galactic free-free, synchrotron and dust emissions at $|b| > 30°$ are represented by dots+short dashes, dots+long dashes, and long+short dashes, respectively; the lower long/short dashed curve gives a lower limit to fluctuations of the Galactic dust emission. The dotted line represents fluctuations from discrete extragalactic sources fainter than 100 mJy. The same models as in the previous figure have been adopted. The solid line shows the quadratic sum of contributions from all foreground components; the filled circles on it mark the Planck/LFI frequencies.

been claimed; in some high galactic latitude patches the power spectra are closer to $\ell^{-2.5}$, but with amplitudes differing from patch to patch.

Of course, dust contamination in the LFI maps would be easy to identify using the HFI channels.

Extragalactic sources

A Poisson distribution of sources over the whole sky would produce a simple white-noise power spectrum, with the same power in all multipoles, so that it becomes the dominant contaminant on small scales. Clustering would add some power on larger scales; however, its contribution is found to be generally small in comparison with the Poisson term (Toffolatti *et al.* 1997).

A detailed analysis has been recently carried out by Toffolatti *et al.* (1997); the main results of interest here are summarized in Figs. 1.8 and 1.9. Predictions are based on extrapolations to high frequencies of evolutionary models, which fit the observed counts of radio sources up to 8.44 GHz. As such counts are actually much deeper than those achievable with Planck, the critical ingredient for the extrapolation in not the evolution model but rather the assumptions on the high frequency spectral behaviour of these sources. The estimates shown are based on the assumption of flat ($\alpha = 0$) spectra for compact radio sources up to 200 GHz; since a good fraction of them do show spectral breaks at tens of GHz, the contribution of radio sources to fluctuations may be, if anything, somewhat overestimated.

1.5.2 Foreground versus CMB Power Spectra

Fig. 1.8 shows that, over a large portion of the sky ($\simeq 50\%$) foreground fluctuations for any angular scale $\geq 10'$ (or for any multipole $\ell \leq 1000$) are well below the CMB anisotropies predicted by the standard CDM model, at least in the 70 and 100 GHz channels, even under the most conservative assumptions. The best Planck frequency for measuring the angular power spectrum of the CMB at moderate to large angular scales ($\ell \lesssim 200$) is 70 GHz, the closest to the frequency (60 GHz) of minimum Galactic foreground fluctuations (see Fig. 1.9). The optimal frequency increases for smaller angular scales, where extragalactic sources dominate foreground fluctuations; its exact value depends on the uncertain mm counts of galaxies. Taking into account the recent evidences of very strong evolution at far-IR and mm wavelengths both

from counts (Kawara *et al.* 1997; Smail *et al.* 1997) and from the background intensity (Puget *et al.* 1996; Schlegel *et al.* 1997; Hauser *et al.* 1998) a value between 100 and 200 GHz is indicated.

Clearly, the LFI will have no problem in reaching a good accuracy on the CMB power spectrum even without making any foreground subtraction (except for the very brightest extragalactic sources).

In order to quantify this point, we use simulations of the sky that the LFI will produce at 100 GHz. This map is obtained by summing the Galactic emission, extragalactic sources, standard CDM anisotropy and instrumental noise. The Galactic emission is modeled after Burigana *et al.* (1997). As expected, the recovered angular power spectrum of the "total" map at 100 GHz is dominated by the CDM angular power spectrum (see Fig. 1.10). The fractional error in the reconstructed C_ℓ's is shown in the same Figure. Consistently with Fig. 1.8, the Galaxy mostly contributes to these uncertainties at $\ell \lesssim 100$, while radio sources step in at much smaller angular scales. Note that a subtraction of the expected instrumental noise level allows us to reach a precision better than $\sim 2\%$ for $100 \lesssim \ell \lesssim 1000$, if extragalactic radio sources with fluxes larger than 350 mJy can be removed. Sources brighter than 350 mJy will be detected at more than 5σ level by Planck/LFI 100 GHz detectors (Toffolatti *et al.* 1997). Fainter sources may be identified and subtracted by means of higher resolution surveys.

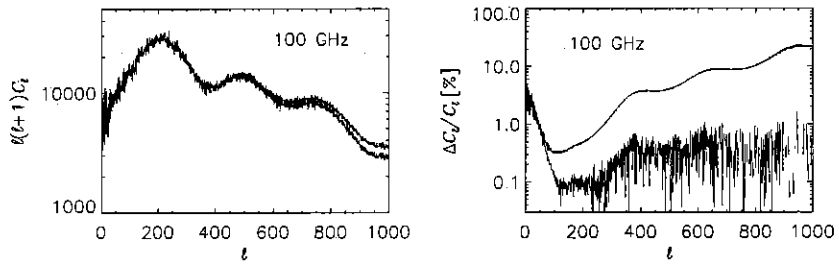

Figure 1.10: Reconstructed angular power spectrum from a simulation of the 100 GHz Planck/LFI map (*left panel*), without subtracting (green line) and subtracting (blue line) the expected instrumental noise. Such a subtraction allows one to reach a precision $\simeq 1\%$ for $100 \lesssim \ell \lesssim 1000$, if extragalactic radio sources with fluxes larger than 350 mJy can be removed.

Although a very detailed modeling of the foreground signals may not be crucial for cosmological studies at the LFI frequencies, preparatory work is underway to improve substantially our understanding of both the angular and frequency behaviour of the foreground emissions. In any case, the multifrequency Planck observations will allow efficient removal of foreground contamination. This will be valuable not just for CMB studies, but also for studying the complex and interesting astrophysical foregrounds.

1.5.3 Methods for Foreground Separation

Tegmark & Efstathiou (1996) have derived a foreground subtraction method that minimizes the residual variance from foregrounds and noise under the assumption that the frequency dependence of all components is perfectly known and independent of position. Their method has been shown to be lossless if the foregrounds are gaussian and if the subtraction is performed mode by mode [working in real space (*i.e.* pixel by pixel) tends to destroy information by not taking advantage of correlations between neighboring pixels]. These methods have been extensively tested with simulations (Bouchet *et al.* 1995, Bersanelli *et al.* 1996) where each frequency channel was the appropriate linear combination of a simulated CMB map, foreground templates such as the Haslam *et al.* (1982), DIRBE 240μm and IRAS 100μm maps, radio sources and random noise. Tegmark (1997) generalized the method to the case where the foreground spectral index depends on the observing direction.

The observed antenna temperature in a given pixel can be written as a vector $\vec{T} \equiv \{T_1, ..., T_{N_{ch}}\}$ whose components are the antenna temperature, T_i, observed in the i-th channel ($i = 1, N_{ch}$). Moreover, $T_i = \sum_{j=0}^{N_{fg}} K_i^j + N_i$, where K_i^j is the antenna temperature due to the CMB ($j = 0$) and to the j-th

foreground ($j \geq 1$) as seen in the i-th, while N_i is the instrumental noise. It is often possible to decompose K_i^j in terms of a spectral dependence S_i^j and a template dependence T^j, *i.e.* $K_i^j = S_i^j t^j$. This is trivial if the assumed foreground spectral index does not depend on the position, but one can easily generalize the method when the latter dependence is weak. If the CMB template T_i^0 is given in thermodynamic temperature, one gets the familiar expression $S_i^0 = x_i^2 e^{x_i}/(e^{x_i}-1)^2$, with $x_i = h\nu_i/KT_{CMB}$, ν_i being the central frequency of the i-th channel. Observations in a given direction can be further arranged as follows:

$$\vec{T} = P\vec{t} + \vec{N}, \tag{1.4}$$

where the matrix $P_{ij} = \int_0^\infty d\nu\ \tau_i(\nu) S_i^j(\nu)$ is introduced to take into account the channels spectral transmission function $\tau_i(\nu)$. It is worth stressing that the template vector $\vec{t}$ has a number of components equal to the number of foregrounds plus one (for CMB); P is not necessarily a square matrix. We must also consider the angular response of the instrument: working in Fourier (or in ℓ-) space, where convolutions reduce to products, allows us to write a similar expression

$$\vec{T}_\ell = A\vec{t}_\ell + \vec{n}_\ell \tag{1.5}$$

where $A_{ij} = P_{ij}\ w_i(\ell)$, w_i being the angular response of the i-th channel.

At this point we face again an "inversion problem", since we want to find $\tilde{t}^j$, the best estimate of t^j: $\tilde{t}_\ell = W\vec{T}_\ell$. The "Wiener matrix" W is obtained by demanding that the difference between the initial and recovered processes is of minimal variance (Tegmark & Efstathiou 1996, Bouchet *et al.* 1996). This leads to an "optimal linear recovery", with the input data weighted according to a generalization of the usual signal-to-noise ratios in Fourier space. This method enables us to recover the angular power spectrum of CMB anisotropies (*i.e.* the C_ℓ's) to better than 1% for $\ell \lesssim 1000$. Although this was done assuming negligible errors in the assumed spectral behavior of the foregrounds, it must be stressed that relatively large errors on the synchrotron and free-free contributions have very low impact on the final CMB accuracy.

The variance of the estimator based on Wiener filtering can be written as (Bouchet *et al.* 1995)

$$\varepsilon_i^2(\ell) = C_i(\ell)\,[1 - Q_i(\ell)]\,. \tag{1.6}$$

The quantity $1 - Q_i(\ell)$ yields the expected $\Delta C(\ell)/C(\ell)$ of the process j, and $Q_i(\ell)$ may be used as a "quality factor" which evaluates the ability of a given experiment to recover process i at scale ℓ. This indicator (Bouchet *et al.* 1996) generalizes the real space "Foreground Degradation Factor". When the number of channels equals or exceed the number of components (as for Planck) complete foreground removal is possible. The Foreground Degradation Factor, introduced by Dodelson (1995), describes how much we loose in sensitivity because of the foreground fitting procedure, under the assumption that the foreground spectra are completely known: it was introduced in the context of a simple analytical model which, by the way, reproduces the Monte Carlo results of Brandt *et al.* (1994) very accurately.

1.5.4 Extracting Cosmological Parameters from the C_ℓ's

The fundamental cosmological parameters can be extracted from the angular power spectrum directly and this can be understood in a straightforward way.

As discussed in § 1.1, the detailed shape of the angular power spectrum of the CMB anisotropy is determined by a number of parameters, that can be considered as components of a vector

$$\vec{s} \equiv \left(\Omega_0, \Omega_b, \Omega_\Lambda, \Omega_\nu, h, A, n, r, n_t, \tau, ...\right) \tag{1.7}$$

Here Ω is the contribution to the critical density in various species (total matter, baryons, vacuum, and massive neutrinos), A and n are the amplitude and slope of the primordial power spectrum of scalar fluctuations, $r = C_2^{(T)}/C_2^{(S)}$ is the ratio of tensor to scalar contributions to the quadrupole anisotropy (primordial tensor fluctuations having a spectral index n_t) and τ is the Thomson optical depth back to the redshift at which the Universe reionized.

TABLE 1.3

UNCERTAINTIES IN EXTRACTED COSMOLOGICAL PARAMETERS

		Planck	
	MAP	LFI	HFI
$\delta h/h$	0.11	0.06	0.02
$\delta\Omega_0 h^2/h_0^2$	0.10	0.04	0.02
$\delta\Omega_\Lambda h^2/h_0^2$	0.28	0.14	0.05
$\delta\Omega_b h^2/h_0^2$	0.05	0.016	0.006
$\delta\Omega_\nu h^2/h_0^2$	0.05	0.04	0.02
δn	0.04	0.01	0.006
δr	0.24	0.13	0.09
$\delta\tau$	0.19	0.18	0.16

The standard method for extracting cosmological parameters from the CMB is the Maximum Likelihood method. The Likelihood of a data set $\{x_i\}$ is expressed as

$$L \propto |C|^{-1} \exp\left[-\frac{1}{2} x_i C_{ij}^{-1} x_j\right], \tag{1.8}$$

where C_{ij} is the data covariance matrix, which depends on $\vec{s}$ and thus contains the theoretical hypothesis one wants to test. If the maximum likelihood solution for the parameter set is $\vec{s} = \vec{s}_0$, L can be expanded to quadratic order about its maximum providing

$$L \propto L_{max} \exp\left[-\frac{1}{2} \delta s_i F_{ij} \delta s_j\right], \tag{1.9}$$

where $\delta s_i = (s_i - s_i^0)$. As discussed in e.g. Tegmark, Taylor and Heavens (1997) the best possible unbiased estimates of the theoretical parameters have a covariance matrix that is well approximated by $F^{-1} \equiv \langle \delta s_i \delta s_j \rangle$, where F is the Fisher information matrix. If all the parameters except s_i are known, the data set contains enough information to determine s_i with error bar $\Delta s_i = 1/F_{ii}$, whereas if we need to determine all parameters jointly, we obtain $\Delta s_i = (F^{-1})_{ii}$. It is in this sense that F is a measure of how much information the data contains about the parameters, and loosely speaking, the larger F the better.

In the present case the data are the a_{lm} coefficients, which are gaussian distributed with zero mean and variance C_ℓ, and the Fisher matrix is given by (Bond, Efstathiou, Tegmark 1997)

$$F_{ij} = \sum_\ell \left(\ell + \frac{1}{2}\right) \left(\frac{1}{C_\ell + \bar{w}^{-1} \tilde{B}_\ell^{-2}}\right)^2 \frac{\partial C_\ell}{\partial s_i} \frac{\partial C_\ell}{\partial s_j} \tag{1.10}$$

where $\bar{w} = \sum_{i=1}^{N_{ch}} (\sigma_i \Delta\theta_i)^{-2}$ and $\tilde{B}_\ell = \bar{w}^{-1} \sum_{i=1}^{N_{ch}} e^{-\ell^2/\ell_{s,i}^2} (\sigma_i \Delta\theta_i)^{-2}$. Here $\Delta\theta_i$ is the FWHM angular resolution of the i-th channel, σ_i is the sensitivity per resolution element and $\ell_{s,i}$ charachterizes the beam window function in ℓ-space.

In Table 1.3 an example is shown of how well parameters could be determined, using the standard CDM model as input (adapted from Bond, Efstathiou & Tegmark 1997). This calculation does not address the systematics arising from inaccurate foreground subtraction. It is however assumed that over 65% of the sky the foregrounds are well below the cosmological signal.

1.6 Summary of the Scientific Case

With the precise maps of the CMB provided by Planck we will be able to address a number of key questions in cosmology, to an extraordinary level of accuracy. As well as providing the ability to extract definitive information about the Universe from CMB anisotropies and possibly polarisation, the LFI will produce all-sky surveys at 4 frequencies between 30 GHz and 100 GHz, covering an essentially unexplored spectral region where large area surveys cannot be made from the ground and where many astrophysically interesting phenomena emerge. The LFI maps will thus have a major impact also on many fields of astrophysics. A summary of some of these science highlights follows.

Parameter extraction is the grand goal of these CMB experiments. Current cosmological models contain of order 10 important parameters (including initial conditions, expansion rate, reionization history and various contributions to the matter density), and Planck's definitive measurement of the CMB angular power spectrum can provide most of these parameters at the few percent level. Moreover, sensitivity to polarisation allows a determination of the reionization epoch for *any* realistic assumption about when it occurs.

Inflation can be directly tested with CMB anisotropy data. If the angular power spectrum is of the form predicted by inflationary models (i.e. $n \simeq 1$), then that will be a strong confirmation of the general paradigm. Topological defect models (the contending idea for perturbation generation) generically give rise to quite distinct power spectra. Moreover, the possibility of detecting the odd-parity polarisation component produced by gravitational waves will provide an even cleaner test of inflation. Either way, precise measurements allow a direct investigation of the initial conditions, and hence a probe of particle physics at energies $\sim 10^{16}$GeV.

Polarisation is a very powerful tool for verifying our basic assumptions about the behaviour of fluctuations in the Universe: it probes the epoch of last scattering directly. This localization in time is a very powerful tool for reconstructing the sources of anisotropy. It provides a clean way of distinguishing the physical processes which determine the temperature angular power spectrum. It also breaks the degeneracies in the determination of cosmological parameters. Adequate sensitivities ($\sim 1\,\mu$K) to meet the challenge of CMB polarisation measurements can be reached by the LFI over areas of about 30 square degrees around each of the ecliptic poles. Radio source polarisation, which is the dominant contaminant on small scales, can be controlled and removed by means of suitable follow-up observations.

The Topology of the Universe is usually assumed to be simple, but it is possible that space is compactified with negative curvature, 'toroidal' and flat, or multiply-connected. The CMB contains information about the largest scales accessible to observation, and hence is the best arena in which to constrain such global properties (topology, rotation, shear, etc.).

Contamination by astrophysical foregrounds. Although we expect that Planck will provide sufficiently rich samples of sources for astrophysical studies, only a small fraction of high Galactic latitude pixels will be strongly contaminated by astrophysical foregrounds. Luckily enough, the crossover between the radio and dust emission components, determining a minimum in the spectral energy distribution of sources, is roughly coincident with the peak of the CMB intensity, making the mm region ideal for mapping primordial anisotropies. The Galactic emission reaches a minimum near 60 GHz. The confusion noise due to extragalactic sources is minimum in the range 100–200 GHz and increases steeply with frequency above $\sim$ 300 GHz due to the strong evolution of galaxies in the far-IR/sub-mm region, further boosted by the large and negative K-correction. Thus the LFI frequencies are optimal to minimize foreground fluctuations.

Inverted spectrum radio sources. The LFI surveys will be unique in providing complete samples of bright radio sources with inverted spectra, essentially undetectable in radio-frequency surveys. One example is the GHz Peaked Spectrum (GPS) sources, which may be the youngest stages of radio source evolution and may thus provide insight into the genesis of radio sources.

Physics of compact radiogalaxies. The LFI will provide spectral information for a relatively large, complete sample of "flat-"spectrum radio sources (compact radiogalaxies, radio loud QSOs, BL Lacs, blazars), covering a region where spectral features carrying essential information on physical conditions of sources show up (breaks due to energy losses of relativistic electrons, self-absorption turnovers of flaring components).

Study of the Galaxy. Planck will also provide a rich database for studies of the interstellar medium (distribution of the interstellar magnetic field, relativistic electrons, hot gas, and dust), and discrete Galactic sources, including supernova remnants, Sagittarius A and, again, sources self absorbed up to high frequencies like some symbiotic stars and planetary nebulae.
Sunyaev-Zel'dovich effects in several hundreds clusters of galaxies will be detected.
Synergies between LFI and HFI. The sharp rise of dust emission spectra with increasing frequency (typically $S_\nu \propto \nu^{3.5}$) causes a drastic change in the composition of Planck detections above and below $\simeq 1$ mm. The source counts in Planck/LFI channels will consist essentially of radio sources, while at high frequencies the dominant population will be evolving dusty galaxies, detectable up to substantial redshifts. LFI and HFI will deal with different astrophysical processes which coexist in real sources; the broad spectral coverage is thus invaluable for a thorough understanding of their physics. For example, large mm/sub-mm fluxes attributed to dust emissions have been reported for several distant radio galaxies, implying that dust masses are 1–2 orders of magnitude higher than found for nearby radio galaxies. The combination of LFI and HFI data will then be essential to elucidate physical and evolutionary connections between nuclear activity and processes governing the abundance and the properties of the interstellar material. Also, tests for unified models can be performed by comparing data on isotropically emitted radiations (such as thermal emission by dust) which are least affected by obscuration with possibly anisotropic components (e.g. radio core luminosities).

Chapter 2

Technical Description

2.1 Introduction & Overview

The Planck Low Frequency Instrument will have the sensitivity to measure CMB anisotropies in the frequency range 30–100 GHz to the fundamental accuracy limits imposed by cosmic variance and by astrophysical foregrounds. It uses state-of-the-art, cryogenic, coherent receivers based on ultra-low-noise indium phosphide (InP) high-electron-mobility transistors (HEMTs), taking full advantage of the dramatic advances in this technology over the last few years.

Both the LFI and the HFI *alone* would be major steps beyond any other CMB experiments achieved or being planned. Together, they give Planck unprecedented sensitivity and angular resolution over the full spectral range 30–900 GHz, ensuring the imaging power, the redundancy, and the control of systematic effects and of foreground emissions needed to achieve the mission science goal.

The LFI represents the third generation millimeterwave instrument designed for space observations of CMB anisotropies, following the COBE Differential Microwave Radiometer and the Microwave Anisotropy Probe (MAP). The DMR, launched in 1989, detected structure in the CMB angular distribution at angular scales $> 7°$ with two Dicke-switched radiometers at each of three frequencies, 31, 53, and 90 GHz, with noise temperatures of 250, 80, and 60 times the quantum limit, respectively, fed by pairs of feed horns pointed at the sky. MAP, scheduled for launch in 2000, will observe the whole sky at 20, 30, 45, 60, and 90 GHz with small arrays of radiatively-cooled radiometers fed by a differential two-telescope optical system, with radiometer noise temperatures at the five frequencies of 15–25 times the quantum limit, and angular resolution of 56′, 41′, 28′, 21′, and 12.6, respectively. The LFI, with its large arrays of cryogenically cooled radiometers, represents another significant advance in the state of the art.

The LFI design proposed here differs in three important respects from that developed during the COBRAS/SAMBA Phase A Study. These changes result in increased performance and reliability for the Planck payload and easier integration with the HFI.

- InP, rather than gallium arsenide (GaAs) HEMTs are used.
- The radiometers are split into two subassemblies connected by waveguides (100 and 70 GHz) and coaxial cables (44 and 30 GHz), one located at the telescope focus, the other on the Equipment Platform.

Taken together, these two changes result in a decrease in the power dissipated by the LFI in the focal assembly from 6 W in the Phase A design to <0.6 W in the new design, along with significantly better noise performance, particularly at high frequencies. The large power dissipation of the LFI focal assembly in the Phase A design was the principal driver of the COBRAS/SAMBA thermal design; the large reduction in the new design enables the third important change:

- The LFI focal assembly is cooled to 20 K with a vibrationless hydrogen sorption cooler, which also provides 18 K precooling to the HFI helium J-T cooler. Because the sorption cooler is necessary to both LFI and HFI, a redundant cooler is included in the flight hardware as a backup.

This allows radiative cooling of the Planck telescope, optical bench, and related structures to a temperature of 60 K or less (end of life), as well as elimination of the 50–80 K and 20 K Stirling coolers used by the HFI in the Phase A design. Integration of the sorption cooler with the instruments is much easier than integration of the Stirling coolers, because the only part of the cooler in the focal assembly is the J-T valve and associated small inflow and outflow tubing, with the compressor and control electronics located remotely on the Equipment Platform. Also, since the cooler is vibrationless, it eliminates a substantial concern with the Stirling coolers. Rough equality of the mass and power resources

consumed by the Stirling coolers and the sorption coolers means that there is essentially no change in the spacecraft resources required. These advantages are obtained whether Planck flies separately or merged with FIRST.

2.1.1 Physical configuration, functional description, and thermal design

As shown schematically in Figure 2.1, the LFI consists of four main units: the Front End Unit (FEU); the Back End Unit (BEU); the Radiometer Electronics Box Assembly (REBA); and the Sorption Cooler System (SCS). The FEU is located at the focus of the telescope, as one component of the joint LFI/HFI focal assembly. The BEU is mounted on the equipment platform, and the REBA and the warm parts of the SCS can be located either on one of the lateral panels of the service module or on the equipment platform. As described in Chapter 5, the FEU and BEU and all of their interconnections will be assembled in a self-supporting Radiometer Array Assembly (RAA). All four units are linked together by the LFI harness, which also connects to the spacecraft interface. The FEU and the Sorption Cooler Compressor (SCC) are connected by concentric stainless steel tubes of OD 6.35 mm and 3.18 mm. The smaller tube carries hydrogen at ~60 atmospheres (TBR) from the cooler compressors to the FEU, while the larger tube returns the hydrogen at ~0.3 atmospheres (TBR). These units are described in detail in following sections.

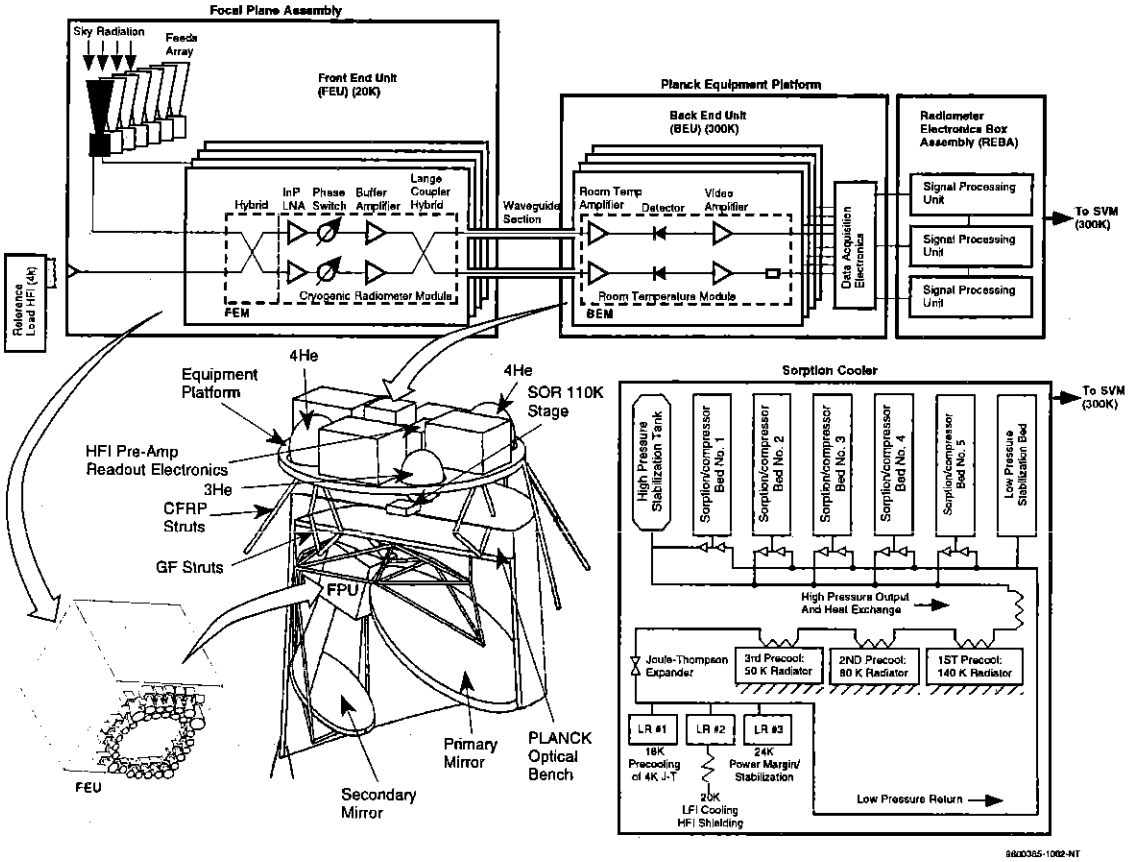

Figure 2.1: Block diagram of the LFI.

The FEU contains the feed array and associated polarizers, hybrid couplers, amplifiers, and phase switches, all cooled to 20 K by the sorption cooler. It also contains the Joule-Thomson expansion valve for the cooler. Reference loads are mounted on the HFI Front End Unit, where they have a temperature

of 4 K. The loads are coupled radiatively, with no mechanical contact allowed. The extra radiative load on the HFI 4 K cooler due to the addition of the 4 K reference loads for the LFI is less than 0.1 mW, easily below the allowed value of 1 mW. The thermal design has been worked out in close cooperation with the HFI team, and is based on three principles:

- Minimize the power dissipated in the focal assembly
- Maximize the effectiveness of radiative cooling by providing good views of cold space, and by intercepting conductive heat loads and radiating them away.
- Segregate the warm and cold components, and keep them as far from each other as possible.

2.1.2 Radiometer design and systematics

To meet the challenging performance goals of the LFI requires not only great sensitivity and angular resolution, but also stringent control of systematic errors. Table 1.2 gives the average values over the sky of the noise per resolution element that the LFI and HFI are expected to achieve. These are unprecedentedly low. But because of the way Planck scans the sky, with integration time concentrated toward the ecliptic poles, the raw instrumental noise near the poles will be lower still by a factor of 3–5. Almost certainly near the poles the true sensitivity of both the LFI and the HFI will be determined not by raw instrumental sensitivity, but rather by systematics.

There are many possible sources of systematic error, including Galactic and extragalactic foregrounds, sidelobe pickup of the Galaxy, Sun, Earth, and Moon, distorted beam shapes, beam smearing due to the spacecraft spin, temperature variations of the telescope and instruments, non-white noise in the instruments, spacecraft pointing errors and nutation, the effect of changing magnetic fields on sensitive components, as well as problems such as ground loops, EMC, and EMI that can be evaluated before launch. Many of these sources of error have been studied in some detail by the Planck instrument teams, with the goal of understanding the magnitude of the error and estimating to what extent it can be removed. The results are extremely encouraging. No insuperable obstacles to the achievement of spectacular sensitivity by Planck have been found.

Nevertheless, caution is required. The effects have been studied one at a time, and removing them if they are large is often extremely demanding computationally. Moreover, no realistic simulations have been done of the effects in combination (e.g., removing the effects of Galactic foregrounds observed with distorted beams smeared by spacecraft motion, with contamination from far sidelobes). Even if the instruments were "perfect", the analysis of Planck data would be a huge effort. Every instrumental effect added to the mixture increases the magnitude of that task, and increases the risk of residual, not fully understood effects in the final maps. The LFI philosophy, therefore, is to reduce the magnitude of potential systematic errors as much as possible within cost and resource constraints by careful design of the hardware, rather than to rely on "removing them in software."

Systematic errors can be divided into three categories: astronomical; environmental; and instrumental. Astronomical sources of error (i.e., foregrounds) are discussed in § 1.4. Here we discuss environmental and instrumental effects.

Environmental sources of error

COBE had to deal with rapidly changing local conditions—temperature variations in the instrument and surroundings, changes in the position of the Sun, Earth, and Moon with respect to the instrument, varying magnetic fields, etc. Differential measurement techniques were required.

The Planck orbit, design, and scan strategy reduce most such sources of error by orders of magnitude. For example, the largest systematic error for the COBE DMR was modulation of the ferrite Dicke switches by the Earth's magnetic field. The magnetic field at L_2 is orders of magnitude smaller than experienced by COBE; moreover, for the LFI instrument the effect of system susceptibility to variations in the solar magnetic field will be well below 1 μK.

Further, with the Planck spin configuration there is no first-order process to induce spin-synchronous thermal variations. In COBE these produced effects only at the $\sim 1\,\mu$K level, and in Planck the effects will be smaller still. The extreme thermal stability at L_2 means that the time scale of thermal drifts will be long compared to the 60 s Planck spin period. The frequency dependence of the emissivity of the telescope surfaces and shields means that temperature stability requirements for Planck are driven by the HFI. For example, the HFI requirement for the temperature stability of the primary mirror is spin-synchronous variations of no more than $200\,\mu$K, compared to the LFI requirement of 1 mK (assuming that the mirror emissivity is that of vacuum deposited aluminum).

The primary environmental sources of error for the LFI are those due to imperfect off-axis rejection by the optical system of radiation from the Sun, Earth, Moon, planets, and Galaxy. It is *variations* in response as the spacecraft spins that cause errors. Jupiter is the strongest compact source that can actually pass into the beam, and data must be corrected or excluded when it falls within the 56 dB contour.

Sidelobe structure sweeping across the Galaxy can produce artifacts in any direction. We have simulated this effect, using the actual two-dimensional radiation pattern of the Phase A TICRA telescope for one of the LFI 100 GHz feeds, as shown in Figure 2.2. Convolving this with a model of galactic emission at 100 GHz, we obtain the results shown in Figure 2.3.

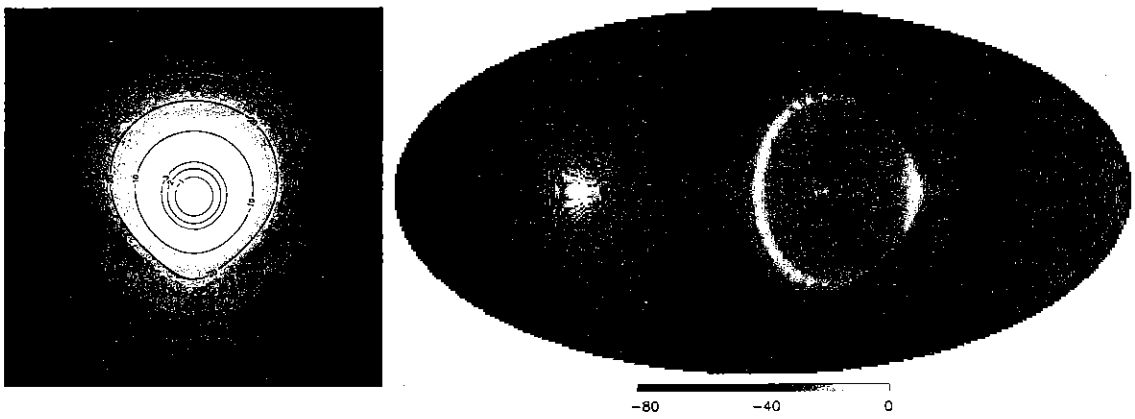

Figure 2.2: Beam directivity for LFI feed #1, a 100 GHz feed located 3° from the axis of the TICRA 1.3 m telescope.
Left panel — Main beam directivity relative to the peak (gain = 59.6 dB). The coordinates $U = \sin\theta\cos\phi$ and $V = \sin\theta\sin\phi$ are the projection of the sky coordinate on the focal plan. The plan described by the telescope optical axis and the spin axis is parallel to $V = 0$.
Right panel — Mollweide projection of the full beam absolute directivity in dB (for clarity only directivities below 0 dB are color coded). For a 90° offset angle the spin axis would be exactly at the center of the plot.

Planck itself will obtain enormously better data on galactic emission than are now available. Given a good characterisation of the far sidelobes of the optical system before launch, a self-consistent reconstruction of both the Galaxy and the telescope radiation pattern could be made. But there will be residual errors in the reconstruction, and the purpose of Planck is to image the CMB, not the Galaxy. To ensure that the residual errors do not compromise Planck's primary science, we require that the level of galactic contamination be below the noise level at 100 GHz for 12 months of observations, with a factor of two margin to allow for uncertainties in the level of galactic emission, over 50% of the sky. For a two-dimensional sidelobe pattern like that in Figure 2.2, this can be translated into a requirement on the sidelobe levels outside the central beam, calculated for the actual positions of the feeds. The exact number depends on the details of the sidelobe pattern and can be calculated as we have shown, but is in the range −60 to −70 dB.

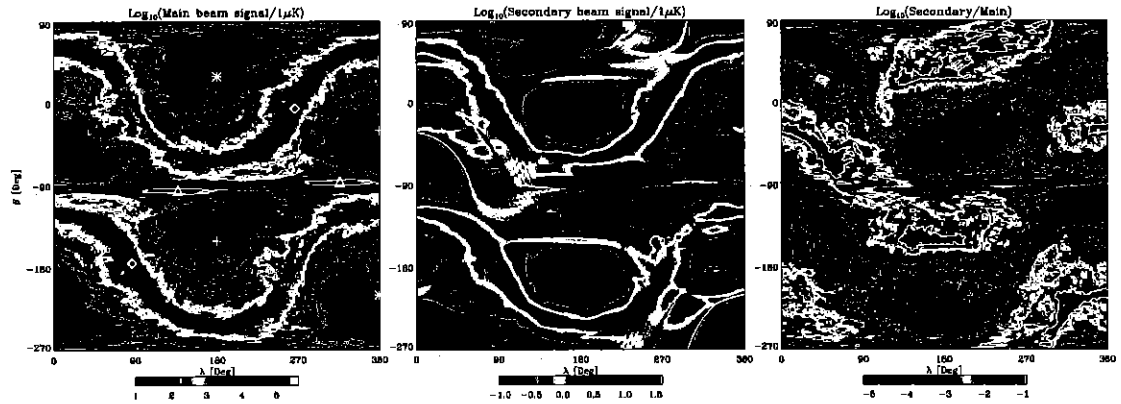

Figure 2.3: Comparison of Galactic emission detected in the central beam and sidelobes of one LFI feed at 100 GHz, assuming the TICRA 1.3 m telescope. Galactic emission is simulated by using the spatial pattern of Galactic dust, and scaling to 100 GHz using models of dust and free-free emission (Kogut et al. 1996). Ecliptic coordinates are used. The telescope beam is assumed to follow great circles on the sky through the ecliptic poles, as would be obtained by Planck with an angle of 90° between the optical axis of the telescope and the spin axis. The north Galactic pole is marked with a star, the south Galactic pole with a cross, the Galactic center with a diamond, and the Large Magellanic Cloud with a triangle.
Left panel — Contributions from the central beam of LFI Feed #1, a 100 GHz horn 100 mm (3°) from the optical axis in the $-x$ direction, out to a radius of 0.°5 around the peak directivity (see Figure 2.2).
Middle panel — Contributions from sidelobes, i.e., outside the central 0.°5-radius central beam area. This panel clearly demonstrates that sidelobe contributions are dominated by the contribution of features relatively near the optical axis. But the contribution from sidelobes in the direction of the primary mirror as seen from the feed (~100° from optical axis) is noticeable in the quiet sky areas near the Galactic poles, where the foreground emission seen by the central beam is the lowest.
Right panel — The ratio of sidelobe to central beam signals. This demonstrates clearly the areas where the sidelobe pickup is most harmful. Contour lines delineate the areas in excess of 0.01 in this ratio. The peak contamination reaches 10% in the ratio.

Instrumental sources of error

An important potential source of instrumental errors is the combination of gain, noise temperature, and phase fluctuations in the amplifiers that leads to variations in the detected power of a constant input signal which have a non-white spectrum. Measurements on many HEMT amplifiers, made from both discrete transistors and monolithic microwave integrated circuits (MMICs), show that the spectrum of detected power is given accurately by $a/f + b$ for $0.01 \lesssim f \lesssim 100$, where a and b are constants for a given amplifier. The frequency at which the white and non-white spectral contributions are equal, $f = b/a$, is defined as the *knee frequency*, $f_{\rm knee}$.

A detailed analysis of the effect of $1/f$ noise in the case of a CMB mission with a spinning spacecraft and "total power" radiometers is given by Janssen et al. (1995). For the Planck spin rate of 1 rpm and the knee frequencies measured to date for HEMT amplifiers, a total power radiometer design would have unacceptably high $1/f$ noise, giving strong striping in the sky images. For this reason the LFI uses "pseudo-correlation" receivers (see Figure 2.1). In this scheme, signals from the sky and from a reference load are combined by a hybrid coupler, amplified in two independent amplifier chains, and separated out by another hybrid. The sky and the reference load power can then be measured and differenced. Since the reference signal has been subject to the same gain variations in the two amplifier chains as the sky signal, the true sky power can be recovered. Similar insensitivity to fluctuations in the detectors themselves is realized by switching in and out ±90° phase shifts synchronously in each amplifier chain.

The differencing receiver greatly improves the stability if the two input signals are almost equal, at

a cost of a factor of $\sqrt{2}$ in sensitivity compared to a perfectly stable total-power radiometer with the same noise temperature and bandwidth. A detailed analysis of the performance of pseudo-correlation radiometers is given by Seiffert et al. (1997). The performance has been tested and verified in prototype radiometers at 10 GHz and 44 GHz. A photograph of the 44 GHz prototype is shown in Figure 2.4a.

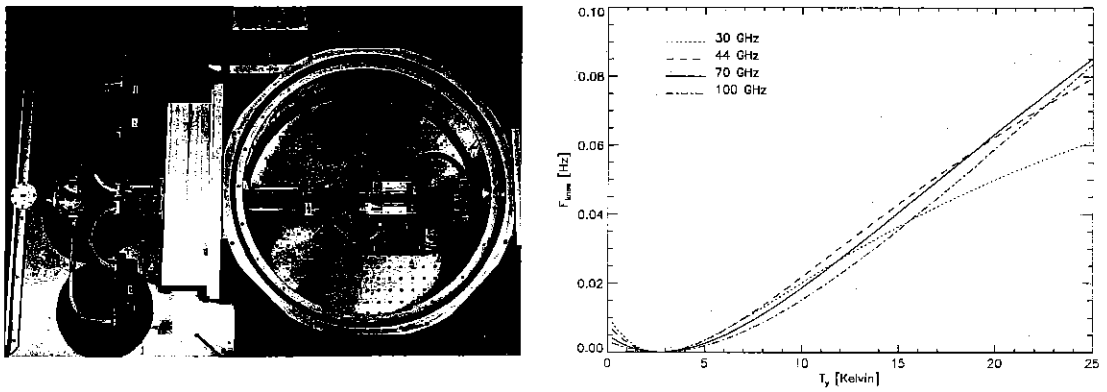

Figure 2.4: **a)** Prototype 44 GHz radiometer used to test the LFI radiometer design concept.
b) Dependence of $f_{\rm knee}$ on the temperature difference between the sky signal and the reference load.

Figure 2.4(b) shows how $f_{\rm knee}$ for the pseudo-correlation radiometers depends on the mean temperature difference between the sky signal and the reference load. It is clear from the figure that the closer the load temperature is to that of the sky, the more perfectly gain and noise fluctuations in the transistors themselves are suppressed in the overall radiometer.

Based on analysis as well as measurements on the prototypes, the knee frequency of the radiometers is acceptable with the reference loads at 20 K, assuming amplifier and detector stability comparable to current values. Some striping would be visible in the unprocessed images, almost all of which can be removed with further processing. By reducing the temperature of the reference loads to ~4 K, however, additional performance margin with attendant reduction in risk can be obtained. A higher level of gain fluctuations could be accepted in the amplifiers and detectors, for example, and there would be essentially no striping to remove in the image processing. The common thermal design adopted by the LFI and HFI teams makes this possible with no impact external to the two instruments, and has been agreed to in principle by the two teams. Accordingly, the LFI design includes reference loads at ~4 K, described in § 1.2.3. Temperature stability is achieved passively. There are no extra wires, no change in volume of the focal assembly, no change in the spacecraft power required, and no increase in the mass of the focal assembly.

Since changes in the physical temperature of the reference load show up directly as errors in the instantaneous output signal from the radiometer, the temperature of the load must be stable. The stability requirement depends on the time scale of the temperature variations—variations on timescales long compared to the 60 s spin period are supressed when the multiple observations of a given spot on the sky are combined; variations on timescales short compared to the radiometer sampling time are averaged out in a single sample. Figure 2.5 shows the factor by which load temperature fluctuations are suppressed by the spacecraft spin, as a function of frequency. Spin-synchronous fluctuations obviously cause the most trouble, and we expect them to have an amplitude less than the maximum allowable value of 1 μK.

A second potential source of instrumental error is temperature fluctuations from the sorption cooler. During the 800-s cycles of the sorption cooler the pressure above the liquid hydrogen downstream from the expansion valve changes slightly as one sorbent bed fill up and another is switched in. As the gas pressure above the liquid changes the equilibrium temperature of the liquid changes, with the dynamic temperature lagging the pressure changes because of the large thermal mass of the FEU. Although the gain of the HEMT amplifiers is temperature dependent, the radiometers are insensitive to gain

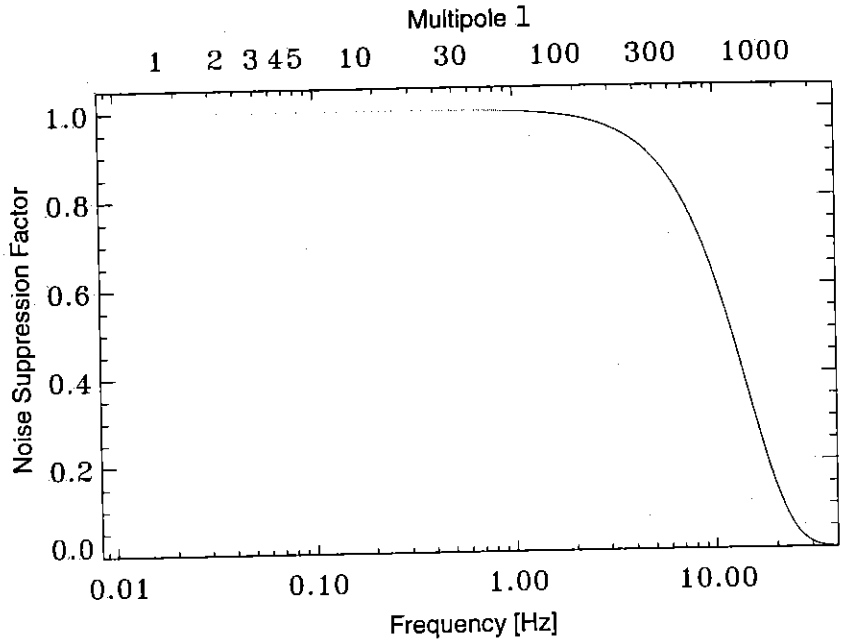

Figure 2.5: Factor by which fluctuations in the temperature of the reference loads are suppressed by the spacecraft spin, as a function of the frequency of the fluctuations. The suppression factor is near zero (noise suppressed completely) except at the spin frequency and its harmonics, seen here as the discrete points starting near unity at $\nu = 0.0167$ Hz, and becoming at the resolution of the figure an apparently solid line. Spin-synchronous fluctuations are not suppressed at all. For great circle scans (90° angle between optical axis and spin axis) each multipole order corresponds precisely to a single spin frequency, given by the top label. For slightly smaller angles the correspondance between multipole and frequency is slightly smeared out. For a two hour scan, the ratio of non-zero to near-zero values is approximately 120, i.e., the noise suppression is large except for about 1% of the bandwidth around the points centered on the spin frequency and its harmonics. This plot assumes a Gaussian beam shape with 10′ FWHM, which together with the spin rate sets the high frequency cutoff.

fluctuations, whatever their cause, as described above. On the other hand, the horns, OMTs, and input hybrids have loss ~ 0.1 dB higher on the sky side than on the reference side of the amplifier inputs. This will lead to differential emission with noise temperature roughly 1/20th of the change in physical temperature. As shown in Figure 2.5, the effect of these emission fluctuations on the data will be suppressed by a large factor by the fact that the cooler cycle is non-synchronous with the spacecraft spin. The gas pressure changes, corresponding temperature changes, and their effect on the data can and will be made negligibly small by proper sizing of the low pressure stabilization bed (Figure 2.1) and perhaps by increasing the thermal mass of the FEU through the addition of small quantities of certain rare earth intermetallics, which at 20 K have ratios of thermal mass to mass 600 times as large as that of aluminium.

A third and extremely important source of instrumental error is distortions in the shape of the telescope beams on the sky. This is an important issue for the LFI especially, because change in the HFI/LFI division of the focal surface and the addition of 100 GHz feeds to the HFI since the Phase A study increase dramatically the distance from the optical axis of the highest frequency LFI feeds. The LFI feeds are all located ~3° from the optical axis, far enough for such a fast optical system that distortions can be large and highly variable from feed to feed. There are two important effects of beam distortions: 1) if the distortions of the beams at a given frequency are different (and they are), combining them together is difficult, especially on-board (see Chapter 6); 2) distorted beams degrade the effective angular resolution on the sky. We have performed extensive analysis and simulations of the second effect, and can now quantify the effects for a given telescope accurately. The current focal surface arrangement places more stringent requirements on the size of the undistorted focal surface of the telescope than existed

during the Phase A study.

2.1.3 LFI performance

Table 2.1 summarizes the performance goals of the LFI

TABLE 2.1

SUMMARY OF LFI PERFORMANCE GOALS

Characteristic	LFI			
Detector technology	InP HEMT arrays			
Detector temperature	20 K			
Cooler technology	H_2 sorption			
Center frequency [GHz]	30	44	70	100
Number of detectors	4	6	12	34
Number of polarized detectors	4	6	12	34
Angular resolution (FWHM) [']	33	23	14	10
Bandwidth $[\Delta\nu/\nu]$	0.20	0.20	0.20	0.20
Noise/res. element, 12 months $[\mu K]$	4	7	10	12
Noise/res. element $[\Delta T/T \times 10^6]$	1.6	2.4	3.6	4.3

The LFI is sensitive to polarization in all channels. The sensitivity to polarization fluctuations will be lower than the sensitivity to intensity fluctuations because the number of channels per polarization is only half as great; moreover, there will be additional complications in removing polarized foregrounds and other potential instrumental effects will have to be copnsidered. Nevertheless, especially at the ecliptic poles, the LFI should have the sensitivity to polarization required to answer the most important question about CMB polarization, namely whether the correlation scale for fluctuations in the polarization is limited to the horizon scale.

2.1.4 Operating modes

There is only one mode for normal operations. All detectors are sampled every 6.9 ms and the difference data are stored, suitably compressed, for transmission to the ground.

There are two diagnostic modes. In the *full-data* mode the raw 16-bit sampled outputs of the detectors associated with any six specified channels are stored for transmission to the ground. The overall data rate is slightly lower in this mode than in the normal operating mode. The *total-power* mode is like the full-data mode, except the phase switches are turned off.

More details on in-flight operation are given in Chapter 6.

2.2 The LFI Front End Unit

The Front End Unit (FEU, Figs. 2.1 and 2.6) is the heart of the instrument. There are 28 modules, each containing one feed horn, one orthomode transducer (OMT), two hybrid couplers, two phase switches, and four cryogenic amplifiers. The modules are mounted on a plate that provides mechanical support and adds thermal inertia. The FEU is cooled to 20 K by a hydrogen sorption cooler (§ 2.6). The phase centers of the feed horns lie in the focal surface defined by the telescope, and the horns are pointed optimally. Details of the FEU components are given below.

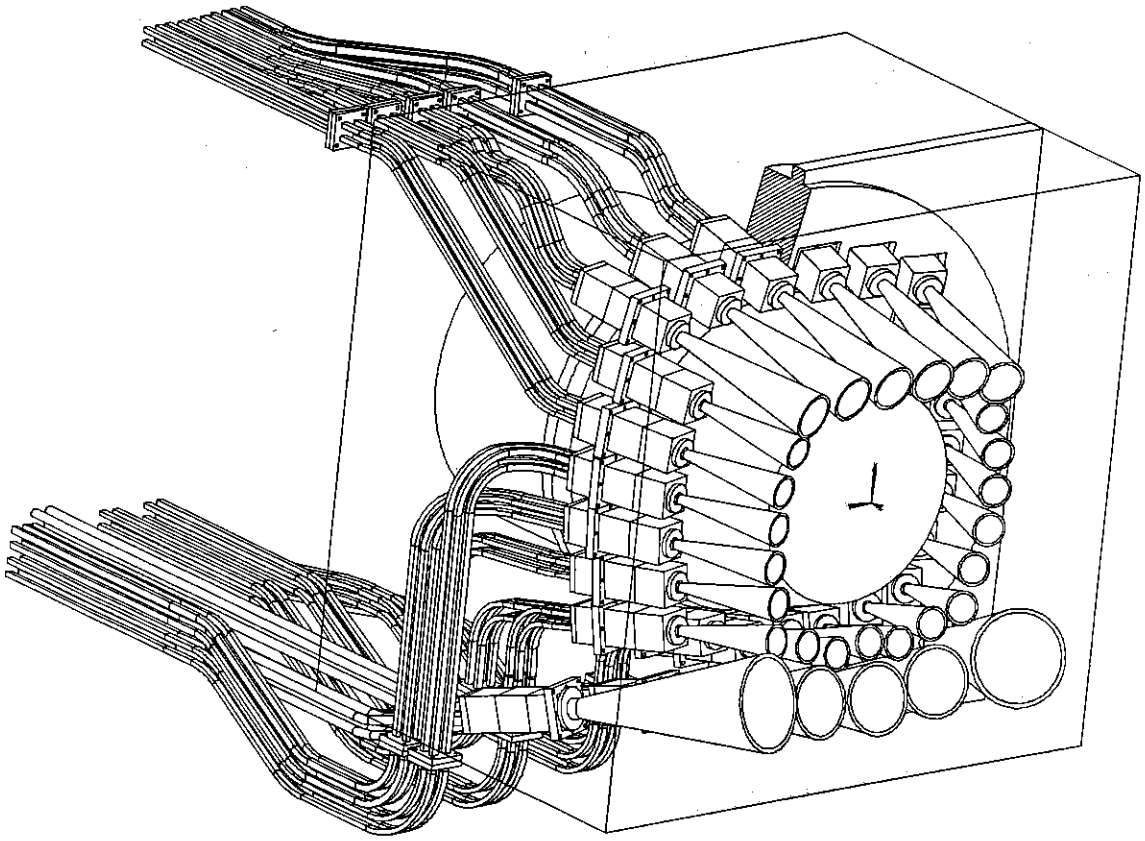

Figure 2.6: The FEU. The waveguides and coaxes that connect to the BEU, only some of which are shown, are configured to facilitate integration with the HFI.

2.2.1 Feed horns and OMTs

The radiation focused by the telescope is coupled to the radiometers by conical, corrugated feedhorns, whose mechanical properties are summarized in Table 2.2. The radiation patterns of the horns must be highly symmetric, with very low sidelobes and a beam width that matches the telescope edge taper requirement. In addition, the electromagnetic field inside the horn must propagate with low attenuation and low return loss. The OMTs separate the orthogonal polarizations with minimal losses and cross-talk. Electrical performance characteristics are given in Table 2.3. The return loss and the insertion loss are to be considered upper limits over the whole 20% bandwidth. The illumination properties, the sidelobe power levels, and the cross-polarization are referred to the central frequency ν_0. The isolation between the two ports of the OMT must be better than -25 dB.

The design procedure for the horns is as follows: 1) Choose the aperture diameter to satisfy the edge taper requirement. 2) Choose the geometry of the corrugations, which determines the cross-polar characteristics and the frequency of operation. 3) Choose the flare angle—a linear taper is assumed as a baseline. Flare angles $\leq 10°$ are chosen to ensure low phase error on the aperture surface, taking into account the configuration constraints imposed by the feed arrangement in the FPU. 4) Design the junction and the throat section; the diameter of the smooth-wall waveguide is set to propagate the TE_{11} mode only. The throat region is designed to match the TE_{11} mode with the HE_{11} hybrid mode, to obtain highly symmetric radiation patterns, low sidelobe levels, and low attenuation.

Both the width and the depth of the corrugations changes along the length of the horn to minimize return loss and attenuation over a wide band. The profile gradually changes the propagation from a

TABLE 2.2

MECHANICAL CHARACTERISTICS OF THE LFI FEEDHORNS

ν_0	D/λ_0	α_f	N_{corr}	N_{corr}/λ_0
30 GHz	~ 6.5	10°	47	3
44 GHz	~ 6.5	10°	47	3
70 GHz	~ 6.5	6°	90	3
100 GHz	~ 6.5	6°	90	3

ν_0 (λ_0) is the central frequency (wavelength), D is the aperture diameter, α_f is the semi-flare angle, and N_{corr} is the number of corrugations.

TABLE 2.3

ELECTRICAL CHARACTERISTICS OF THE LFI FEEDHORNS AND OMTS

ν_0	$\Delta\nu/\nu$	Edge Taper [dB]	Sidelobe Power Level [dB]	Cross Polarisation [dB]	Return Loss [dB]	Insertion Loss [dB]
30 GHz	20%	−30@22°	< -35	< -25	$< -25(-20)$	< 0.1 (0.2)
44 GHz	20%	−30@22°	< -35	< -25	$< -25(-20)$	< 0.1 (0.2)
70 GHz	20%	−30@22°	< -35	< -25	$< -25(-20)$	$< 0.15(0.25)$
100 GHz	20%	−30@22°	< -35	< -25	$< -25(-20)$	< 0.2 (0.3)

Numbers in parentheses include the OMTs.

smooth-wall waveguide to a corrugated waveguide with corrugation depth about $\lambda/4$ at the horn aperture.

Typical asymmetric Orthomode Transducers are considered as a baseline. The circular waveguide is connected to the smooth wall waveguide of the horn. A thin iris inside the circular waveguide will be located in order to maximise the bandwidth and to increase the isolation between the two orthogonal ports. Other kinds of OMTs will be considered as options. The refinment of the feed horns and OMTs design will be performed using a dedicated software package based on multi mode matching analysis.

Because of the small size of the corrugations, especially at 100 GHz, fabrication by direct machining is excluded; however, silver electroforming techniques are capable of producing corrugations fine enough for frequencies well above 100 GHz (Bersanelli et al. 1998), and are quite suitable. Moreover, silver has excellent electrical properties. A thin flash of gold deposited on the silver surface prevents oxidation.

It is anticipated that the OMTs will be manufactured in a similar way, although machinable prototypes can be made. The compact focal array calls for miniaturized designs with no sacrifice in performance. To eliminate loss connecting the horns to the OMTs, the horns and OMTs may be manufactured as a single electroformed component; however, prototypes of the feeds and OMTs will be produced and tested first as independent components.

2.2.2 Hybrids, phase switches and amplifiers

The OMTs are followed by blocks containing hybrid couplers and amplifiers (including phase switches and output hybrids), all cooled to 20 K by the sorption cooler (see Figure 2.1). This front-end is designed to minimize $1/f$ noise in the radiometer while maintaining low thermal noise or T_{sys} (§2.1.2).

The hybrid blocks each contain two hybrid couplers. Each hybrid has two inputs, one of which sees the sky, the other of which looks at the 4 K reference load through a small horn fabricated into the block, as shown in Figure 2.7.

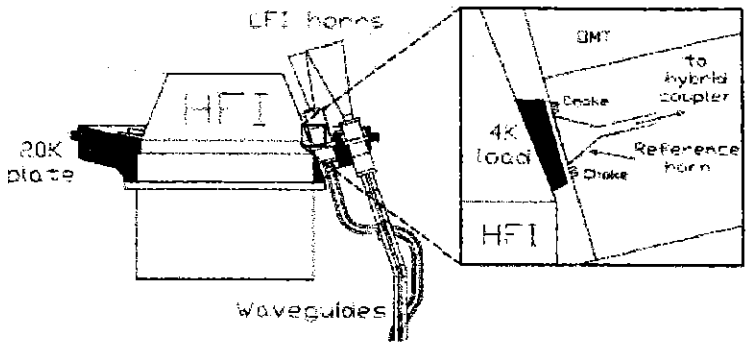

Figure 2.7: Configuration of the 4 K reference load. There is no mechanical contact between the 20 K LFI components and the 4 K absorber. The extra radiative load on the HFI from the feed horns built into the hybrid blocks, which look like 20 K blackbodies, is < 0.1 mW, well below the acceptable limit.

Four amplifiers are contained in each amplifier block, illustrated in Figure 2.8, with multiple inputs and outputs on a single flange to minimize size. The hybrid coupler (short-slot or magic-tee) combines the signals from the sky and cold load with a fixed phase offset of either 90° or 180° between them. It has the necessary bandwidth, low loss, and amplitude balance needed at the output to ensure adequate signal isolation.

Figures 2.9 and 2.10 show 30 and 100 GHz prototype amplifiers and their performance. The input signals are coupled from waveguide to microstrip via a low-loss antenna probe. Broadband probes exist spanning all four LFI bands with less than 0.2 dB loss.

The low-noise amplifiers use InP HEMTs in cascaded gain stages. HEMTs are Field Effect Transistors fabricated on a heterostructure confining the carriers to a two dimensional conduction channel. The dominant heat input into the focal plane is due to power dissipation in the transistors; since this has a significant impact on the payload module, it is desirable to reduce it as far as possible. Of all transistors, InP HEMTs have the highest frequency response, lowest noise, and lowest power dissipation. InP amplifiers have demonstrated superior performance at frequencies as high as 160 GHz (Lai et al. 1997).

In the baseline LFI design, amplifiers at 30 and 44 GHz will use discrete InP HEMTs incorporated into a microwave integrated circuit (MIC) with microstrip networks fabricated on a low loss material and connections made with bond wires that also act as circuit tuning elements. At these frequencies the parasitics and uncertainties introduced by the bond wires in a MIC amplifier are controllable, while the additional tuning flexibility makes optimization for low noise easier than in a monolithic microwave integrated circuit (MMIC) design. There will be four channels at 30 GHz and six channels at 44 GHz; with this relatively small number of amplifiers, fabrication of the MIC amplifiers is a manageable task. Using the MIC approach, it will be possible to integrate the input and output couplers, front-end gain of approximately 30 dB, and the phase switch, as each can be constructed using microstrip technology. However, for low loss it may be necessary to use a waveguide input coupler. The 'chip-and-wire' approach

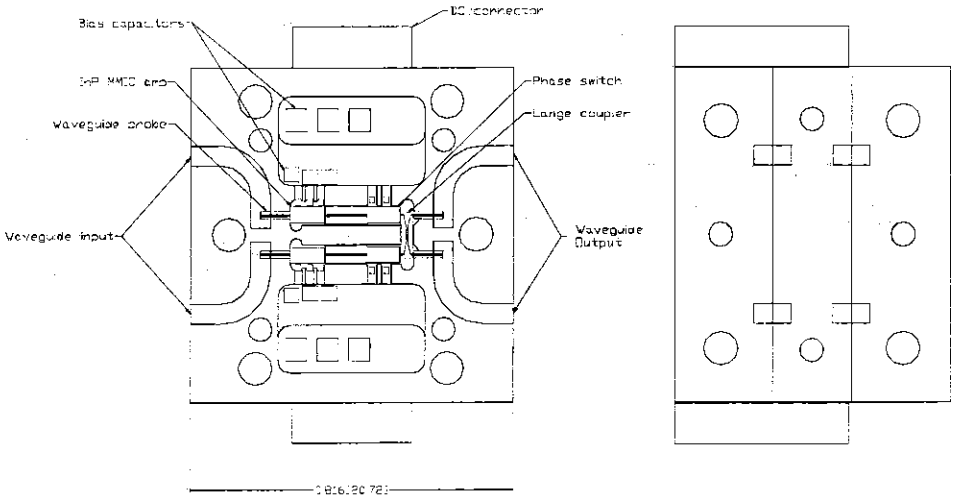

Figure 2.8: Physical layout of an amplifier block, which contains four amplifier chains. The scale shows that extremely compact size can be obtained, thus allowing the array of feeds to be closely packed.

will enable the optimization of the sensitivity and gain flatness of the amplifiers.

Use of InP HEMTs for the gain stages will ensure not only the minimum noise contribution from the receiver but also minimum heat dissipation. Amplifiers have been demonstrated with noise figures of 9 K at 30 GHz and 12 K at 44 GHz, with 20% bandwidth.

At 70 and 100 GHz there will be 12 and 34 channels, respectively. Amplifiers at these frequencies will use MMICs. The MMIC approach incorporates all circuit elements and the HEMT transistors on a single InP chip. The material system employed for Planck is lattice-matched InGaAs/InAlAs/InP with a 0.1μ gate length. The amplifiers can thus be mass-produced in a controlled process, a real advantage given the large number of amplifers at 70 and 100 GHz .

The only connections to the MMICs are single input and output wires, and DC voltage bias to the circuits. The dramatically reduced number of connections increases reliability and reduces circuit parasitics. TRW has produced thousands of wafers of InP MMIC circuits and has demonstrated state-of-the-art performance including the highest frequency low noise amplifier at 155 GHz. TRW/UMass/JPL have demonstrated a 75–115 GHz cryogenic amplifier which exhibits $\leq$50 K noise from 90–105 GHz. While this amplifier dissipates 5 mW of power for 17 dB of gain, similar amplifiers have been demonstrated dissipating only 0.8 mW of power per 5 dB of gain (Gaier et al. 1996).

For all frequencies, 30–40 dB of gain is sufficient to guarantee that the overall noise is dominated by the front end amplifiers. In order to achieve the required 15 dB of isolation, gain and phase matching of the amplifiers is required. If additional gain were located in the front end, the power dissipated would grow significantly, putting too much load on the cooler (the last stages of a radiometer must be run at higher power to guarantee linearity). It is necessary to provide bias controls to the first two stages per amplifier to ensure an adequate range of tunability over a wide range of operating temperatures. A summary of expected performance of the LFI amplifiers is shown in Table 2.4.

Following amplification the signals are passed through a phase switch. TRW has demonstrated a broadband switch using the source-drain contacts of a HEMT biased only on the gate. The switch consumes microwatts of power, is broad band, and works at cryogenic temperatures with switch rates in excess of 1 kHz. The phase switch adds 90 or 180° of phase lag to the signals, thus selecting the input source as either the sky or the reference load at the radiometer output. Two wires per FEM are required to provide phase switching signals.

The phase lagged pair of signals is then passed into a second hybrid coupler, separating the signals.

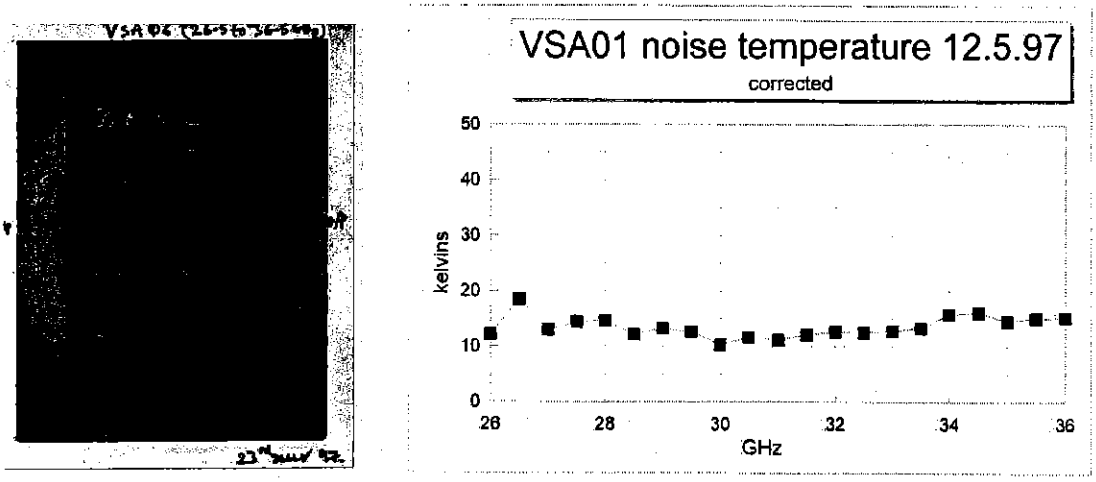

Figure 2.9: Photograph (left) and measured state-of-the-art performance at Jodrell Bank (right) of a 30 GHz MIC prototype Planck amplifier.

The signals are then transitioned to either coaxial cables (30 and 44 GHz) or to gold-plated stainless waveguides (70 and 100 GHz). The inclusion of the phase switches and second hybrids eliminates the need for phase matching of the long transmission paths to the BEU, greatly simplifying integration and testing. It also allows extensive testing of the individual FEMs as compact units, reducing the cost of testing and verification (Chapters 4 and 5).

2.3 Waveguide and Coax Sections

Each pseudo-correlation radiometer unit needs two waveguides or coax cables to carry the double chain signal to the BEU. Each horn feeds two radiometers, so that each cryogenic unit is connected with the room temperature section with four waveguides or cables, grouped together. This results in a total of 20 coax cables and 92 waveguide sections running between the FEU and the BEU.

TABLE 2.4

PERFORMANCE OF THE LFI FRONT-END AMPLIFIERS

Characteristic	30 GHz	44 GHz	70 GHz	100 GHz
Configuration	InP MIC	InP MIC	InP MMIC	InP MMIC
Number of amplifiers	8	12	24	68
Number of stages per amplifier	3	3	4	4
Gain per stage [dB]	13	12	10	9
Power dissipation per stage [mW]	< 3.2	< 2.2	< 1.3	< 1.0
Power dissipation per frequency [mW]	< 77	< 78	< 132	< 262
Amplifier noise temperature [K]	6	11	17	24
System noise temperature [K]	9	15	22	31

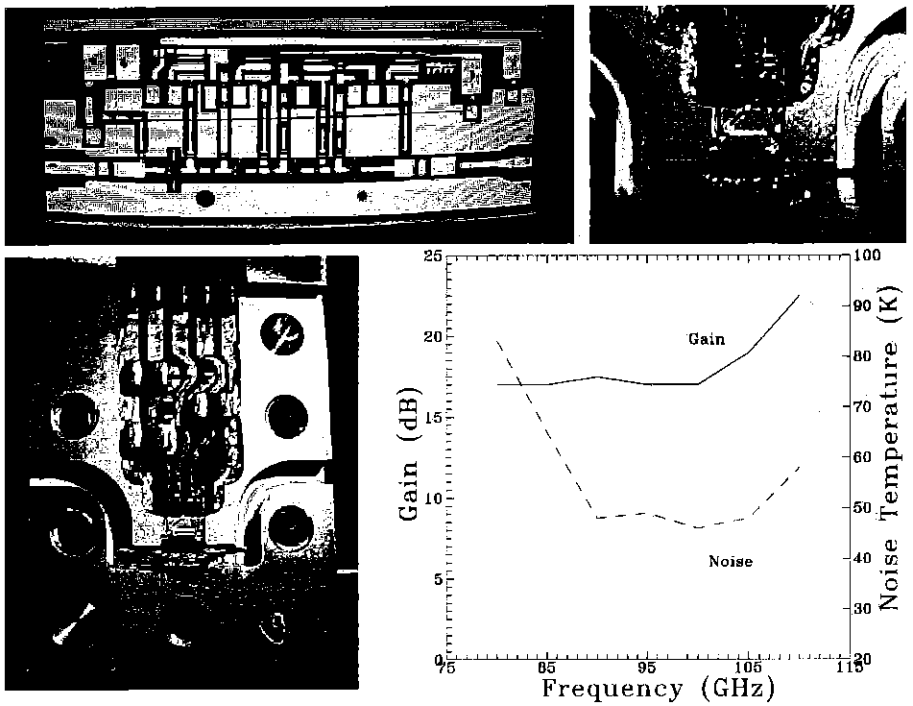

Figure 2.10: Photographs and measured performance of a W-band MMIC amplifier. The MMIC chip shown at the upper left is mounted between the input and output waveguides of the amplifier housing (upper right). The entire housing is shown at the lower left. Measured performance is shown at the lower right. Although this represents record low noise performance for a MMIC amplifier in this frequency range, the design of the amplifier has several known defects, and the overall performance characteristics of the wafer on which it was fabricated are by no means the best that TRW can produce. Design improvements will be implemented in the next and following MMIC fabrication runs, and multiple fabrication runs in the LFI schedule will ensure delivery of several wafers of the highest quality. This early success puts the LFI Consortium ahead of schedule in achieving its amplifier performance goals.

The waveguides and coaxial cables must have low insertion loss and VSWR while minimising parasitic heat loads on the 20 K Front End Unit. Thin-wall metal waveguides and high quality coaxial cables meet the required radiometric performance above and below 50 GHz, respectively. For good performance, waveguide fabrication errors must be no more than $\lambda/100$ (30 μm at 100 GHz). Specially designed flanges are required for low VSWR and for compactness.

Thermal parasitics in the 20 K stage are dominated by conduction in the waveguides and coaxes. Radiative loads can be intercepted by lossless foam inserted in the waveguides at positions matching heat sink plates. The thermal requirements are met by standard waveguides with 0.20 mm stainless steel wall, flashed with 1 μm of gold for good electrical performance. To reduce the heat load on the 20 K stage, the waveguides are heat sunk at approximately 140 K, 80 K, and 50 K.

Adequate clearance for integration of the HFI and the LFI FEUs (see Figure 2.6 and Appendix A). The mechanical requirements on the waveguides and coaxes can be met if they are grouped into four bundles and configured to allow the required flexibility and clearance. Mechanical constraints imposed by launch vibration loads are largely relaxed by the RAA rigid structure.

The bending radius R of the waveguides will be such that it will not compromise the radiometric performace, which is obtained with $R \gtrsim \lambda/2$.

Dielectric waveguides made from polytetra-fluoroethylene (PTFE) have significantly lower insertion loss and thermal conductivity, and much greater flexibility, than gold-flashed stainless steel waveguides.

All three properties are desirable for the waveguides connecting the FEU and the BEU. PTFE waveguides are commercially available, although custom flanges may be required for compactness. A study to assess this backup option is currently underway.

2.4 The Back End Unit

The BEU comprises the radiometer Back End Modules (BEM) and the Data Acquisition Electronics (DAE), which are connected by an internal harness. The BEU is connected to the FEU by 92 waveguides and 20 coaxes. Wires for DC biasing of the amplifiers and for one switch control signal are also required. A unidirectional, synchronous serial interface is used for transmitting science data to the Signal Processing Unit (SPU). Communication, timing, and analog housekeeping interfaces are transmitted to the Data Processing Unit (DPU). Internally, each back end anolog output is connected, by coaxial cables, to the DAU. Table 2.5 summarizes the key properties of the back end unit. As in the FEU, InP HEMTs offer the highest gain, lowest power consumption, and lowest noise.

TABLE 2.5

BACKEND CHARACTERISTICS

	FREQUENCY [GHz]			
CHARACTERISTIC	30	44	70	100
Bandwidth [GHz]	6	8.8	13	20
RF gain [dB]	29	31	20	22
Noise temperature [K]	< 350	< 350	< 350	< 600
DC gain [dB]	20	20	20	20
Power dissipation [W]	0.6	0.9	1.8	4.8

2.4.1 Back end modules

Each back end module (BEM) comprises two parallel chains of amplification, filtering, detection, and integration. The detected signals are amplified and a low-pass filter or integrator reduces the variance of the random signal, providing in each channel a DC output voltage related to the average value. Post-detection amplifiers are integrated into the BEMs to avoid data transmission problems between the radiometer and the electronics box. A block diagram of a BEM is shown in Figure 2.1

The sky and reference signals are at different levels, which are equalized after detection and integration by modulating the gain synchronously with the phase switch. Because of the phase switching in the front end modules, a given detector alternately sees the sky and the reference signals. Differences between the detectors are therefore common-mode in the output signals and have no effect on the final difference, which is calculated in the Signal Processing Unit.

Phase match is unimportant in the BEU because the second hybrids for the pseudo-correlation radiometers are in the FEU; only the amplitude of the signals is important in the back end. Both back end chains in a given BEM can be fabricated in the same MMIC. This is convenient for packaging and advantageous in matching the properties of the two chains. Each backend module will be packaged, including A/D converters, into a box of a few centimeters on a side, including the biasing circuitry and the input and output connectors.

2.4.2 Data acquisition electronics

The Data Acquisition Electronics (DAE) comprises the analog conditioning electronics, the multiplexers, the analog-to-digital converters, the parallel-to-serial converters, the control electronics, the communication interface, and the power conditioning and distribution electronics. It performs the following

functions: Communication with the DPU, including command reception (identification, acceptance, interpretation, and execution) and status transmission; acquisition, conditioning, and multiplexing of the signals; control of the data acquisition chain; transmission of raw data to the SPU; power supply conditioning and distribution; DC biasing of the FEU and BEU amplifiers; synchronous control of the FEU phase switches; and ON/OFF control of FEU and BEU amplifiers.

The time at which each sample is acquired must be known accurately so that the corresponding position on the sky may be determined accurately, so the DAE must have access to both the main spacecraft clock and to the spin-phasing reference pulse from the star mapper.

The analog outputs are conditioned to provide signal levels suitable for quantification. Antialiasing filters limit the noise higher than the signal bandwidth. Each detector is sampled and held synchronously, multiplexed, and digitised using 16-bit analog-to-digital converters. There are at least four analog acquisition chains corresponding to the four frequency bands. The acquired data are converted to a serial stream and automatically transferred to the SPU, through the synchronous serial link, for later processing and compression.

2.5 Radiometer Electronics Box Assembly and Software

The Radiometer Electronics Box Assembly (REBA), shown schematically in Figure 2.11, comprises three sub-units: the Signal Processing Unit (SPU), the Data Processing Unit (DPU), and the Power Supply Unit (PSU).

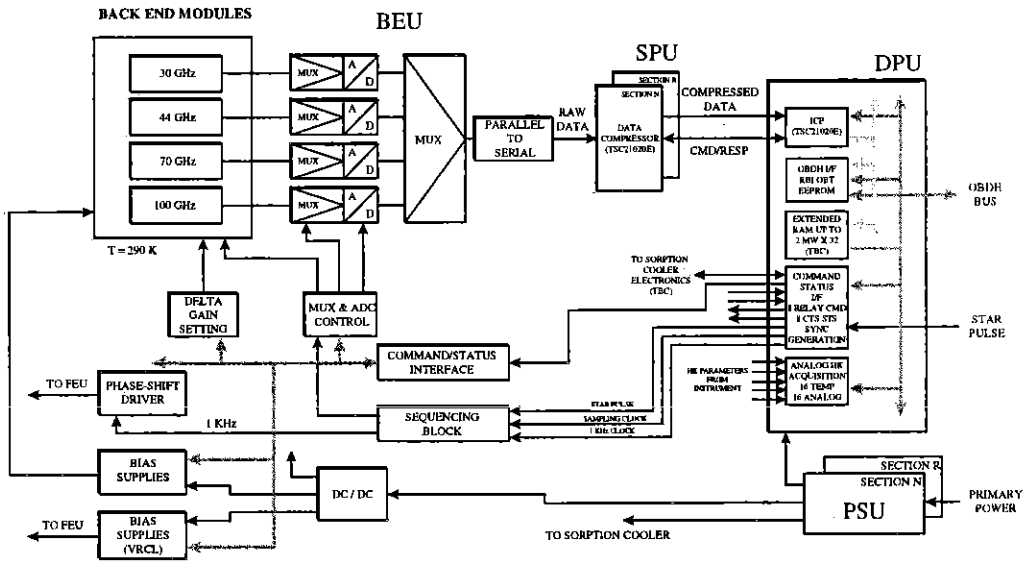

Figure 2.11: Schematic of the Radiometer Electronics Box Assembly.

2.5.1 Signal processing unit

The baseline Signal Processing Unit (SPU) processes and compresses the science data. It is fully redundant, with two TEMIC TSC21020E Digital Signal Processors running at 20 MHz. The TSC21020E is a radiation-tolerant version of the 32-bit Analog Devices ADSP 21020 processor. It has two complete bus systems, one 48 bits wide dedicated to instructions, the other 32 bits wide to data, allowing simultaneous access to instructions and data, multiple data accessing, and parallel execution of arithmetic instructions. The throughput of this machine at 20 MHz (design baseline) is 75 MFLOPS peak and 50 MFLOPS

sustained performance. The instruction rate is 25 MIPS. Although this machine is a general purpose processor, it is especially efficient at signal processing tasks. For example, it can compute a 1024-point complex FFT in 780 μs, a division in 240 ns, and an inverse square root in 360 ns.

2.5.2 The Data processing unit

The Data Processing Unit (DPU) comprises the synchronisation generator, the Instrument Control Processor (ICP), the memory subsystem, and has four interfaces, with the spacecraft OBDH, the Back End Unit (BEU), the Sorption Cooler Electronics (SCE), and the instrument Power Supply Unit (PSU).

The DPU is fully redundant. It performs the following functions: communication with the spacecraft CDMU via the OBDH interface, including telecommand reception (identification, acceptance, interpreting, and execution), and telemetry transmission (science and housekeeping data acquisition and formatting); monitoring and control; initialisation and error management; management of operating modes; time stamping, time and synchronisation management; and conditioning and acquisition of housekeeping data.

The baseline DPU processor is the same TEMIC TSC21020E Digital Signal Processor as used in the SPU. Other options will be studied to take advantage of commonality with the HFI and the FIRST instruments. The DPU has two RAM Memory banks, one 128 K $\times$ 32 bits for data and one 128 K $\times$ 48 bits for program storage.

The SPU is controlled by the DPU through an asynchronous serial link . The SPU has two unidirectional synchronous serial interfaces (FIFO based) for receiving scientific raw data from the BEU and transmiting compressed data to the DPU. The SPU accesses these interfaces by means of FIFO buffers, decoupling the execution of the software from the hard synchronism of the serial lines. Both the asynchronous and synchronous serial links are standard RS 422 type.

2.5.3 Power supply unit

The Power Supply Unit (PSU) conditions the S/C bus power and distributes it to all of the warm LFI electronics boxes. The PSU provides galvanic isolation and converts the S/C bus voltage into a number of regulated output voltages that are current limited and protected from both short circuits and overvoltages. Two DC/DC converter modules operate in cold redundancy, meaning that only the main or the redundant unit is powered up at a given time. The S/C power bus is connected to the Buck converter via a so-called soft starter and input filter, providing a regulated and current-limited voltage to the push-pull converter, which supplies the voltage outputs obtained from the voltage regulators.

2.5.4 On-board software

On-board software can be classified into two categories: the Low-Level Software (LLS) and the High-Level Software (HLS). The LLS, which is common to both DPU and SPU, comprises the bootstrap code and the software drivers to access the I/O devices. The HLS includes the data handling and instrument control software that run in the DPU, and the data processing and compression software that run in the SPU.

DPU-LLS, DPU-HLS and SPU-HLS programs are stored in the DPU-PROM bank. On instrument switch-on the DPU bootstrap program will execute an initial self-test and then the user program, DPU-HLS, will be loaded from PROM to RAM. In the SPU, where the SPU-LLS program is stored in the SPU-PROM bank, the SPU bootstrap program will execute an initial self-test, then load the SPU-HLS program from the DPU to SPU-RAM by means of the asynchronous serial line. After commanding from the DPU, the SPU control will be left to the HLS user program. It is also possible to provide basic on-flight support functions running in PROM, such as specific self-test programs or patch-and-dumps of the user program in RAM.

On-board software shall comply with ESA standard PSS-05-0 and its amendments (BSSC(96)2). It will have the autonomy functions and memory capabilities stated in the FIRST/Planck IID-A document, i.e., on-board memory loading and dumping.

2.5.5 Harness and grounding

Signal and power will be maintained separated in different bundles and retained up to the interface connectors. Nominal and redundant signals will be routed on the same bundle. The same criteria will be used for the power lines. A redundant S/C harness will provide interconnection between the PSU, DPU and the S/C Power and Data handling subsystems respectively.

The grounding scheme minimises ground loops, using DC/DC converters to isolate loads located in different boxes.

2.5.6 Redundancy

The FEU and BEU are inherently redundant. All other electronic sysbystems are fully redundant and free of single point failures. In general complete systems are duplicated; "criss cross" between the two channels is avoided. The system operates in "cold redundancy" mode, which means the redundant channel is powered up or functional only when it is needed.

2.6 The Sorption Cooler

The FEU is cooled to 20 K by a hydrogen sorption cooler, shown schematically in Figure 2.1. It is a simple Joule-Thomson cooler in which $0.0045\,g\,s^{-1}$ of hydrogen expands from 6 MPa to 0.03 MPa through a Joule-Thomson (J-T) expander. The cooler also provides < 18 K precooling to the HFI 4-K cooler. In a sorption cooler the high and low gas pressures are maintained not by a mechanical pump, but rather by the fact that the equilibrium pressure of gas above the sorbent bed is a strong function of temperature.

The cooler has two principal components, the Sorption Cooler Compressor (SCC) assembly containing a metal hydride sorbent material, and the Joule-Thomson (J-T) expander. The refrigerant is hydrogen. In addition to meeting temperature and capacity requirements, 20 K hydrogen sorption coolers have three major advantages for Planck: 1) they are efficient; 2) there are no cold moving parts, no vibration, and very low EMI; and 3) integration with the instruments and spacecraft is simple. Since the cooler is used for both the LFI and the HFI, two identical coolers (compressor + expander + connecting tubing + electronics) provide full redundancy.

2.6.1 Sorption compressor and its operation

The Sorption Cooler Compressor (SCC), as well as the redundant unit, each 100 × 750 × 750 mm in size with a mass of 30 kg, are located on the SVM at a temperature < 280 K. During operation, hydrogen is desorbed from the metal hydride at 6 MPa as one compressor element after another is heated to 485 K, then precooled in a tube-in-tube heat exchanger and expanded through a J-T orifice to create a gas/liquid refrigerant mixture at 0.03 MPa and < 18 K. The orifice is sized to set the flow rate at $0.0045\,g\,s^{-1}$. The liquid evaporates as it absorbs heat from the instruments. The gas is warmed as it returns through the tube-in-tube heat exchanger, and is then reabsorbed in a cool (< 280 K) compressor element, completing the cycle. The flow of gas through the various components is directed by a gas manifold with passive check valves, one inlet and one outlet for each compressor element.

The SCCs contain five compressor elements. At any given time, one compressor element is warming up, one is hot and desorbing gas, one is cooling down, and two are cold and absorbing gas. The five compressor elements are cycled successively through the steps in this process with one complete cycle taking 4000 s. Cycling is accomplished simply by turning on and off at appropriate times heaters embedded in the compressor elements, using solid-state relays. Gas-gap thermal switches are incorporated into the compressor element design to isolate the compressor elements thermally during the heating and desorbing phases, and to connect the compressor elements thermally to the < 280 K temperature sink during the cooling and absorbing phases.

Stability of the cold temperatures is achieved by virtue of the large thermal mass of the FEU, and by maintaining a stable low pressure at the liquid reservoir. To help accomplish this, the pressure is buffered

by an extra sorbent bed maintained at the 280 K sink temperature. The buffering provided by this bed is equivalent to that of a 200 liter plenum.

The J-T expander assembly contains a contamination filter, a porous plug flow restrictor (the J-T expander), and three liquid reservoirs. The first reservoir of each cooler is mated to the HFI 4 K cooler to provide precooling at < 18 K. The second reservoir provides cooling to the LFI and the HFI 20 K shield, and intercepts parasitics to both instruments. The total cooling capacity at 20 K is approximately 1.2 W. The third reservoir is controlled at approximately 24 K to wick and then sublimate any excess liquid refrigerant.

The expander and compressor assemblies are connected by a tube-in-tube (3.18 and 6.35 mm o.d.) heat exchanger approximately 5 m long, which is thermally connected to several radiatively cooled shields to minimize the heat rejected on the optical bench. The heat rejected to shields at 140 K, 80 K and 50 K is 364 mW, 511 mW and 727 mW, respectively.

Table 2.6 summarizes the heat loads that must be lifted by the cooler, and the total input power required by the cooler, for the 50 K baseline temperature of the telescope enclosure and precool, and for three higher temperatures. The cooler is sized with substantial margin. In the baseline case the input power to the cooler is 360 W for an output cooling capacity of 1.2 W. It is easy to modify the cooler to accomodate changes in the temperature of the precool and telescope enclosure through linear scaling of the compressor length and increased input power; however, it is clear from Table 2.6 that the environment should be maintained below 70 K.

TABLE 2.6

COOLING LOADS AND SORPTION COOLER POWER

	ENCLOSURE TEMPERATURE [K]			
HEAT LOAD [mW]	80	70	60	50
HEMTs	550	550	550	550
Waveguides and coaxes	303	243	186	132
Struts	40	30	20	16
Cables	20	14	12	10
Redundant cooler	25	15	10	7
Radiation	237	140	75	40
HFI load	160	140	120	100
SUBTOTAL	1335	1132	973	855
40% margin	534	453	390	342
TOTAL	1869	1585	1363	1197
Cooler efficiency [W/W]	600	475	360	300
TOTAL POWER REQUIRED [W]	1121	753	491	359

2.6.2 Sorption cooler electronics

The sorption cooler electronics (SCE), housed in two boxes each roughly 250mm×200mm×140mm, provide the following functions for the coolers: switching control for the sorption bed heaters; switching control to the heat switches; timing signals for the switching; proportional control of 30 W of power to the compressor elements in the "hot" state; temperature control of one of the liquid hydrogen reservoirs; and control of a number of temperature, pressure, voltage, and current sensors. Power at 28 V is supplied to the cooler electronics and to the coolers via the LFI Power Supply Unit.

The cooler electronics receive commands and clock synchronization signals from the data processing unit (DPU) and return telemetry signals to it, but are otherwise independent. Timing sequences

are generated internally, but synchronized with the DPU and the spacecraft computer so that possible switching transients cannot affect the data. The autonomy of the cooler electonics has the advantages that the cooler control software does not have to be integrated into the control software of the LFI and HFI, and the instrument computers are not required for operation of the cooler during initial integration and testing.

2.6.3 Development

Recent advances have substantially improved the flight readiness level of sorption technology. The Brilliant Eyes Ten-Kelvin Sorption Cooler Experiment (BETSCE), flown in May 1996, tested all design characteristics affected by microgravity environments, and qualified and validated all component and assembly procedures required for future hydrogen sorption coolers. Moreover, the flight data validate the design and performance predictions of future periodic and continuous sorption coolers.

Two aspects of sorption cooler performance not addressed by the BETSCE flight—operational stability and capacity as a function of lifetime—are being studied by the NASA-funded Vibration-Free Cooler Program at JPL. Compressor elements designed for long life, shown in Figure 2.12, will be tested for stability and performance in life tests begining in the summer of 1998.

Figure 2.12: Prototype compressor element for Planck, designed for long life. These elements will be tested for stability and performance as a function of time beginning in the summer of 1998.

In addition, a 25 K sorption cooler being developed for the UCSB BEAST CMB experiment has a configuration similar to that of the Planck coolers. BEAST is a long duration balloon flight scheduled for to fly in Antarctica in December 1998. The single-stage cooler, shown in its original configuration in Figure 2.13, was designed for stable performance with extremely high insensitivity to contamination. It is currently being modified to increase its capacity from 480 mW to 800 mW at 25 K. The proof of detector compatibility, as demonstrated by the quality of the science data gathered, and verification of cooler reliability and ruggedness will add significantly to the heritage of sorption cooler development for Planck. The BEAST cooler will be upgraded following the 1998 flight with the new compressors developed for Planck, and flown again in 1999.

A single Engineering/Qualification Model cooler will be built, characterized, flight qualified, and delivered to TESRE in 2000. After refurbishment, this cooler will serve as the flight spare to the two Planck flight coolers.

To develop mechanical and thermal interfaces to the HFI and to validate compatibility with the bolometers, a cryostat identical to the EM sorption cooler cryostat will be delivered to the IAS for integration with the HFI. This will allow parametric characterization of the combined performance of the HFI coolers as well as any interactions between them and the detectors to be fully mapped early in the development of the HFI instrument.

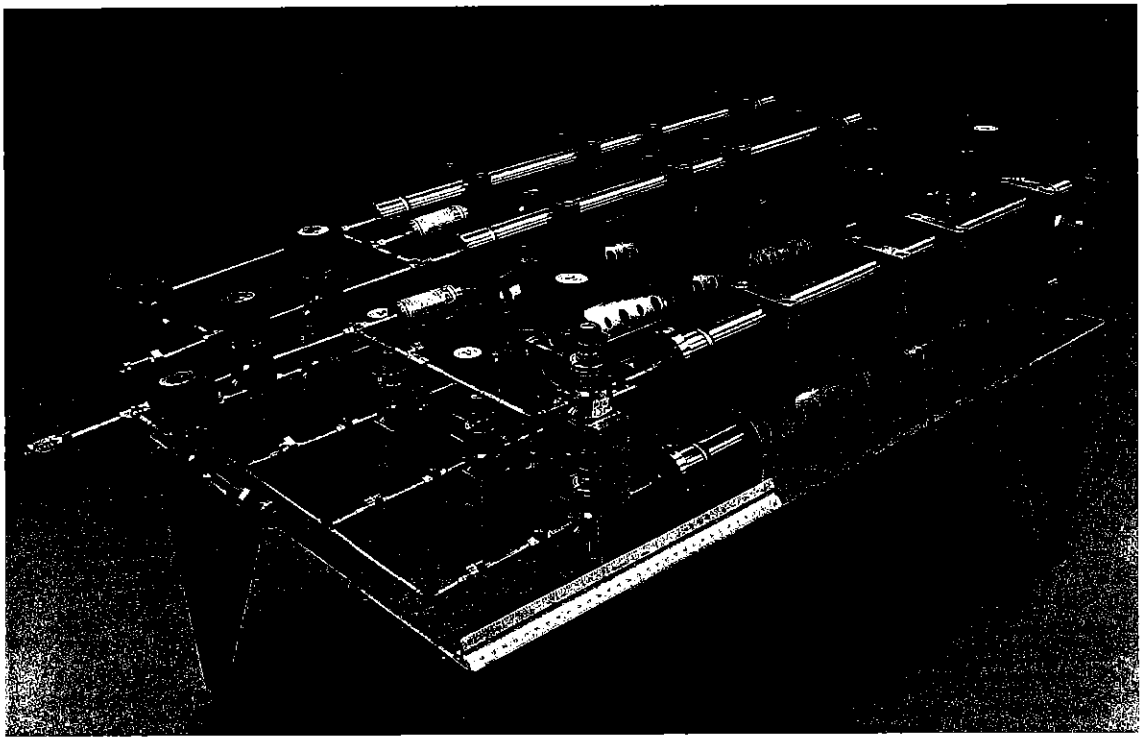

Figure 2.13: Photograph of the BEAST 25 K hydrogen sorption cooler in its original configuration with a capacity of 480 mW.

2.7 Risk Assessment and Heritage

No new technology development is required for the LFI; however, the LFI will introduce sorption coolers to space science missions and actively cool HEMT amplifiers in space for the first time. A design maturity level has been assigned to all components of the flight system, as follows: 1) An identical design has operated in space; 2) A prototype or engineering model has been qualification tested in preparation for operation in space; 3) Similar components using the same technology, materials, design, and fabrication processes have been demonstrated in space; 4) Subcomponents of a custom design have been demonstrated on the ground or in space.

The equipment list in Table 2.7 gives source, heritage, design maturity level, mass, power, and contingency for the components of the LFI. The heritage column shows missions that used subcomponents, materials, and design and manufacturing techniques that the LFI will use.

Mass and power contingencies are based on design maturity, inheritance, and also on the nature of the component. For example, the heritage and maturity of the cooler lines is high, but their mass depends on exact lengths, etc., so a high contingency is assigned. Contingencies range from 25% (on estimates based on hardware sketches or schematics) down to 3% (for estimates based on measurements of a component or engineering model expected to be identical to the flight hardware). This contingency scheme will be used throughout flight system development as part of the margin management effort.

All components at maturity levels 3 and level 4 will be tracked. All components at maturity level 4 go through breadboard and engineering models. The radiometers set the critical path for the payload development.

Although the LFI will be the first science instrument to use a hydrogen sorption cooler in space, sorption coolers are a relatively mature technology. BETSCE (§ 2.6) flew in May, 1996 and achieved a cold-end temperature of 10.4 K in under 2 minutes from a starting temperature of 65 K (Bard et al 1993,

TABLE 2.7

LFI EQUIPMENT LIST

ELEMENT	Number	HERITAGE[a]	Maturity[a]	MASS Est. [kg]	MASS Cont. [%]	MASS Total[b] [kg]	POWER Est. [W]	POWER Cont. [%]	POWER Total[b] [W]
Thermal/Mechanical Components									
Struts & fittings	11	various	3	11.6	25%	14.5			
Front support plate	1	various	3	10.0	25%	12.5			
Cryocooler									
Compressor and expander	1	BETSCE/BEAST	2	30.0	20%	36.0	267	35%	360
Tubing	1	BETSCE/BEAST	2	2.0	10%	2.2			
Control electronics	1	BETSCE/BEAST	2	3.0	25%	4.0	20	25%	25
Radiometer									
Feed horns	28	various	3	2.0	40%	2.8			
Orthomode transducers	28	various	4	1.7	40%	2.4			
Hybrid couplers	28	various	4	1.7	40%	2.4			
Cryo amplifier blocks	56	MILSTAR	4	4.5	25%	5.6	0.5	25%	0.7
Waveguides & coaxes	112	various	3	4.0	25%	5.0			
Back end unit	1	MILSTAR	3	22.0	10%	24.2	40	20%	48
Signal processing unit	1		3	3.8	10%	4.1	7	10%	8
Data processing unit	1		2	6.7	10%	7.4	10	10%	11
Power supply unit	1		2	3.0	10%	3.3	12	10%	13
Harness	1	Various	3	3.0	40%	4.2			
TOTAL				**109.0**	**20%**	**130.6**	**356.5**	**31**	**465.7**

a See text for definitions and explanation.
b Total including contingency. In the case of power, also multiplied by duty cycle(=DC).

1997). It offered the first opportunity to measure microgravity effects on a wide variety of performance characteristics, of which the most important were the thermal conductivities of the $LaNi_{4.8}Sn_{0.2}$ and ZrNi hydride powders. The in-flight conductivities were identical to those measured on the ground. These are the same hydrides to be used on Planck. Also verified in flight were the ability of the cryostat liquid reservoir to separate and retain both liquid and solid hydrogen. Again, no adverse microgravity effects were observed. As a result of the BETSCE mission, the components and assembly procedures required to build future hydride sorption coolers such as the Planck 20 K cooler were developed, qualified and validated.

Unlike the Planck coolers, BETSCE was designed for intermittent, not continuous, operation. It went through 18 cycles in flight, reaching the same gas pressures in the compressors each time; however, it cooled below 11 K only on the first cycle because a valve became contaminated by a particle shaken loose from a buffer tank. In-stream filters at each valve would have prevented the problem, and are included in all Planck valves. In fact, the Planck cooler has been designed to be extraorinarily insensitive to contamination, at the same time as construction techniques have been designed to achieve full cleanliness inside the cooler.

High frequency MMIC radiometers have been flown in space missions such as MILSTAR. Jodrell Bank, University of Manchester, and NRAO operates some 44 telescope each with $\sim$ 10 cryogenic HEMT receivers including frequencies up to 86 GHz. Although ground-based these systems operate remotely over long periods of time, only requiring maintainence to some mechanical parts not present in the LFI receivers.

Chapter 3

Information management and data processing plans

3.1 Introduction

In order to take maximum advantage of the capabilities of the Planck Surveyor mission and to achieve its very ambitious scientific objectives, proper data reduction and scientific analysis procedures need to be defined, designed, and implemented very carefully. The data processing should be optimised so as to extract the maximum amount of useful scientific information from the data set and to deliver the calibrated data to the broad scientific community within a rather short period of time, as stated in the Science Management Plan. As demonstrated by many previous space missions using state-of-the-art technologies, the best scientific exploitation is obtained by combining the robust, well-defined architecture of a data pipeline and its associated tools with the high scientific creativity essential when facing unpredictable features of the real data. Although many steps required for the transformation of data can and must be defined early in the development of the pipeline (and some of them have been already tested and implemented in the simulations made by the teams of the proposing Consortia), some of them will remain unknown before flight data are obtained.

Planck is a PI mission, and its scientific achievements will depend critically on the performance of the two detector systems, LFI and HFI, and on the telescope. The data processing will be performed by two Data Processing Centres (DPC). However, despite the existence of two separate distributed DPCs, the success of the mission relies heavily on the combination of the measurements from both instruments. Moreover, some phases of the data processing are almost identical for both instruments and optimisation of resources demands a common implementation of those parts.

A unifying approach is thus necessary in order to fully achieve the scientific objectives of the mission, and to obtain a single final set of data, derived optimally from all products of the two DPCs.

The HFI and LFI Consortia and the Telescope Provider have agreed on the need to completely integrate the data reduction and scientific analysis approaches; thus in this chapter, sections 3.1 to 3.4 are common to both the HFI and LFI responses to the AO.

This section deals with a topic of wider scope than data processing (reduction and scientific analysis): it also discusses aspects related to information management, which pertain to a variety of activities concerning the the whole mission, ranging from instrument information (technical characteristics, reports, configuration control documents, drawings, public communications, etc.), to the analysis of the impact on science implied by specific technical choices. In particular, an Integrated Data and Information System (IDIS) will be developed to allow proper intra-Consortium and inter-Consortia information exchange. IDIS is described below (section 3.4). IDIS is deemed essential for the proper information management in a project with many CoIs, Associates, engineers and technical and scientific staff (the estimated number of participants is around 200), located throughout countries in both Europe and North America.

For a proper discussion of data processing, the following subsection breaks down data processing tasks into levels, and proposes a scheme for the two DPCs. Organisational aspects, relations between the two DPCs, management, and coordination are discussed in section 3.3. Section 3.5 finally details instrument-specific aspects of the DPCs.

3.2 Data Processing Tasks

The Planck DPCs are responsible for the delivery and archiving of the following scientific data products, which can be considered as the deliverables of the mission (page 10 of ESA/SPC(97)27):

- Calibrated time series data, for each receiver, after removal of systematic features and attitude reconstruction.
- Photometrically and astrometrically calibrated maps of the sky in the observed bands.
- Sky maps of the main astrophysical components.

Others can be added to the formally defined products of Planck mentioned above, e.g.:

- Catalogs of sources detected of the main astrophysical components.
- Data sets defining the estimated characteristics of each detector and the telescope (e.g. detectivity, emissivity, time response, main beam and side lobes, etc ...)

Being naturally dependent on each other, all those products will progressively be built up from raw data. Iterative processing is required to successively refine all the results. As an example, for the evaluation of the beam, a first estimate of the main beam can be made from ground calibration data. A first photometric map of the sky emission can be then be obtained from observations. The next step will then be to use this map for evaluating the contribution of the side lobes, thus obtaining a complete map of the beams.

In the following, four levels of processing (numbered 1 to 4) are defined. They are listed as if some ordering in their execution was implied; however, as stated before, there will be iterative loops among them. The chosen scheme is more "logical" than "chronological". It should be added that all levels will operate simultaneously (although with different time constants) since it is necessary to get the full mission data for extracting information at the different steps.

The activities of the Mission Operation Centre (MOC), carried out by ESA staff, are to be added to this scheme. The MOC is responsible for the tasks listed in page 6 of ESA/SPC(97)27.

Besides MOC activity (to be considered as Level 0), Levels 1 and 2 of the DPCs described below, or some part of them, plus the preliminary step of acquiring data from the MOC, plus other possible steps TBD, should be active on a day-to-day basis during the mission, in order to provide information to the Science Team for possible corrections to be implemented by the MOC, and generally to provide the requested feedback and support.

The actions corresponding to the various levels which are the responsibility of the instruments DPCs are detailed in the following sections.

3.2.1 Level 1 (Telemetry Processing)

Level 1 can be conceived as being accomplished by a single, independent centre acting as an interface between the MOC and the two Instrument DPCs. It is to be noted that the actions of Level 1 are expected to be performed automatically using pre-defined input from the technical teams, and *do not include scientific processing of the data.*

Level 1 operations lead from P/L and S/C raw data to organised data time-lines for each parameter or signal. The input to Level 1 is the data as released by the MOC. The processing is intended to:

a) Lead to the full mission raw-data stream in a form which is suitable for successive data processing by the LFI and HFI DPCs.

b) Perform a routine analysis of the S/C and P/L Housekeeping (H/K) data, in addition to what is performed at the MOC, with the aim of monitoring the overall health of the payload and detecting possible anomalies.

c) Perform a quick-look analysis on the data to monitor normal operation of the observation plan and verify normal behaviour of the instruments. No processing of the scientific data is included.

All actions of Level 1 are supposed to be performed on a "day-to-day" basis during observation. In some more detail, the tasks to be performed by this level are:

- Acquire time ordered P/L scientific and housekeeping data (from FINDAS).

- Record the reconstructed pointing information from the MOC.
- Analyse attitude reconstruction performance (accuracy, stability, etc.) comparing field camera to pre-defined point source catalog.
- Perform data de-compression (TBC).
- Check data integrity.
- Produce time-ordered raw data in a pre-defined format, which should include at least:
  - absolute time (by synchronising all on-board clocks and timers);
  - signal in digital units (DU) from each detector;
  - S/C Attitude;
  - H/K data;
  - other.
- Monitor all housekeeping data. E.g.:
  - temperature sensors output and stability;
  - power consumption of individual units (when recorded);
  - cooling system parameters.

  and generate derived parameter time-lines useful for further steps.
- Quick-look at scientific data allowing real-time links to the ST through the Data Processing Managers (DPCMs) in case anomalous behaviour is detected.
- Self-consistency checks on telemetry vs. "pre-processed" raw data.
- Monitor observation plan and sky coverage. Perform analysis to optimise possible corrections to the pre-defined observation plan.
- Report to ST for new pointing programs for the S/C and/or modifications of the instrument operation mode (compression mode, on-board S/W, gain modification ...) to be possibly fed back to the MOC.
- Archive all data and H/K processed up to this point (raw TOD archive).

The output of Level 1 is the following:

- Data product 1 (deliverable): Raw time series data per receiver after attitude reconstruction, flagging information, etc.
- "Day-by-day" inputs to MOC (instrument health)

3.2.2 Level 2 (Data Reduction and Calibration)

At this level, the data processing steps requiring detailed instrument knowledge (data reduction proper) shall be performed. The Level 2 reduction steps will therefore be concentrated at two separate sites, one for each detector system, processing only data acquired from the related instrument.

Level 2 will utilise the raw time series from Level 1 to reconstruct sets of calibrated scans per detector, instrumental performances and properties, and maps of the sky for each channel. The processing must be iterative, since simultaneous evaluation of a number of parameters is to be made before the astrophysical signal can be isolated and averaged over all detectors in each frequency channel. Continuous exchange of information between the two DPCs, achieved through the IDIS, will be necessary at Level 2 in order to identify any suspect or unidentified behaviour or results from the detectors. When appropriate, time-ordered data and maps, together with all other relevant material, will be made available to Level 4 to be prepared for public access.

The instrument-dependent actions to be performed will be detailed in the Science Implementation Plan, as it evolves from its current draft stage. As an example, it is to be noted that utilisation of the Earth, Moon (if available) and planets for beam pattern reconstruction and absolute calibration will require detailed models (or measurements) of their microwave emission at Planck frequencies. Similarly, there will need to be some sensible evaluation of Galactic foreground emission and systematic error contributions to the error budget. The development of these models is currently not considered part

of the calibration process, but as simulations and modelling developments of each of the instrument Consortia.

Level 2 actions can currently be summarised as follows:

- Evaluation of instrument health and performance, and quick-look analysis (QLA)
- First-level statistics and checks for systematics
  - For each data set and for each pixel, check distribution of the measured voltage in that pixel, V_{pix} (LFI+HFI). Remove spikes and glitches, etc.
  - Evaluate all noise components for each detector (e.g. white noise, $1/f$ noise).
  - Comparison of data relative to various coordinate systems (S/C centred, orbit-angle, spin angle, etc.) and time-periods
  - Perform "relative calibration", i.e., control of gain drifts in each receiver (or correlated) and possible subtraction of their effects. This typically involves monitoring of voltage differences dV_{pix} from opposed pixels in the observed circle or combination of signals from successive circles on the sky.
  - Control possible thermal drifts of the LFI reference load of the radiometers (and check for internal correlations). Perform analogous procedure for the HFI, in particular for monitoring the offset of bolometric channels.
  - Perform correlation between data (V_{pix}, V_{rms}) and H/K data (e.g. temperature monitors, attitude/Solar-aspect angle, etc.)
  - Identification of and quick-look at strong-signal data (e.g. planets, strong HII sources, etc.).
  - Identification of any other systematic behaviour of signal (e.g. cross-talk among detectors, systematic errors synchronised with spin, etc.)
  - Extraction of a preliminary point source catalog (needed for astrometric verification and photometry checking)
- Beam pattern reconstruction
  - Reconstruct the beam pattern using Earth and Moon radiation if possible during transfer to L2 and/or using an iterative process evaluating the contribution of the Galaxy in the far side-lobes
  - Reconstruct the main lobe of each beam using external planets or bright known objects as sources
- "Absolute Calibration"
  - Evaluate the response (from volts to watts) of the detectors by using the on-ground calibration database and in-flight signals.
  - Calibration with CMB dipole (NB: at the necessary accuracy, this will require an iterative procedure between calibration and identification of CMB quadrupole and higher multipoles) or the galactic ridge according to the channel frequency.
  - Absolute calibration with planets.
  - Calibration using spacecraft orbital velocity.
  - Definition of procedures to cross-check data and systematics between HFI and LFI.

- Frequency Maps production
  - At each frequency, combine all data according to the chosen pixelization scheme (HEALPIX is the current baseline) and using an optimisation technique for properly weighting each detector. Given the number of detectors per frequency there is probably enough redundancy to build more than one map: this would be extremely useful for attempts at assessing noise contributions (cfr. 'sum' and 'difference' maps with COBE-DMR).
  - Long-term closure checks.

The output of Level 2 is the following:

- Data product 2a (deliverable): Time series data per receiver after removal of systematic features, etc.)
- Data product 2b (deliverable): Maps of the sky in the observed bands
- Data product 2c (internal): Maps of the sky per detector
- Data product 2d (internal): Point-source catalog associated with the sky maps
- Data product 2e (internal): Performances and beam of each detector, flagging information, variance estimation for each pixel, maps of the systematic effects
- Data product 2f (internal): Updates to the Calibration Database
- "Day-by-day" inputs to MOC and Level 1 (instrument health and performance)
- "Longer-term" inputs to MOC and Level 1 (e.g. modifications of the acquisition mode to be uplinked to the on-board computer, feedback parameters for Level 1 automatic processing, etc.)

3.2.3 Level 3 (Component Separation and Optimisation)

The aim of Level 3 is to transform by means of pipeline processing the frequency maps produced by both instruments into preliminary maps of the underlying astrophysical components. Deliverable products will be prepared in Level 4 under the supervision of the ST. Data from both HFI and LFI need to be analysed jointly to produce the desired result. While it is expected that a number of institutes will participate in this work, two centres (representing the 2 instrument consortia and the Telescope Provider) will be responsible for performing the processing, and to guarantee the integrity and quality of the data products and their availability through the IDIS.

The final maps for each component shall be produced jointly by the two DPCs, under the supervision of the Planck ST. When appropriate, they will be made available through the IDIS, together will all other relevant material, to Level 4 to prepare for public distribution and for further detailed scientific analysis by CoIs and Associates.

It is to be noted that scientific exploitation is outside the scope of the Level 3 pipeline as described here. A specific policy for the "secondary" science goals of the mission, and based on peer-reviewed proposals has been defined in ESA/SPC(97)27 (pages 12-14).

The actions to be performed at Level 3 can be summarised as follows:

- Component separation – This section will require the development of software capable of disentangling the various contributions with no (or minimal) assumptions on the parameters:
  - point sources catalog
  - extended source catalog
  - synchrotron (using polarisation information)
  - free-free
  - dust components
  - SZ effect
  - CMB anisotropies
  - checks with external data and surveys (e.g. DMR, Haslam, IRAS, FIRAS, balloon experiments, ...)
- Noise maps and statistics data set

- Inter-frequency cross-check
  - Internal correlation (at proper angular resolution) of (frequency independent) CMB maps at the various LFI frequencies
  - Internal correlation (at proper angular resolution) of CMB maps at the various HFI frequencies
  - Correlation of LFI/HFI maps
  - Analysis of possible systematic anomalous features in the correlations, e.g.:
    - If from instrumental effects, then refine processing carried out in Level 2, then continue
    - If residual foreground contamination, refine relevant analysis carried out in Level 3, then continue
- Component Maps production
  - Combining all data, produce all-sky maps of CMB, SZ, dust, etc. according to the chosen pixelization scheme (HEALPIX is the current baseline)
- Produce catalogs of radio sources, IR-sources, SZ, etc. to be eventually delivered to the scientific community through IDIS.

The output of Level 3 is the following:

- Data product 3a (deliverable): Preliminary maps of the sky for each of the main underlying components).
- Data product 3b (internal, to be eventually distributed with relevant S/W and documentation TBD): Source catalogs and object cross-identifications.

3.2.4 Level 4 (Generation of final products)

The action to be performed in Level 4 is reception, archiving, and prerelease preparation of all material needed for public release (at least final TOD, frequency maps and component maps), with procedures to be defined in more detail, which will be built in accordance with ESA/SPC(97)27 and with the Science Implementation Requirements Document (SIRD).

- Time-Ordered Data
  - Convert to a format convenient for access by the astronomical community sets of files of Time-Ordered Data, generated by Level 2, with full calibration and systematic error information.
- Final maps
  - Convert to a format convenient for access by the astronomical community the maps at each instrumental frequency generated by Level 2
  - Produce maps for each diffuse component (CMB and separated foregrounds) from the preliminary maps generated by Level 3, according to a pre-defined pixelization and suitable data format(s).
- Prepare all related documentation and explanatory reports.
- Support transfer to FINDAS and maintenance of all S/W for reading, displaying and manipulating data.
- Transfer to FINDAS data products and documentation for distribution.

The output of Level 4 is the following:

- Data product 4a: Files of the Time-Ordered Data with calibration and systematic error information
- Data product 4b: Final maps of the sky at each of the Planck detector frequencies
- Data product 4c: Final maps of the sky for each of the main underlying components
- Data product 4d (To be distributed through FSC and FINDAS): Associated explanatory documentation and basic S/W for Final Data Product I/O and display
- Data product 4e (To be distributed with procedures TBD): catalogs of sources extracted from the sky maps

3.3 Organisation of the pipeline

To achieve the goals mentioned in the previous sections, two separate DPCs will be created, performing operations related to Levels 2 (only on associated instrument) and 3 of the pipeline. This guarantees specific competence on the associated instrument during the daily checking and reporting of instrument performance, and during the process of data calibration. At the same time, the scientific competence available at the DPCs can be used for part of the component separation and inter-frequency cross-checks using data from both instruments. Thus, a proper level of cross-checking can be achieved, by allowing redundant scientific analysis at Level 3, where data from both LFI and HFI are processed in both DPCs.

Level 1 is carried out by a separate Centre common to the two instrument consortia and the TP. This choice leads to optimisation of costs, and allows quicker reaction and immediate cross-checking between telemetry from the two instruments. On the other hand, tasks included in such a Level are not expected to be instrument-critical, and detailed instrument knowledge can be concentrated elsewhere.

To help homogenise the work of the two DPCs, a separate group common to the two instrument Consortia and the TP will carry out tasks related to Level 4. Such a group could also participate in the definition of the processing related to Level 3 in parallel with the other sites, so that a proper level of duplication and cross-checking is made on scientifically-usable (calibrated) data.

The selected approach respects most of the concepts of the original scheme defined in the ESA/SPC(97) 27 document, it allows the optimisation of resources in the preliminary steps of the processing chain, and to exploit instrument knowledge where it is most needed (Levels 2 and 3). At the same time it allows scientific redundancy and cross-checks together with a greater amount of flexibility necessary in the critical phase of the data processing work (Levels 3 and 4). The Planck Science Team (ST) is always kept in the focus of scientific operations.

As a consequence, the two DPCs are organised in a geographically distributed fashion, to take maximum advantage of the expertise available throughout the Consortia, without the heavy costs associated with gathering many experts at two localised centres. This approach is also justified by the indispensable sharing of the high costs of the data processing activities within all participant countries. The field of networking is currently developing extremely rapidly and by the time the full Planck data processing system becomes operational, it is unlikely that its distributed nature will cause any difficulty. In particular, the Integrated Data and Information System (IDIS) to be developed is expected to ease communication and information exchange among the different locations constituting the DPCs. IDIS is described below (section 3.4).

From the geographical point of view, the DPCs will be organised in 5 Principal Sites, based on the following scheme:

Level 1 - A single site representing the two instrument consortia and the TP, at the Observatory of Geneva, at the premises where the Integral Science Data Centre (ISDC) is currently located.

Level 2 - Two sites, one for each instrument: Orsay (POSDAC) for the HFI Consortium, and Trieste (OAT and SISSA) for the LFI Consortium. The TP consortium will participate in the work at both sites.

Level 3 - Two sites, one for each instrument: Cambridge (CPAC) for the HFI Consortium, and Trieste (OAT and SISSA) for the LFI Consortium. The TP consortium will participate in the work at both sites.

Level 4 - A single site representing the two instrument consortia and the TP, at the MPA in Garching.

It is to be noted that Levels 2 and 3 for the LFI Consortium are carried out at the same physical location. For HFI, three major sites are involved and will coordinate closely their activities : Orsay, Cambridge and London (LPAC).

It is the responsibility of the Principal Sites to perform the related steps of the processing pipeline, and to guarantee the integrity of the information and data stored therein.

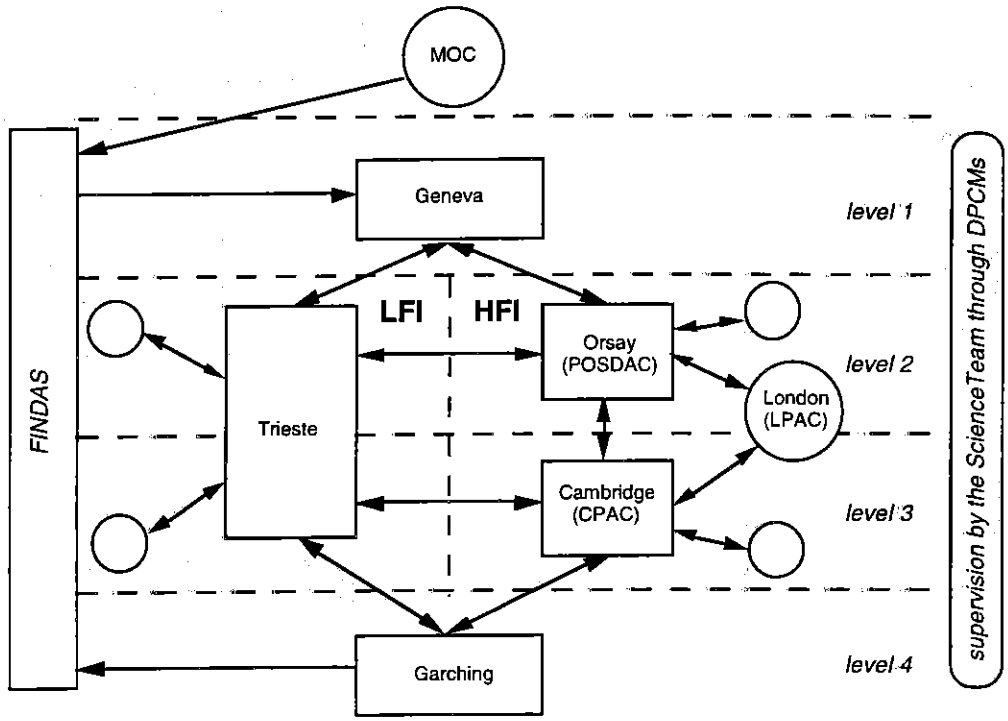

Figure 3.1: Data flow among sites forming the Planck data processing distributed structure. Five Principal Sites (rectangles) and several Secondary sites (circles) are identified. Principal Sites have the responsibility of guaranteing the integrity of data and of processing procedures. In the figure, lines indicate the logical flow of data (all these lines do not imply a physical link between all locations: the implementation of these links will be done according to the best and cheaper available network); information exchange among the sites (inside the boxes) occur within IDIS.

A number of Secondary Sites are envisaged as participants in the various levels of data processing. Some secondary sites are already well identified: London for HFI and IPAC (Infrared Processing and Analysis Center, Pasadena) which should act as the entry point in the USA for the Planck project (TBC). Other sites are still TBD. Each Secondary Site will have some specific expertise on particular aspects of the Planck mission, either technical or astrophysical. In each of these sites one or more mission Co-Is are expected to be working.

Each Secondary Site will be allowed to gather information from the Principal Sites, and to feed back information (with appropriate filtering) to them through the IDIS and according to ST-prescribed data access rights. It should be easy for project staff at a Secondary Site to retrieve information and data from a Principal Site, while ingesting information in a Principal Site will be rigidly checked.

3.3.1 Data Flow

Two figures are presented in this section, representing the data flow among different sites and levels related to Planck data processing.

Figure 3.1 shows the flow of data among the various Principal and Secondary Sites envisaged for the Planck DPCs.

Figure 3.2 describes data exchange for the overall data processing activity in Planck, regardless of geographic distribution. Each Level produces and maintains data in proper archiving structures, which are to be shared with other Levels of the data processing system.

From both diagrams, the complexity of the data flow in Planck data processing can be appreciated.

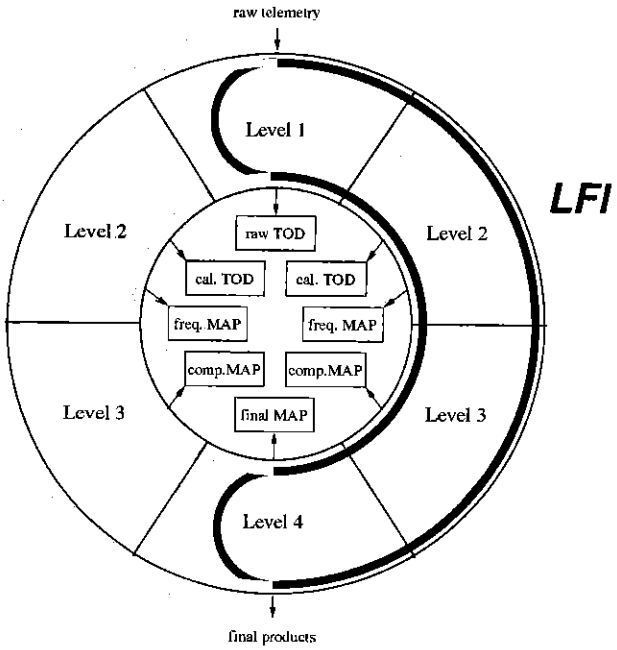

Figure 3.2: Diagram illustrating interactions and commonalities between the HFI and LFI DPCs. Data archives produced by the various Levels of processing are also illustrated: they are to be shared by the two instrument Consortia and the TP through IDIS.

While the time-lines and rules for data exchange between Consortia are still TBD, it is clear that a common mechanism for data sharing is absolutely necessary. This will be provided by IDIS, which is described in the next section.

3.3.2 Management of Overall DPC Structure

The complex and distributed structure of the Planck DPCs requires proper management to be effective, in particular during day-by-day operations.

A DPC Coordination Group (DPCCG) will be created. This group will have representatives of all Principal Sites and Consortia, and will closely liaise with the Science Team. The DPCCG will be a distributed management structure for the overall Planck data processing working on a day-by-day basis, and is expected to have continuous exchange of information among its members, by means of e-mail or tele-conferences which will occur at least on a daily basis during critical periods (launch preparation and initial phase of operations).

3.4 Integrated Data and Information System (IDIS)

Large amounts of information, data and software will be generated during the various stages of the Planck project. These include the development, test and operation of the Planck instruments, and the subsequent processing of the observed data. The IDIS conceptualises a system to provide the infrastructure and the tools necessary to manage these objects efficiently and flexibly. The general requirements for the IDIS have been layed out in the URD (→ Science Implementation Plan). FINDAS will be evaluated as a baseline for satisfying these requirements in the implementation phase.

Hereafter, the term "the IDIS" refers to the system that provides the functionality of the IDIS environment, while the term "software" encompasses all kinds of software running under the control of IDIS.

3.4.1 IDIS Philosophy

Integration. The IDIS must comprise (at least) three different components to carry out its broad diversity of tasks:

- A *data management component* that allows the ingestion, efficient management and extraction of the data (or subsets thereof) produced by Planck activities.
- A *software management component* that encompasses the software required to administer, handle, and analyse these data.
- A *document management component* that contains documentation pertaining to both software and data controlled by the other two components, or other relevant documents.

Efficient use of the IDIS requires that these components be inter-connected. It must be possible to relate objects under the control of one component to objects controlled by another component.

Accordingly, the IDIS can be thought of as a *federation layer* consisting of software, data and documentation standards, and software supporting these standards (cfr. Figure 3.3). It provides the infrastructure within which all Planck-related activities may be performed in a consistent and coherent way, from the development of the payload to the delivery of the final data products.

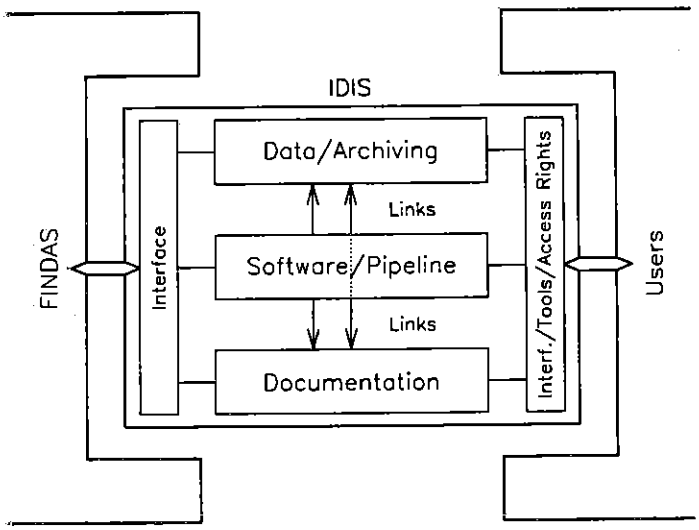

Figure 3.3: IDIS structure

Distributed Environment. Users of the IDIS will be situated at many institutes in several European and North American countries. Efficient use requires that the IDIS be a system geographically *distributed* over many sites (see also §3.4.3). Certain types of tasks can then be performed locally at these sites in order to minimise access and execution times. Sites need to communicate regularly, in an automated fashion if practical, in order to guarantee consistency of the system and maintain configuration control. Sufficiently fast and reliable network connections between the sites are thus necessary, and the system must provide automated procedures for mirroring data and replication of software to all appropriate sites.

Classes of Users; Typical Tasks. The prospective users of the IDIS can broadly be grouped into four classes. They are listed and described here together with the typical tasks they are likely to perform within the IDIS.

- *Site Managers* are people chiefly responsible for the operation of the IDIS at their site. Their detailed responsibilities are given in §3.4.3. The IDIS must support the tasks of site managers via federation components which track the objects and users in different parts of the system.
- *Planck Scientists* form the largest group of the IDIS users. Typical IDIS tasks performed by this group include

  - accessing and up-loading documentation and data;
  - communicating with other users of the IDIS using standard mail protocols;
  - accessing, visualising, analysing, and processing data stored in the IDIS;
  - creating and distributing data and documents;
  - creating and running software modules on data stored within the IDIS, in the process generating new data;

  The IDIS must provide such users with the necessary tools and access rights required to carry out these tasks. Apart from data and document management tools, the issue of software pipelines is particularly important. It will be further detailed below.
- *Developers* are people who develop and test new components for the IDIS. IDIS standards for coding and interfaces must be defined. All IDIS components must conform to these standards. Developers must be able to access data and software controlled by the IDIS, and to submit new or revised components together with the respective documentation for insertion into the IDIS. For that purpose, a software release policy needs to be defined, and the IDIS must contain tools that allow site managers to implement this policy. Configuration control is essential to track the released versions of software and documentation across the distributed system.
- *Astronomical Community*: Ultimately, Planck data, software, and documentation will be released to a broader astronomical community. A limited number of the IDIS services must then be accessible to such users, and the IDIS must contain web-based components implementing and facilitating such use of the IDIS.

It is envisaged to use the IDIS also to prepare and distribute all kinds of material required for PR activities as requested by ESA in the Public Relations Plan.

Given the diversity of prospective users and tasks, the IDIS must provide a mechanism to control the access rights of users to all objects within the IDIS components. This requires tools with which the IDIS managers can set, change, and track user privileges across the distributed system. Evidently, corruption of the system by users must be prevented.

External Interfaces. There must be an IDIS user interface to query the system. Tools and application programming interfaces must be provided for basic visualisation and analysis of data objects. Application programming interfaces will be written for component developers. Web-based interfaces will be developed at a later stage to allow the general astronomical community access to a limited number of IDIS services.

The IDIS must support an interface to receive data from, and deliver data to, FINDAS. An estimated 5 GBits per day will be transmitted from FINDAS to the IDIS. To allow the ingestion of this amount of data within a few hours, data transfer rates of order ~ 0.5 MBits per second are necessary between FINDAS and one of the IDIS principal sites.

Software Pipelines. Data sets produced during the development, testing, and operational phases of the Planck instruments will be visualised and analysed by a multitude of users in many different ways. Sufficiently flexible use of the IDIS calls for modular software whose components can be combined to form complex *software pipelines*. This has several implications:

- Software components must be modular, and they must comply with coding and interface rules.
- Users must be able to construct sufficiently complex software pipelines from the IDIS software modules. Several such pipelines can exist in parallel, and they can be partially identical. It should also be possible to run parts of existing pipelines independently, and it must be possible to run pipelines iteratively.

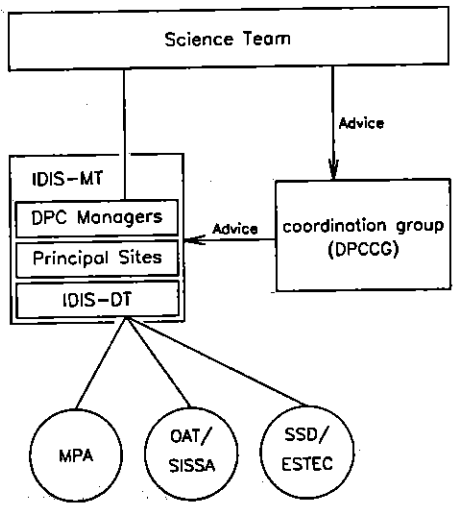

Figure 3.4: IDIS management structure

- The IDIS should allow parts of pipelines to be run locally, and parts remotely. This requires appropriate messaging between sites, and the control of access rights.
- The IDIS must allow the storage of existing pipelines for later re-use.

Self-Documentation; Linking of Objects. Flexibility and efficiency also demand that all objects in all the IDIS components be uniquely identified, and that software and data be documented. The IDIS must therefore link together objects managed by different components, and maintain a controlled relation between software, data objects, and their respective documentation. In addition, data objects should contain headers clearly and uniquely defining them, their originating software and the parameters with which they were generated.

Final Data Products. The IDIS will maintain a complete, distributed archive of all data produced by all processing Levels, including house-keeping data. Final data products will be released to the public, with the IDIS managing the corresponding data archive and relevant software for exploitation and analysis of the data. Complete documentation of instruments, data products, and software will be prepared and released through the IDIS. Finally, the IDIS will deliver data products, documentation, and relevant software (TBD) to FINDAS.

3.4.2 Development

Development Tasks. The development of the IDIS components and their integration into the complete system will be carried out by three *development sites*, MPA Garching, OAT Trieste, and SSD/ESTEC Noordwijk. Their joint activities will be monitored and coordinated by the IDIS Development Team (see below). The development sites will provide the manpower and resources required to develop the IDIS. Work-packages will be defined and assigned to the IDIS development sites. A preliminary breakdown of work-packages is given as an attachment to the Scientific Implementation Plan (SIP).

Planck Pilot Project. The development and integration of the IDIS must begin very early in the project. For that purpose, a *pilot project* will be launched, aiming at a preliminary implementation of the IDIS by December 1999. In the course of the pilot project, the IDIS prototype will be tested on a

realistic simulated data stream and will incorporate a preliminary documentation system for the Planck project.

3.4.3 IDIS Development Organisation

Sites; Site Managers. The IDIS will be geographically distributed over many sites. Three of them (MPA Garching, OAT/SISSA Trieste, and SSD/ESTEC Noordwijk) will be *development sites* concerned with the development, implementation and management of the IDIS itself; there will be a larger number of *user sites* making major contributions to the Planck project in other areas. Accordingly, the IDIS must operate and be managed in a decentralised manner.

The *development sites* jointly guarantee the integrity of the IDIS. They support the setup and the initial phase of operation of the IDIS at user sites. Apart from this, each site will be responsible for proper operation of its own resources.

Each site will nominate a *site manager*. These will be responsible for the proper operation of the IDIS at their sites. In particular, sites must run the appropriate tools to maintain communication between sites. Site managers will administer access rights to the IDIS, and they will also be responsible for carrying out specific tasks assigned to their site. Finally, development site managers will decide about the acceptance of any object to be ingested into the IDIS at their site, following established guide-lines.

IDIS Development and Management Teams. An additional *IDIS manager* will be nominated who coordinates and oversees the efforts of the three development site managers. These four managers form the IDIS *development team* (hereafter IDIS-DT). The IDIS-DT will be chaired by the IDIS manager. While the IDIS-DT is responsible for implementing and maintaining the software providing the functionality of the IDIS environment, the responsibility for the overall data reduction and analysis pipelines ultimately rests with the DPC managers. An IDIS *management team* (IDIS-MT) will be formed comprising the IDIS-DT, the DPC Managers, and the Principal Site Managers. It will be the responsibility of the IDIS-MT to direct the design, development, integration, and testing of the IDIS, keeping track of the current status of the IDIS and assigning specific IDIS-related tasks to sites as required. The IDIS-MT will meet at regular intervals and report to the Planck Principal Investigators directly through each instrument's data processing manager. The IDIS-MT will resolve conflicts among the IDIS parties.

The IDIS-MT will liaise to the Planck Science Team via a coordination group (identical with the DPCCG once this is set up). This group will advise the IDIS-MT on all aspects of the IDIS development, maintenance, and operation (e.g. by suggesting guide-lines for granting access rights of individual users to the IDIS, etc.). Further detail on IDIS management is given in subsection 2.3.2 of the IDIS URD.

3.5 LFI-specific implementation

In the previous sections, the concepts of data reduction and scientific analysis, together with some information management aspects, which are in common between the HFI and LFI consortia have been described and discussed. In this section, the peculiarities of the implementation planned by the LFI consortium are described.

In particular, the organization of the work in the various phases of the LFI DPC (development, operations, and post-operations/archive), the Quality Assurance procedures, the responsibilities and allocated resources, and the organisation structure are described in this section. Furthermore, for each Principal Center of the distributed DPC structure, the infrastructure and hardware configuration and the logistical aspects are discussed, as can be possibly envisaged at the time being.

3.5.1 DPC Development

The LFI consortium has an organization in which Working Groups (structures open to interested individual scientists and technologists) play an important role. They provide advice, but also prototypal inputs

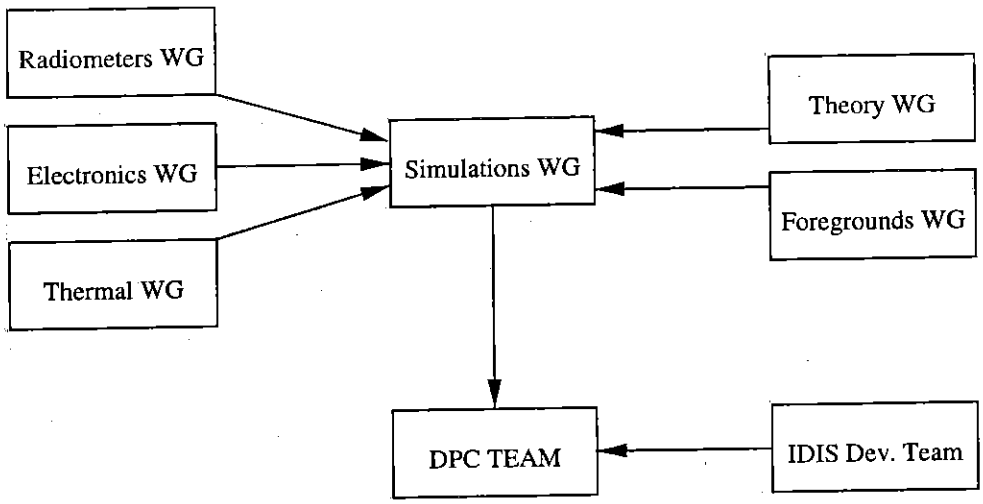

Figure 3.5: Diagram evidencing the inter-relations among LFI Working Groups. Instrument and scientific WG provide inputs to the Simulations WG, which produces prototype software for the DPC Team. The software is integrated into the pipeline using the environment software provided by IDIS.

to different aspects of the project (see Section 8 for details). Their impact on LFI data processing and on the DPC development is described in the following, and is shown in figure 3.5.

The Working Groups dealing with hardware components (Radiometers, Electronics, Thermal WGs), and those dealing with the scientific aspects of the mission (Theory and Foregrounds WGs) all provide inputs to the Simulations WG. The latter is already developing simulations which represent an ideal sky in the various frequency bands covered by LFI and, introducing realistic degradations due to the instrument performance, is producing simulated observations, i.e. timelines. Information on instrument performance will be kept in a preliminary Calibration Database, which will be based on ground measurements of instrumental characteristics (see Section 4.2.1).

The various Working Groups will define the requirements the data processing S/W, subdivided in Data Reduction Software (DRS, basically corresponding to the Levels 1 and 2 defined in section 3.2) and Scientific Pipeline Software (SPS, basically corresponding to Level 3), shall satisfy to allow the scientific goals of the mission to be accomplished.

The Simulations WG will also develop prototype Data Reduction S/W, which will make use of the preliminary Calibration Database to derive from the simulated timelines the sky degraded by the instrument performance. Science analysis S/W will also be developed freely by scientists participating in the LFI consortium, in order to test the most effective ways of extracting science from calibrated data. This software will be provided to the LFI DPC as prototypes for the SPS.

In this development, the scientists in the Simulations WG will take advantage of IDIS tools, and namely of some of the Application Programming Interfaces (APIs), especially those related to data formats, data visualization and management. However, it is clear that prototype S/W developed by scientists for simulation purposes is not expected to have the robustness, documentation and maintainibility that DPC pipeline S/W is expected to provide. For this purpose, an integration team (the DPC Team) will engineer the prototype Data Reduction and Science Analysis S/W into production S/W, satisfying all requirements defined in the phase described above. Efforts will be also specifically concentrated on the possibility of correct recovery in the case of hardware failures, and on the concept of providing "warm" or "cold" backup capabilities at operations time.

The development phase will consist of four main phases for the S/W built to support each of the levels of processing defined in section 3.2:

Design - in this phase, the architecture of the data processing pipeline will be defined in detail, so as to

be fully compatible with the IDIS structure defined jointly with the HFI consortium. While S/W related to common phases of the processing (Levels 1 and 4) are expected to be designed with the HFI consortium, S/W which is LFI-dependent or which is expected to provide redundancy and cross-checking will be designed independently by the LFI consortium.

Integration - in this phase, the pipeline S/W will be developed. Prototype S/W developed by the Simulations WG will be re-engineered to fit design, requirements and constraints. The integration phase will be carried out in close contact with the scientists to avoid divergence of results from expectations.

Testing - the results of the pipeline S/W will be compared with those of the prototype S/W; they should be reproducible within the error margins specified in the requirements. Global testing of the pipeline will also be implemented, to verify its ability to perform unattended, and its robustness. The driver for the testing phase will always be correctness and data integrity.

Maintenance - once the pipeline S/W has been integrated and has become operational at the DPC, further refinements of the DRS or SPS may continue inside the Consortium, or bugs may be discovered. A proper S/W maintenance scheme will be developed, in accordance to the decisions made in the IDIS collaboration, to allow a proper maintenance scheme for pipeline S/W.

3.5.2 DPC operations and interaction with spacecraft operations

The functional scheme for the LFI DPC at operations time follow tightly the requirements set by ESA in the Science Implementation Requirements Document (SIRD).

On a daily basis, two basic tasks will be performed:

- Instrument health and performance monitoring will be performed with Real-Time Analisis (RTA) software at the Level 1 of the LFI DPC. This includes acquisition of all telemetry from the MOC (via FINDAS), the display and monitoring of relevant information on instrument status, checking of limits, and deriving and display of additional parameters.

- Instrument Quick-Look Analysis (QLA) will be performed at the Level 2 of the LFI DPC. This includes acquisition of all data from the Level 1 of the DPC, selection and display of science data, deriving and display of additional parameters, assessment of detector behaviour, pointing verification, identify and propose possible changes in the instrument parameter settings and operations scenario. The latter will be provided as change requests to the MOC via FINDAS.

With less stringent time requirements, Levels 2 and 3 of the LFI DPC will provide both continuous data processing during operations (including quality checks on scientific data, calibration and updating of the Calibration Database, understanding and removing the systematics decribed in section 1.2.2, cleaning, and preliminary separation of astrophysical components) and DPC maintainance (including infrastructure, hardware, software, documentation, backups, updates). At regular intervals (TBD) intermediate data products will be exchanged (through IDIS) between Levels 2 and 3 of the LFI DPC and the corresponding Levels of the HFI DPC for comparison and cross-check.

No direct interaction of DPC operations with spacecraft operations is foreseen. All communications with spacecraft operations (handled by the MOC) occur through the FINDAS interface.

3.5.3 Post-operations / archive phase

During the post-operations phase (i.e. after the completion of the second Planck survey), the MOC and Level 1 of the LFI DPC will become inactive, Levels 2 and 3 will gradually decrease their activity, and Level 4 will start (or increase) its own activity. As described in the SIRD, three sub-phases can be envisaged:

Data reduction phase - lasts at most 1 year after end of operations. In this period, the final calibration is achieved by the Level 2 of the LFI DPC and the final version of the Calibration Database is produced. At the end, the data products will contain at this stage only well understood anomalies and/or peculiarities. Level 3 of the LFI DPC, through data exchange (through IDIS) with Levels 2 and 3 of the HFI DPC, will continue implementing preliminary separation of astrophysical components.

Proprietary period phase - lasts at most 1 year after end of data reduction phase. Level 2 of the LFI DPC will remain active only for possible (minimal) revisions of the DRS, while Level 3 will finalize the separation of astrophysical components using the final SPS. Data products will be exchanged (through IDIS) with the corresponding Level of the HFI DPC for comparison and cross-check. Level 4 starts preparing procedures and documentation for the distribution of the final products.

Data products distribution and access phase - the final products of the mission are made available (through IDIS) to Level 4 of the LFI DPC (in common with HFI). Level 4 will finalize the distribution of the data products and of the associated documentation to the astronomical community via a convenient medium (TBD) and, where appropriate, through FINDAS.

3.5.4 Quality Assurance procedures

All products (software and data) will undergo standard assurance and quality control procedures, in accordance with the rules set in the PSS-05 document, as required and/or appropriate. Such procedures are at the moment TBD. A Quality Assurance workpackage is foreseen in the management scheme for the LFI, described in Chapter 8.

3.5.5 Organization structure

In figure 3.6, a scheme for the organization of the data reduction and science analysis section of the project is depicted. The overall effort includes a Requirements section, a Prototyping section, a Pipeline Production (and maintenance) section, and an Operations section (including also post-operations). Coordination and Quality Assurance are guaranteed by the Data Processing Center Manager (DPCM) and by a Quality Assurance team dedicated to the data processing S/W and to the resulting data products.

The task of the Requirements section is to gather all requirements, from the user point of view, the DRS and SPS operating in the pipeline shall satisfy to accomplish the scientific goals of the mission. The task of the Prototyping section includes the production of prototype software performing data reduction and science analysis to the precision desired. The responsible of such Sections will coordinate the efforts of the Instrument, Simulations, Theory and Foregrounds WGs and liaise with the DPCM.

The Pipeline Production (and maintenance) section shall be responsible of the integration of all software, either prototypal (imported from the Requirements and Prototyping section), or project-wide (e.g. imported from the IDIS development effort), or built independently, into a robust pipeline. Such software shall at the end of the effort support DPC operations. Design, integration, and testing of the pipeline are foreseen as activities; each will deal with the production of the various levels of DPC software (Levels 1 through 4, as defined in Section 3.2). Design, integration, and testing will be managed separately, and the responsibles of each of such activities shall be coordinated by the responsible of the section, who shall liaise with the DPCM.

The Operations (and post-operations) section shall ensure the actual implementation of the pipeline in the three Principal Centers defined for LFI (Geneva, Trieste, and Garching). An operational structure is defined for every level (from 1 to 4) of the data processing. There will be a responsible for operations for each of the levels. During spacecraft operations, Levels 1 through 3 will be active, and Level 4 will be in a preliminary stage; after spacecraft power-off, Level 1 will cease operations, and Levels 2 through 4 will be active. The responsibles for each of the levels shall be coordinated by the responsible of the section, who shall liaise with the DPCM.

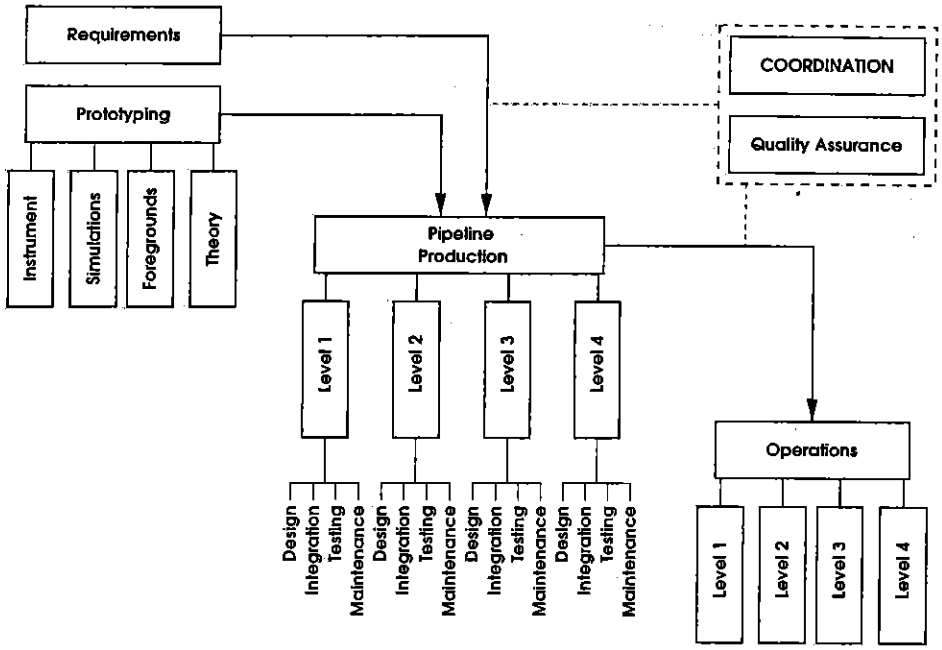

Figure 3.6: Diagram showing the organization of the work (from the gathering of requirements down to operations, through the phases of prototyping and integrating the software in the pipeline) for the LFI DPC. Standard Quality Assurance procedures will apply to the formal phases of software production.

The Quality Assurance team shall perform standard assurance and quality control procedures (currently TBD), as required and/or appropriate, on all products (data processing S/W and resulting data). The responsible of such activity will coordinate with the DPCM.
This organization scheme is reflected in the Workpackage breakdown structure described in Section 8.

3.5.6 Staffing required

During the various phases which the DPC will undergo (development, operations, post-operations), different staff with different competences will be needed. The following professional profiles have been identified for the LFI DPC, and the relative responsibilities are listed below:

Managers	coordination and management
	reporting to ST, if relevant
	contacts with MOC and ST, if relevant
Network Specialists	network management
	system management backup
System Specialists	system management
	IDIS management
	network management backup
	database/archive management backup
Database Specialists	database administration
	archive management
	IDIS management backup
Instrument Scientists	analysis of instrument health & performance
	quick-look analysis
	data quality monitoring
	pipeline monitoring

Data Proc. Scientists	pipeline monitoring & maintenance
	overall quality assurance
Programming Staff	writing specific data processing procedures
	writing system software
	software maintenance
Operators (2)	running the pipeline & archive
	handling of backup tapes from MOC
Support Staff	system hardware maintenance
Secretaries	secretarial support

The additional presence of guest astronomers (duly authorized by the PI) would be highly desirable for such activities as sources identification and the definition and processing of follow-up observations. In any case, collaborations with institutes where knowledge in the field of cross-correlation of identified sources with existing catalogues is available (e.g. the CDS, Strasbourg) will be considered as an integral part of the LFI DPC activities.

As for the duration of the project, the Development phase is expected to last 6.3 years, the DPC Operations phase 3.5 years, and the Post-operations phase 2.5 years, for a total project length of 12.3 months. The duration of the Operations phases is estimated taking in account the maximum length of the various FIRST/Planck operational phases (LEOP, Commissioning, PV, Science Demonstration, FIRST Key Programmes, Planck Routine Ops), as described in the SIRD.

The total manpower, to be expressed in FTEs (personyears), and to be computed over a project lifetime of 12.3 years, has not been fully defined, being the definition of the data processing blocks quite preliminary. An estimate for the overall effort results in a total of about 330 FTEs over a period of 12.3 years. This effort includes design and implementation of all the system and data processing software, including participation to IDIS development (shared with the HFI and TP Consortia), and running DPC operations at the 3 foreseen Principal Sites (Geneva, Trieste and Garching). To the above manpower, the effort put in simulations and prototypal software development has to be added. It is furthermore assumed that a part of the project-specific Data Reduction Software (DRS) can be procured, if necessary, by means of contracts with external providers.

3.5.7 Local implementations

This section describes the status or the plans concerning computer infrastructure, networking, logistics and staffing of the Principal Sites for the LFI DPC (Geneva, Trieste and Garching), and of the Development Sites for IDIS (Trieste, Garching and the Astrophysical Division of ESA). It is to be noted that all of these sites participate in the IDIS definition.

Geneva

The activities of the Level 1 processing will be based on the experience gained in the INTEGRAL Science Data Centre (ISDC). This centre has responsibilities for the INTEGRAL mission that include those proposed here in Level 1. The centre is attached to the Geneva Observatory which is the institute of astronomy of the Geneva University. The Planck Level 1 data processing will be performed by a group of people independent but closely related to the ISDC, who will also participate in the definition of IDIS. The funding for this element will be requested from the Swiss confederation.

The INTEGRAL system that is being developed now is based on several subsystems. Three of them are relevant here:

The data receipt that receives all the spacecraft and instrument telemetry together with the associated auxiliary data (attitude and orbit) from the MOC in near real time.

The preprocessing which decodes the telemetry and stores the data in appropriate formats (FITS) in the archive for use in all subsequent analysis.

The observation status monitoring which is a set of tools to monitor the progress of the operations and data collection and matches this with the expected data based on planning information. This subsystem has an automatic and an interactive part.

We intend to use a very similar architecture and to modify the tools that will be available for INTEGRAL to match the needs of the Planck mission and data, following the concepts of the IDIS. The daily operations will also be based on the experience gained during the life of INTEGRAL, in particular for what concerns the daily monitoring of the housekeeping telemetry which we expect to be very similar.

The total manpower requirement based on this scenario is 18 manyears for the developement and 5 manyears per year during operations, for an estimated total of 38 manyears.

It is not possible now to define the hardware that will be used in 2005 for the type of work envisaged here. The evolution of the products is such that any prediction will be highly inaccurate. We nonetheless foresee that each person will require the equivalent of a present day workstation and that some central archiving facility will be needed (it is quite possible that by the launch all data can be stored on a disk system).

Planck data will be sent from the MOC to the ISDC location via a dedicated network connection, possibly using the tools in place for INTEGRAL. The bandwidth needed is still TBD, and will be defined in the Science Implementation Plan (SIP). We expect to use the international network for further dissemination of the data. The ISDC is linked to the Swiss network now with a bandwidth of 34Mbits/sec, sufficient also for the Planck mission (few Gbytes per day). This will be upgraded in the coming years to some 600 Mbits per sec. The costs related to the use of these networks by university institutes will depend on political decisions and cannot be assessed now. In any case, the Geneva team will participate, in the framework of the IDIS work, in the definition of the networking requirements for the data flow between Levels 1 and 2 of the Planck DPCs, and will support data delivery to Level 2 with the adequate bandwidth.

It is expected that the University of Geneva will meet the costs related to office space and telecommunication.

Trieste

Levels 2 and 3 of the LFI DPC will be hosted in Trieste as a joint effort carried out by the Astronomical Observatory of Trieste (OAT) and the International School for Advanced Studies (SISSA). A close collaboration among the two institutions and the Astronomical Observatory of Padova (OAPd) for the scientific organization of the work is already active since late June 1996. Furthermore, OAT will design, develop and integrate the LFI pipeline; it will participate in the development of the IDIS infrastructure, and will verify its suitability to the LFI pipeline.

From the point of view of infrastructure and hardware configuration, it is reasonable to assume that appropriate and much more powerful hardware and software will be available when LFI DPC operations will start. In the following an estimate for the hardware/software configuration needed is given, using products commonly available in 1998 as the baseline.

Network: connection with guaranteed bandwidth to the Level 1 Site (requirements TBD, probably 512 kbps), connection with guaranteed bandwidth (requirements TBD) to the Level 4 Site, router, upgrade of Internet line to the Italian Research network, fast dedicated line OAT-SISSA, extension to FDDI LAN, bridges

Computers: 2 computational servers of adequate power (multi-CPU) for running the pipeline, 1 network server, 1 database server, 1 data server, 10 science analysis workstations, 10 X-terminals, 5 PCs

Peripherals: disk storage (500 GByte typical), juke-box of magneto-optical disks, 1 magneto-optical disk unit, CD-R (and/or DVD) writer with juke-box (2 units), 2 CD-ROM (and/or DVD) readers, 2 DAT units (with autoloader), 2 laser b/w printers, 2 color printers

System software: DBMS (client-server, development, mirroring licences), data processing environment system (multi-CPU licence), CD-R (and/or DVD) writer software, juke-box handling software, project-specific Data Processing Software

The OAT will provide a total of 104 manyears over the expected 12.3 years duration of the project (over 70 manyears covered by internal permanent staff scientists and engineers). SISSA is planning to provide a total of 70 manyears, the OAPd additional 25 manyears.

The OAT will provide the related infrastructures and logistics. The OAT is currently expanding its premises: a building near OAT headquarters has been recently acquired, and a new building will be built in the Basovizza branch station (construction will start within 1998). Funding for construction has already been allocated by the local government. The Board of Directors of the OAT has already approved to host the LFI DPC and to allocate an area of $\sim 200\ m^2$ for it in one of the new buildings. Personnel from SISSA and the OAPd participating in the LFI DPC will have proper facilities and work places at the OAT, in the area dedicated to the LFI DPC.

A proper conditioned room shall be provided to keep the computer servers (computational, network, database, data). In such a room, proper cabinets shall be available to store off-line data (*e.g.* CD-ROMs, DATs, DVDs). Being this room devoted to operations, and being likely to contain off-line proprietary data, restricted access (*e.g.* via magnetic card) must be enforced.

During operations and post-operations time, logistics will be provided for the DPC staff ($\sim$ 15 people), plus 3 to 5 work places for guest scientists.

Garching

Level 4 of the Planck Data Processing will be supported in Garching by the Max-Planck Institute for Astrophysics (MPA) for both the LFI and HFI consortia. The Garching data centre will support the two instruments equally. MPA will also take a substantial role in developing the IDIS for both instruments and is responsible for ensuring that it conforms to the needs of the HFI pipeline.

From the point of view of infrastructure and hardware configuration, the equipment listed in the following is available or will be provided.

Network: assured average bandwidth to Trieste, Paris, Cambridge (requirements TBD), router

Computers: multi-CPU server for running Pipeline elements (dedicated 2-CPU SUN UltraSPARC II workstation with 1 GByte core memory already in place), network servers, database server, data server, science analysis workstations X-terminals. Access to the Computer Centre of the Max-Planck Society in Garching (RZG), operating among others a 688-CPU Cray T3E supercomputer with 85 GBytes core memory (currently the ninth largest in the world), a 20-CPU IBM/RS6000 SP2 workstation cluster, and several high-end graphics workstations.

Peripherals: disk storage (of order a TByte), CD-ROM juke-box, disk units, CD-ROM writer and reader, DAT units, tape robots, color- and grayscale laser printers. Access to mass-storage devices at RZG with a capacity of over 130 TBytes.

Software: DBMS (client-server, development, mirroring licenses), data processing environment (multi-CPU license), software for peripherals, project specific Data-Processing Software.

The MPA will provide the infrastructure and logistics to support Level 4 of the Planck Data Processing. About 200 square meters of the institute building currently occupied by MPE has been allocated for use by the Planck Level 4 facility, and will be available by the beginning of 1999. This area will be modified to accomodate an appropriate environment for the Planck-dedicated computer system and user terminals, together with offices for the MPA Planck staff. Further office space will be available to support guest scientists.

In Germany the total requested support for Planck Surveyor is at the level of 105 man-years of personnel over the mission lifetime in addition to in-house scientific and computer support at MPA. Additional in-house technical support for the Garching data centre is already in place (currently about 25 man-years plus the necessary space allocation). The in-house scientific support for the mission is not included in the funding request and is estimated at about 25 man-years. The Max-Planck Society has already agreed to provide additional funds for the initial phases of IDIS development beginning in 1998 (about 6 man-years

until 2001) and agrees in principle to fund an appropriate part of the additional hardware request. Negotiation with the Observatory of Munich's Ludwig-Maximilians University is underway for participation at the level of 12 man-years of a technical position. Finally, the DLR is currently evaluating a funding request for the balance of resources required until the end of the project.

Astrophysics Division of ESA

The Division will contribute in approximately equal part to both the LFI and HFI projects by means of developing part of the IDIS system for use by the DPCs and development teams. It is ideally placed in establishing interfaces with FINDAS. Post launch we will assist in maintenance of IDIS and would be willing to host a data-repository.

SSD has a well equipped Computing Infrastructure based mainly on SUN Solaris work-stations. Office automation uses both PC's and Macintosh. An in-house developed Document Management System is available for Planck use.

Presently the division shared in 2 Mbps connections to NL-NET, which must be supplemented to support the Plant Intranet of IDIS.

Bulk data are stored on a, multi-project, Terabyte optical storage device in an AMASS hierarchical data-management system dedicated to divisional use. This incorporates a AIT/DLT robot system, initially sized at 9 Tbyte (multiply expandable).

The in-house DBMS is Oracle 7 (8).

The computer system is supported by a full-time system administrator/manager and several part-time operators.

Chapter 4

Testing and Calibration

The overall LFI philosophy will be to test and measure the performance of individual units separately as early and as fully as possible. Figure 4.1 shows the radiometer flow of testing from the device, to the component, to the subsystem, and on to the system level. Testing will ensure compliance with performance and environmental requirements. At each level, test procedures will be established and followed to assure repeatability and compliance with standards. In all cases, the tests will be done against established requirements. Items not passing will be rejected, and if possible, reworked until acceptable.

TABLE 4.1

LFI SUBASSEMBLIES

Assembly	Subassembly	Component/Unit
Radiometer	Front end unit (FEU)	Horns and OMTs/phase switches
		Hybrid couplers and amplifiers
	Back end unit (BEU)	Amplifiers and detectors
		Video amplifiers
		Multiplexers and ADCs
		Amplifier bias supplies
		Interfaces to SPU and DPU
	Waveguides (WG)	Waveguide and Coaxial cables
	Radiometer Electronics Box Assembly (REBA)	Data Processing Unit
		Signal Processing Unit
		Power Supply Unit
Sorption Cooler .	Sorption Cooler Compressor (SCC)	Sorption Compressor Elements(5)
		Joule Thompson Expander
	Sorption Cooler Piping (SCP)	
	Sorption Cooler Elecctronics (SCE)	

4.1 Testing

4.1.1 Front end unit

The FEU is the most critical assembly in the LFI, and requires the most exhaustive testing. Testing begins at the wafer level during processing, at which time the MMIC amplifiers or discrete transistors are screened for DC characteristics. After processing, on-wafer measurements of noise and gain are used to identify devices with low noise. Following dicing of the wafer, selected chips are matched for gain, noise, and other characteristics. in order to balance the two legs of the pseudo-correlation radiometers. At this point the selected chips are bonded into housings, mated with input and output hybrids, and measured for noise temperature, gain, bandwidth, gain stability, phase-switch balance, VSWR, power dissipation, and variation of gain, phase, and noise with temperature and bias, all at room temperature. Since these units will be operated at 20 K in the LFI instrument the assemblies with good performance are then mounted in a vacuum dewar and cooled to 20 K, by a closed-cycle helium refrigerator whose temperature can be accurately controlled, and the measurements repeated.

Cryogenic tests will be performed to optimise and verify the gain and phase match, as well as the receiver noise and stability. Optimisation will be carried out primarily with bias tuning, possibly including

mechanical phase tuning for the 30 and 44 GHz channels. Bias settings and noise and gain data will be maintained for room temperature and cryogenic tests in order to facilitate ground calibration verification.

TABLE 4.2

PERFORMANCE TESTS

Item	Performance tests
Horn	FOV, Beam efficiency
OMT	Inserion loss, Return Loss, Isolation.
Front end modules	Noise, gain, phase, DC power, VSWR, stability.
Back end modules	Noise, gain, phase, DC power, VSWR, stability.
Radiometer(FEU to BEM)	Noise, gain, linearity, DC power, stability, spectral response.
Radiometer Electronics Box Assembly	Functional test, DC power, PSU noise and stability.
Sorption Cooler System	Temperatures, heat flows, input power, stability

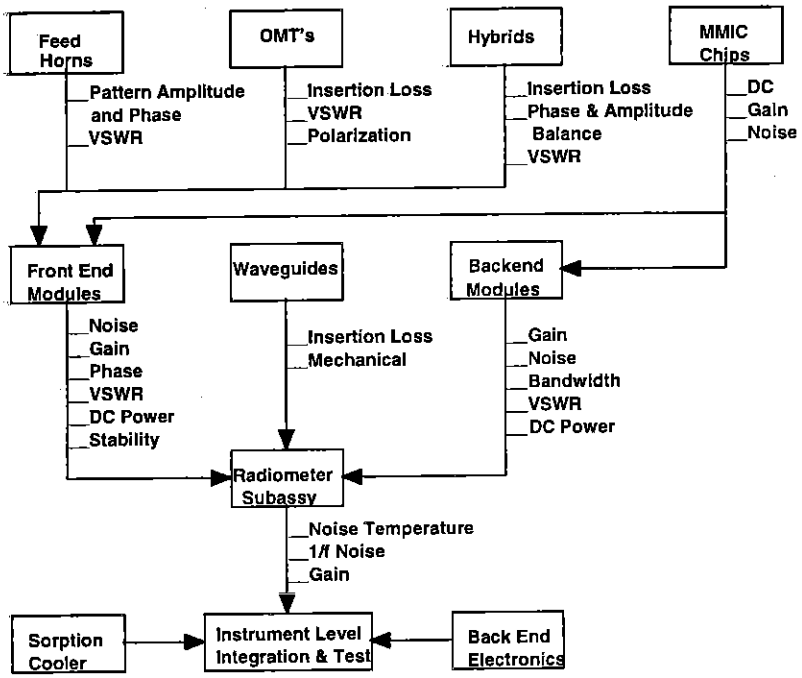

Figure 4.1: Test flow of the Low Frequency Instrument.

4.1.2 Back end unit

The approach to assembly and testing of the Back End Modules (amplifiers, detectors and video amplification) is similar to the one described for the front end modules, the main difference being that no cryogenic measurements are made since the unit is not cooled. The BEU has no requirement for phase matching and the gain match requirement is less stringent than for the front end modules. In addition, since the BEU includes the detector diodes, the output will be DC through audio frequency rather than RF, placing different requirements on the test facility.

After module testing, the back end modules and the data aquisition electronics are integrated, and the Back End Unit performance tested by inspection and analysis of the raw output data.

The DC amplifier bias supplies, which are housed within the Back End Unit, will be characterised for stability, noise and bias range. Due to the sensitivity of the amplifiers to small amounts of noise in the bias supply lines, the bias supply units will be carefully checked for conducted susceptibility.

4.1.3 Horns, OMTs, waveguides

The electrical properties of the horns, OMT's and the combination, including scattering parameters and radiation patterns will be measured in an anechoic chamber equipped with a vector network analyzer. Aperture coupling pairs of horns or pairs of OMT's, and measuring in the time domain, will enable estimates of return loss and attenuation as a function of distance alng the horn/OMT axis. In addition, return loss will be measured by heating a thermally isolated feed horn.

For the horns full, two-dimensional radiation patterns will be measured in the anechoic chamber, including the effect of possible mutual coupling between the horns. All pattern measurements will be done first for the horn alone, and then for the horn-OMT assembly in order to check the OMT contribution to the beam.

Individual waveguides, as well as the single-flange 2×2 goups of waveguides connecting the radiometers chains, will be extensively tested for radiometric performance (attenuation, return loss, stability) and for thermo-mechanical compilance.

4.1.4 Radiometer Tests

Following the tests described in the previous subsections, the front end modules will be mated with feed horns and OMTs, interconnecting waveguides, and back end modules, and performance tested as subassemblies. For these tests, the cryogenic section will be cooled to 20 K while the back end module will be kept at room temperature outside the dewar. (The only difference from the eventual space operating conditions will be that the temperature gradient in the interconnecting waveguides will be somewhat different. This difference, however, will not be significant to the performance.) For these tests, liquid cryogens will be used for cooling to avoid the vibrations inherent with mechanical coolers. A test box that will simulate the analog-to-digital converters and data processing portions of the Radiometer Electronics Box will be used to accumulate the test data. The radiometer noise temperature and $1/f$ noise will be measured using well matched and temperature controlled loads as inputs. During these tests, phase and amplitude adjustments will be made for optimal performance. Thereafter, each particular combination of interconnected components will be kept together as a numbered radiometer subassembly and environmentally tested to the required level. Performance will be verified following environmental tests, then the radiometer subassemblies will be delivered for overall integration of the LFI.

TABLE 4.3

LFI INSTRUMENT PERFORMANCE/CALIBRATION TEST MATRIX

Test	Unit	Sub-system	Instrument
F.O.V direction	Horn assembly	Horn assembly + telescope	
Beam efficiency	Horn assembly	Horn assembly + telescope	
Cross polarisation	Horn assembly		
Spectral response	FEU+BEM		
System noise temperature	FEM, BEM	RAA	LFI
Crosstalk Electrical		RAA	LFI
Crosstalk optical	Horn assembly		
Linearity	FEM+BEM		
Stability	FEU+BEM	RAA	LFI
Performance vs temperature and amplifier bias	FEM	RAA	LFI
Compatibility with HFI			LFI + HFI

4.1.5 Radiometer electronics box assembly

The functional testing of the Data Processing Unit and Signal Processing Unit will verify that the engineering and scientific data is properly converted and passed to the Spacecraft for transmission and that all aspects of the Instrument command and control are functional.

Each regulated power output voltage from the power supply unit within the Radiometer Electronic Box Assembly will be tested for current limit, over voltage and isolation in addition to the characterisation of the regulated supplies output.

4.1.6 Sorption cooler system

The coolers will be characterised for on and off design point performance. This approach will allow for full characterisation of the cooler performance and temperature stability allowing correlation with and validation of the design model. This testing will include transient cooldown time and capacity.

4.2 Calibration

4.2.1 Ground calibration

Calibration of the LFI Radiometers will be performed via hot/cold load tests at each level of assembly, with the FEU at room temperature and 20 K for the assembled units. The goal of the ground calibration is to assure appropriate signal levels for the ADC for anticipated on-orbit noise rms, signals and calibration, as well as to verify receiver noise and stability performance.

The data collected from the ground calibration measurements at unit, subassembly and system levels will provide a measurement data set that will verify the operation of the integrated LFI Instrument, as well as providing an in depth understanding of the instruments behaviour.

The parameters required to understand the instrument response and behaviour are shown in Table 4.3. The LFI test and calibration facilities will be required to measure these parameters.

4.2.2 On-orbit calibration

Proper reconstruction of the PLANCK maps requires accurate calibration, i.e., conversion of the signal strength from raw telemetry data into physical units. Fortunately, it will be straightforward to make accurate and frequent measurements of the critical instrument properties—relative and absolute gains, beamwidths, pointing, and stability—in flight, using the $\sim$3 mK CMB dipole signal plus observation of bright discrete sources such as Jupiter.

The dipole signal is an effective calibration signal because it provides a continuous modulation of the sky signal with a convenient amplitude. The amplitude of the modulation is known to about 1% (95% confidence level) from previous measurements, and NASA's Microwave Anisotropy Probe mission will reduce the uncertainties ever further; however, the fundamental calibration signal for Planck will be not the dipole itself, but rather the modulation of the dipole by the orbital motion of the Earth around the Sun, known in terms of fundamental physical constants to high accuracy. This technique was used by COBE but the PLANCK accuracy will be much higher due to the enormously higher sensitivity of the Planck radiometers.

Detailed simulations show that calibration accuracies on the order of 1-2% can be obtained at a rate of a few hours to about one day for most of the mission lifetime.

Accurate measurements of the antenna beam shapes and their relative pointing are critical to the removal of stray signals from bright astrophysical sources entering the detectors through the sidelobes of the telescope, as well as to the reconstruction of images of the CMB from the raw data. The most important sources for sidelobe pickup are the Sun, the Earth, the Moon, planets, and the galaxy. The beam pattern of each detector will be measured to better than 40 dB below the peak using biannual observations of Jupiter and Saturn.

Since all critical performance calibration is done in space, the ground testing program can focus on function, at considerable cost savings in the implementation.

4.3 Test and Calibration Facilities

A first performance test of LFI components or units (radiometers, cooler, electronics, etc) will be carried out by the contractor producing the LFI deliverable part (see Work Packages in SIP). The integration of components into subsystems and of these subsystems into the LFI itself will be mainly carried out at TRW and at LABEN. Both of these organizations have extensive experience in the integration and test of microwave systems for space and have developed advanced facilities to conduct these tasks. These facilities consist of those laboratory instruments necessary to measure and monitor all aspects of the performance of these systems. They also include the thermal/vacuum chambers needed to establish and maintain the environmental conditions required for some of these measurements. In addition to the facilities for conducting performance measurements, these organizations also have in place the facilities required to perform the shock, vibration, thermal/vac and temperature cycling required for qualification and acceptance testing.

Chapter 5

System Level Assembly, Integration and Verification (AIV)

Assembly, integration and verification (AIV) of the LFI will be a very significant aspect of the LFI Consortium effort, particularly due to the strong coupling of the LFI with the High Frequency Instrument and with the Planck payload. Nonetheless a careful integration plan, involving close cooperation with the HFI team, will enable a relatively straightforward strategy for integration and verification at the appropriate levels. The first section of this chapter (5.1) describes the assembly and integration approach at instrument level, and it constitutes the basis for the Design, Development, and Qualification Plan (DDQ Plan) of the LFI Consortium (requirement of IID-A, Sect. 9.2.1.2). Section (5.2) outlines the higher level AI&V at the LFI/HFI instrument, payload and spacecraft level. The proposed integration approach is described in detail in Appendix A and summarised in the IID-B document.

5.1 LFI Baseline configuration

The baseline configuration of the Low Frequency Instrument, shown in Figure 5.1, contains the following subsystems:

- Radiometer Array Assembly (RAA), which is composed of the Front End Unit (FEU), the Wave-Guide and coaxial cable sections (WG), and the Back End Unit (BEU).
- Sorption Cooler System (SCS), which includes the Sorption Cooler Compressor (SCC), the Sorption Cooler Electronics (SCE) and the Sorption Cooler Piping (SCP).
- Radiometer Electronics Box Assembly (REBA), which is composed of the Data Processing Unit (DPU), the Signal Processing Unit (SPU) and Power Supply Unit (PSU).
- Harness (H).

This decomposition leads to well-defined areas for the activities of integration and verification.

5.1.1 Design and development criteria

The overall approach for the instrument integration and verification is based on the following requirements and driving factors:

- the list of the deliverable items as requested by ESA (IID-A, Sect. 9);
- the integration scenarios at LFI/HFI level and at spacecraft level;
- the need to verify by test as many requirements as feasible as early as possible in the life cycle of the assemblies in order to minimise schedule impact in the event of problems;
- the need for an integration and verification flow which minimizes the overall period for development, production and qualification of the instrument;
- the need to take into account different approaches at unit level.

5.1.2 Model philosophy

Breadboards of critical items, such as the front-end and back-end modules, will be produced and tested in order to verify specific performance goals. The end product will be an "Elegant Breadboard" model of the LFI Front End Unit which will be used to refine the overall design.

A LFI Electrical Model (EM) will be the first model to be delivered to ESA. This model will be fully representative of spacecraft electronic interfaces and all software systems that excercise control over any

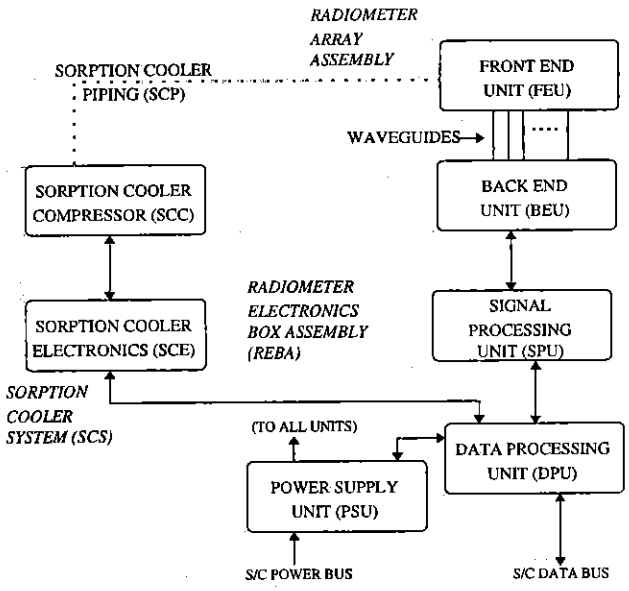

Figure 5.1: Schematic of the LFI baseline configuration

of these electrical interfaces. For the EM, a simulator will be provided for the remaining portions of the instrument.

Two instrument models are planned: An Engineering and Qualification Model (LFI-EQM) and a Flight Model (LFI-FM). The LFI-EQM will be integrated with the HFI QM before being delivered to ESA for the Planck Payload Module (PPLM) thermal and mechanical validation tests, a spacecraft system level test.

The LFI EQM delivered to ESA will consist of all three LFI sub-systems; the radiometer Array Assembly (RAA), the Radiometer Electronics Box Assembly (REBA), and the Sorption Cooler System (SCS).

In accordance with the guidelines laid down in IID-A section 9.2.2.1 the RAA and SCS-EQM will be built to the same standard as the flight models with the exception that, whenever several identical sensors are involved, some of them may be replaced with lower quality items or with appropriate dummies. Additionally the redundant units for the Sorption Cooler System will be replaced by suitable dummies as they are cold redundant with no automatic switch over. The EQM will therefore mimic the thermal, electrical and mechanical properties of the flight instrument and will be capable of undergoing the full environmental qualification program.

The LFI-FM will have full flight standard verified by formal functional and environmental acceptance tests.

Flight Spares (FS) will be produced for replacement of failed or damaged equipment at the integration and launch sites. In order to reduce costs the approach will be to derive the flight spare parts through the refurbishment of the qualification model units, which are built to full flight standard. In the event of this approach not being accepted for any unit, a flight spare unit will be fabricated verified by formal acceptance testing, or if a turn around which is compliant with ESA requirements can be ensured the flight spare may be reduced to a repair kit for unit repair at the manufacturers site.

A schedule for the development and delivery of the LFI models is given in Chapter 8.

5.1.3 Verification method

Verification of LFI units will be performed by inspection, analysis, test, and similarity, or a combination thereof. Inspection will be used to verify dimensions against the Interface Control Document (ICD) for each box and also markings and connector labels. Thermal-mechanical analysis will be carried out at subassembly levels. Thermal analysis for each unit and for the overall cooling apparatus will be performed. Mechanical analysis (static and dynamic loads) and radiation analysis will be carried out for each unit and relevant subassembly. In addition, a reliability analysis for the instrument will be performed. For each electronic unit a worst case analysis and a part-stress analysis will be carried out. Testing is considered the most reliable way to verify the system and unit requirements, and it will be the primary source of verification. Similarity will be used mainly on units which are identical: in this case qualification testing will be applied on a single unit with the other units undergoing acceptance testing.

5.1.4 Integration and verification flow

The integration and verification flows are basically identical for the two instrument models, the EQM and FM. The EQM will therefore be used to verify in detail the integration scheme, whilst at the same time providing crucial training for the integration team. The integration and verification details provided here are of necessity brief. Full test procedures will be detailed in the LFI Instrument Test Plan, which will be prepared after the Instrument Baseline Design Review.

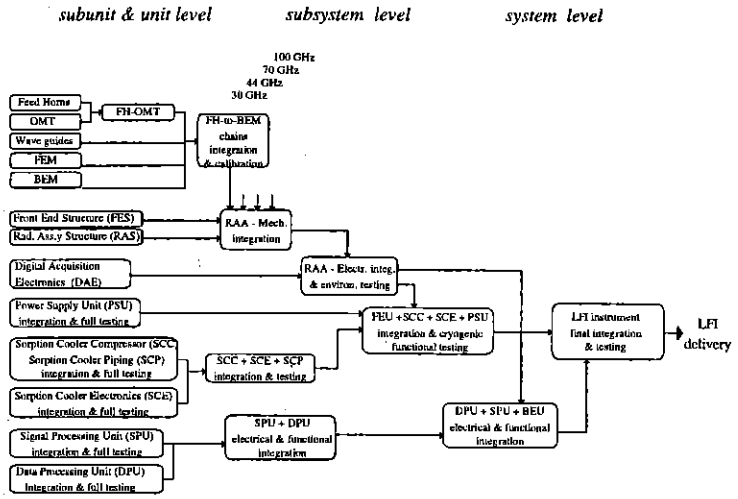

Figure 5.2: AI&V flow chart for both LFI models (EQM and FM)

Unit testing and the testing and calibration of the radiometer chains are described in chapter 4. The thermal vacuum, vibration and EMC testing of these units is detailed in the IID-B document. A basic flow diagram of the assembly integration and test is shown in Figure 5.2. It should be noted that for the initial integration and testing of the Radiometer Array Assembly the Sorption Cooler System is not required, because a suitable cryogenic GSE is planned. Thermal balance will be carried out on the Radiometer Array Assembly with the cooling provided by the cryogenic GSE. The configuration of the Radiometer Array Assembly for these tests will have the electrical and mechanical links from the 20 K stage through to the ambient stage faithfully reproduced. These measurements together with the on/off design point performance measurements of the Sorption Cooler System will allow validation of the

thermal design and model.

At sub-system level the following tests will be carried out: electrical, functional, performance, vibration, thermal vacuum.

At system level the following tests will be carried out: electrical, functional (warm), EMC.

The LFI will then be integrated with the HFI and be subjected to: Ambient temperature functional tests (including cross talk), Ambient temperature EMC, vacuum thermal balance tests, vacuum functional test. Following each of these tests a functional test will be carried out to check the instrument health.

5.1.5 Documentation tree

The documentation will be in accordance with ESA requirements which are laid down in the following documents IID-A, IID-B, First/Planck Product Assurance Requirements, Planck Science Management Plan and Planck Science Implementation Requirements Document. Documentation will be prepared at unit, sub-assembly and instrument level: details of the documentation can be found in the IID-B document.

At sub-assembly level, specific documents will be required to support the specific needs of sub-assembly level activities. The Work Package descriptions for these assemblies will detail these documents.

The group risponsible for each unit will prepare and deliver all the required documentation, which will cover requirements, software and hardware detailed design and product assurance.

The required documentation and the relevant content will be established by the P.I.

5.2 Higher level AI&V

This Section concerns the AI&V at levels higher than the LFI alone, i.e., integration between the LFI and HFI instruments and with the telescope, integration at payload and spacecraft (system) level. For all of these steps a modular approach is suggested for maintaining alignment, minimizing insertion problems, and reducing weight for the Planck instrument assembly. This approach is aimed at minimising the risk and the cost involved.

The LFI and HFI PIs propose to participate in a common team with the PPLM contractor to mechanically and thermally design this aspect of the payload module and at the same time further refine and develop the integration and test plan

5.2.1 Rationale for the modular approach

Once the modular LFI Front End Unit, Wave-Guides and Back End Unit are assembled, aligned and tested as a sub-assembly, it is highly desirable that this assembly not be disturbed. Additionally, if redundant structures are employed, the relative motion (3 mm) between the optical bench and the payload equipment module platform will be a significant problem that the design team will need to address in designing the LFI structure. Therefore, a rigid structure is highly desirable to join the LFI Front End and Back End units into a Radiometer Array Assembly (RAA). A single structure of six struts in a Stewart platform arrangement is suggested, arranged with a clear aperture, so that the side facing the exterior of the telescope has no struts. This is to enable access to the HFI after the LFI has been integrated with the telescope assembly. This arrangement maintains LFI alignment, simplifies the insertion and bolt-up operations, and provides high strength against launch loads.

5.2.2 LFI-HFI integration

The current design of the Planck Focal Plane Unit (FPU) is based on two highly integrated instruments. The HFI front end can either be inserted into the LFI front end prior to the telescope integration (if the 4 K and dilution refrigerators are disconnected) or after the LFI is integrated and secured. In either case, the HFI front end can be inserted from the backend. As shown in Chapter 2, the design of the Wave-Guides (WG) is such that it ensures clearance for insertion of the HFI without requiring any disassembly.

In the event of a failure of a given LFI channel, the corresponding waveguide can be disassembled, allowing replacement of the defective component. This will require the necessary unit and system level verifications tests being repeated in order to ensure that the system is compliant with requirements.

In Appendix A, the proposed integration approach / procedure is described in detail for the Planck Payload Module. The procedure starts with the integration of the LFI radiometer Array Assembly. The integration of the LFI Radiometer Array Assembly with the HFI Front End Unit is then described. Finally a practical approach is outlined for the integration of this assembly into a strawman concept Planck Payload Module.

5.2.3 Electronic Ground Support Equipment

The LFI Electronic Ground Support Equipment (EGSE) is intended to support final integration and testing activities at instrument level, as well as integration activities at spacecraft level. The activities of the first type are internal to the LFI Consortium and their scope is to integrate all the units and/or sub-assemblies, and to verify by test all the requirements at instrument level. The activities of the second type will be carried out by ESA with the support of technical personnel from the LFI team. In order to meet both targets, the LFI EGSE will be designed in a modular way, taking advantage of previous consolidated experiences for ESA payloads (e.g. XMM and INTEGRAL).

The LFI EGSE will be composed of three units: the Interface Simulator Unit (ISU), the Central Check-out Equipment (C-COE), and the Experiment Check-out Equipment (EXP-COE) (see Figure 5.3).

- The Interface Simulator Unit will simulate all the electrical interfaces of the spacecraft and hence will perform the following functions: S/C CDMU simulation, S/C Power System simulation, S/C clock simulation, S/C RTU simulation (if needed). The ISU will receive TC packets from the C-COE and will send TM packets with some additional information to the C-COE and EXP-COE.

- The Central Check-out Equipment (C-COE), a workstation with additional storage capabilities, will serve as the man-machine interface from the commanding point of view. The operator will prepare all the necessary sequences of telecommands in a suitably friendly environment, and the telecommand packets will then be routed to the ISU, which will send them to the instrument. The C-COE will also provide the capability to simulate the behaviour of the S/C bus. The C-COE will store received TM data, and will display housekeeping data to the operator to allow proper monitoring of instrument engineering functions. The C-COE will provide control functions to inform the operator of any non-nominal instrument behaviour.

- The Experiment Checkout Equipment (EXP-COE), a workstation with additional storage capabilities, will serve as the man-machine interface from the scientific point of view. The EXP-COE will store all of the TM data received, and will perform on-line quick-look data analysis for display of scientific data. This verifies just the correct functioning of the detectors; exhaustive data analyses will be performed elsewhere. The EXP-COE will also provide playback capability for previously stored data. It will duplicate the C-COE capability for displaying housekeeping data, primarily for use during the S/C level integration phase, where commanding will be performed elsewhere (through the S/C EGSE and the CDMU) but an overview of the instrument behaviour will be needed. The EXP-COE will be an LFI deliverable item.

The database may be selected so as to have at least a partial commonality with the database of the S/C EGSE, if the latter is known beforehand at the beginning of the development phase.

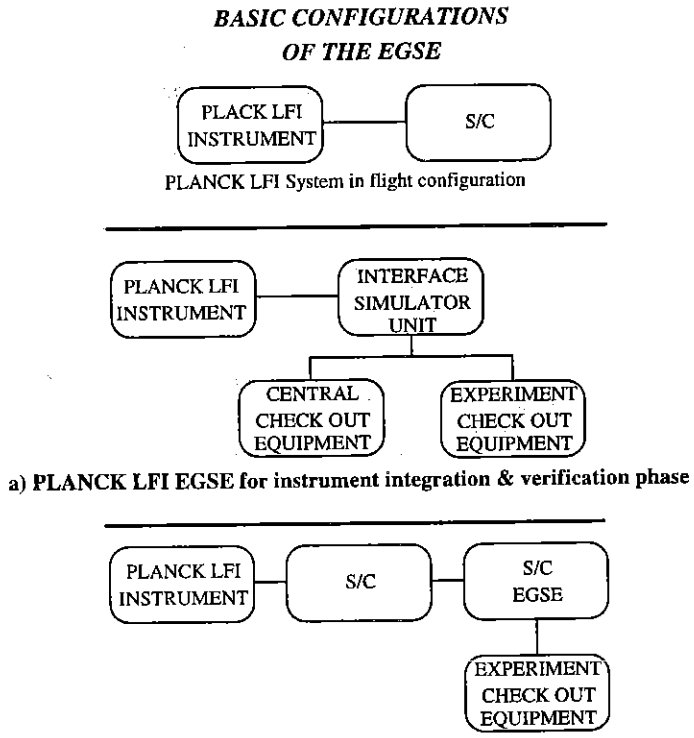

Figure 5.3: Experiment Check-out Equipment

Chapter 6

Flight Operations

6.1 Planck-LFI survey

The Planck operational orbit has been selected to be a Lissajous orbit around the Lagrangian Libration Point $L2$ of the Sun-Earth system, which is at a distance of approximately 1,500,000 km from Earth. This essential feature of the Planck mission, identified during the COBRAS/SAMBA phase A study, allows maximum simplification of the flight operation and reflects the need for an extremely contamination-free and very stable environment for the LFI (as well as HFI) observations. The orbit will be free of eclipses for the entire duration of the FIRST/Planck mission.

The Planck field of view will be directed at 85° (nominal) away from the spin axis. During normal operation the spacecraft will be spinning at 1 rpm around the Z-axis, with the spin axis in the anti-solar direction. Thus the instrument field of view will scan nearly great circles. A period of approximately 7 months will be required to complete a full-sky survey. Planck-LFI will carry out two full surveys. The Planck spin axis will be repointed regularly to obtain full sky coverage and maintain anti-sun attitude. This will be achieved, nominally, with steps of 2.5 every hour. Given the LFI angular resolution (see Table 2.1), this is sufficient to yield continuous coverage of the sky with adequate redundancy.

FIRST and Planck have mutually exclusive modes of operation, so that during FIRST operations the LFI will be switched off. Once begun, each LFI survey will be performed continuously, and simultaneously with the HFI. Both Planck surveys will be completed within the first two years of the FIRST/Planck mission. As detailed in the FIRST/Planck Ground Segment Interface Document (GSID), the first Planck survey will be carried out at the beginning of the FIRST/Planck observational period, followed by ~ 6 months for the FIRST survey, followed by the second Planck survey. During Planck operations, the LFI observation schedule will nominally be executed autonomously from telecommands stored on-board. The command schedule will be up-linked every day from the ground station.

During routine Planck-LFI observations the operations will be conducted through a single ground station. The LFI telemetry data acquired during periods of non visibility will be stored on board, and downlinked during the visibility period in parallel with real-time data.

The LFI instrument control will be performed by ESA's Mission Operations Center (MOC). It is anticipated that during the Satellite Commissioning and Performance Verification phases, instrument specialists from the LFI team will provide support to the MOC operations. This support may be extended to the period of nominal Planck observations, if required, in case of emergency, such as a serious instrument or spacecraft malfunctioning.

6.2 Nominal operations

The LFI flight operations are desgned to be extremely simple, as the best method to obtain the science and the most efficient data processing and analysis effort. Simple operations improve the stability of the instrument which is of the utmost importance. The LFI flight operations have two basic modes:

1. During routine Planck operations, the LFI will operate continuously and steadily, in a single operational mode ("ON mode").
2. During FIRST operations the LFI will be switched off ("OFF mode").

Other instrument modes dedicated to nominal operations include stand-by, sleep, and test modes; any additional instrument configuration refers to non-nominal operations, and will correspond to either a diagnostic mode, or to a fail-safe configuration, as outlined below.

6.2.1 ON mode

Each sky survey will be conducted by the LFI with the instrument always in the "ON" mode. No changing configurations, deployable elements, or mechanically moving parts are included in the instrument design.

Temperature stability during ON operation is of extreme importance for the success of the mission, so that stability of power consumption is critical, particularly in the cold focal unit. No significant changes in power level will be exhibited by the LFI radiometers throughout each sky survey. The only changes will come from power adjustment on the first stage of the HEMT amplifiers, which require extremely small power level variations.

Inherent frequencies of the LFI during the ON operational mode are:

- The center frequencies of the four LFI channels. No down-conversion is performed, as all the amplification is carried out at rf frequency.
- The switching frequency of the solid-state phase switches in the front-end portion of the LFI radiometers. The frequency is anticipated to be 1 kHz.
- The sorption cooler cycle, which has a period of 800 seconds.
- All other frequencies, such as the spin rate and the spin-axis repointing are in common with the rest of the spaceraft, and are described in the IID-A.

6.2.2 OFF mode

All LFI units are switched off. The only reason that the LFI needs to be powered down during FIRST observations is to save power. If there were sufficient power, then thermal stability performance would be enhanced by keeping the power on the LFI or powering it well before operations so that operational thermal stability is reached at commencement of observations.

6.2.3 Stand-by, Sleep, Test modes

The Stand-by mode is entered at power-on, after the initialisation period. The LFI I/F electronics is on, so as to allow communications with the S/C CDMU.

The Sleep mode can be considered as a sub-mode of the Stand-by mode, where most of the elctronics is off, but basic communications with the LFI are still possible.

In the Test mode, a stored pattern of data can be used as input; since the output is known, the downstream electronics can be tested.

6.3 Telemetry and data compression

In the "ON" mode, the radiometers are sampled every 6.9 ms (2.5 on the sky, or 1/4 FWHM at 100 GHz), i.e., at 144.9 Hz. Radiometers at all frequencies are sampled synchronously to eliminate possible interference between channels. There are 112 detectors, so there are 16,232 samples per second, each 16 bits. The raw data rate of the LFI, then, is $260\,\mathrm{kb\,s^{-1}}$.

The average telemetry data rate specified in the Phase A study is $60\,\mathrm{kb\,s^{-1}}$, of which the LFI is allocated $20\,\mathrm{kb\,s^{-1}}$. For the LFI a higher average data rate would be desirable; however the low rate can be accommodated if necessary. One factor of roughly two comes from safe, lossless data compression.

A second factor of two reduction comes from only transmitting the difference between sky and reference temperatures, rather than the separate temperatures, as was assumed in Phase A. Some diagnostic information on the stability of the amplifiers and reference loads is lost this way, but the essential science data come from the difference. To allow the possibility of recovering this potentially valuable information, two channels at a time (a sky/reference pair) will be sent at the full independent rate. The channels sent would be changed each time the spacecraft was repointed, so that all channels could be monitored over a few days.

The data rate for the remaining 110 channels must be reduced by a further factor of roughly 3.6. This can be achieved by on-board averaging of data for a given feed taken at the same point in the sky on successive spins. Since the spin axis remains fixed for 60 revolutions (§ 6.1), a reduction by a factor of four can be readily achieved, with some loss of information.

On-board averaging requires accurate repeatability of the telescope pointing on successive spins. The clock angle of the spacecraft must be known to high precision by the LFI DPU, and the nutation of the spacecraft must be small. The uncertainty in beam position on the sky from the sum of these effects should be 1/10 beam or less at 100 GHz, i.e., 1′, to avoid errors in the averaging. It is possible that after each spin-axis repointing the spacecraft attitude stability will be insufficient to maintain the requirement for a period of a few minutes. In this case the LFI data will need to be stored and down-loaded, for that time period, with no on-board averaging in order for it to be used after a-posteriori attitude reconstruction.

More clever schemes may make possible similar reductions in data volume with less loss of information. For example, the detector output is sampled at 16 bits for adequate dynamic range on the sky signal, which is dominated by the dipole, the Galaxy, Jupiter, etc. The CMB signal and the noise (even including $1/f$ noise) require smaller dynamic range. Simulations show that almost lossless compression ratios of ~ 4 can be achieved even when the noise is $1/f$-dominated by separating out the mean signal on the set of spins at a given spin-axis pointing from the noise, and then requantising the noise component with fewer bits.

On-board processing of the science data (including compression of all sorts) is handled by the Signal Processing Unit (§ 2.5.1), which has adequate processing capacity and memory to handle a broad range of algorithms.

6.4 Calibration

As described in § 4.2.2, in flight calibration will be performed routinely by exploiting the ~ 3 mK signal from the CMB dipole.

Additional calibration and measurements of the LFI beam patterns will be obtained in-flight using the signal from external planets, as they fall in the field of view of the instrument. Jupiter and Saturn, in particular, will provide an adequate microwave source for beam calibration. This places a requirement on the flight plan: each of the two 7-months full sky surveys shall include at least one passage in the field of view of LFI, for each array beam, of these two external planets.

The beam measurements will be performed with the LFI in the ON mode, and will not require additional operational modes or discontinuity with the routine observations.

6.5 Diagnostic modes

Two types of diagnostic modes are envisaged. These are expected to be particularly useful during the Satellite Commissioning and Performance Verification phase for instrument health check out:

1. In the *full-data* mode the raw 16-bit sampled outputs of the detectors associated with any six specified channels are stored for transmission to the ground.
2. The *total-power* mode is like the full-data mode, except the phase switches are turned off.

For both diagnostic modes the overall data rate is slightly lower than in the normal operating mode.

6.6 Fail-safe configurations

Two main fail-safe configurations can be foreseen:

1. *Fail-safe mode 1* – In case one (or more) LFI detectors need to be switched off.
2. *Fail-safe mode 2* – In case the sorption coolers (both operational and spare units) fail.

6.6.1 Fail-safe mode 1

This may be required if a detector fails or if, for unforseen reasons, the physical temperature in the focal plane is unacceptably high. In this configuration the LFI is in the ON operational mode, except that the defective or unwanted detector/detectors is/are turned off. The large level of redundancy of detectors in the focal plane ensures great flexibility in this scenario.

6.6.2 Fail-safe mode 2

In this case, the LFI risk is mitigated by the implementation of the gas-gap thermal switch (see Section 2.6.1). The increased temperature in the focal plane ($\sim$ 60 K) causes the low-pressure nitrogen to sublimate and provide a thermal path for the power dissipated by the LFI radiometers. In this configuration the LFI array will operate in a passive-cooling mode, at an estimated temperature of about 60 K. A dedicated plan will be developed to establish how many and which detectors should be operative in this configuration to maximise the science return.

6.7 Transfer phase

Details of the transfer trajectory for the merged or independent mission are not yet available. It is anticipated that Planck-LFI will exploit as much as possible the transfer phase to perform tests of the far sidelobe response, using the Earth and the Moon as test-sources at various off-axis angles, compatibly with the trajectory and attitude selected for the FIRST/Planck transfer to L2. To carry out these tests the LFI will be in the ON mode.

Chapter 7

Qualification and Experience of the PI Team

Name:	**Nazzareno Mandolesi**
Task:	Principal Investigator
Affiliation:	Istituto TeSRE - CNR
Address:	via P. Gobetti 101 I-40129 Bologna Italy
	Tel: 39 51 6398682 Fax: 39 51 6398724
e-mail:	reno@tesre.bo.cnr.it
Experience:	Doctor in Physics (1969) has more than 25-year experience in CMB experiments. He has proposed the COBRAS mission as PI. Co-I of ISOCAM, former member of the AWG, he served for 6 years the CNR Physics Committee. He is currently member of the European Space Science Committee of the ESF and director of Istituto TeSRE since 1994.
Name:	**Charles R. Lawrence**
Task:	Survey Scientist
Affiliation:	Jet Propulsion Laboratory
Address:	4800 Oak Grove Drive Pasadena CA 91109 USA
	Tel: 1 818 354 5307 Fax: 1 818 354 8895
e-mail:	crl@jplsp.jpl.nasa.gov
Experience:	Ph.D. 1983 (MIT) is the leader of the US LFI team as well as on the Code-X/O-funded device technology effort. He has extensive experience in the application of low-noise amplifiers for astrophysics, including CMB observations in the Owens Valley, and led the first systematic study on the separation of Galactic foreground emission from CMB data. He is a member of the NASA SVLBI Project Science Group, the Submillimeter Science Working Group, the Structure and Evolution of the Universe Subcommittee, and the SEU Technology Working Group.
Name:	**Marco Bersanelli**
Task:	Instrument Manager
Affiliation:	CNR-Istituto IFCTR
Address:	via Bassini 15 I-20133 Milano Italy
	Tel: 39 2 23699308 Fax: 39 2 2362946
e-mail:	marco@ifctr.mi.cnr.it
Experience:	Doctor in Physics at the University of Milan (1986), has 12 years experience in design and fabrication of instruments for measurements of the Cosmic Microwave Background, including ground-based observations of the CMB spectrum from the White Mountain Station and from the South Pole, and balloon-borne CMB anisotropy projects such as BEAST. He has been working on the Planck (ex COBRAS/SAMBA) mission since the very beginning, leading the international instrument team of the Low Frequency Instrument, and participated in the Science Team during the Assessment and Phase A study. He is designated as the Instrument Manager in the Planck-LFI Consortium.

Name:	**Fabio Pasian**
Task:	Data Processing Center Manager
Affiliation:	Osservatorio Astronomico di Trieste
Address:	via G.B. Tiepolo 11 I-34131 Trieste Italy
	Tel: 39 40 3199221 Fax: 39 40 309418
e-mail:	pasian@ts.astro.it
Experience:	Born in São Paulo, Brazil, in 1953. Degree in Physics at the University of Trieste in 1977. Since 1978 with the Astronomical Observatory of Trieste. From 1989 to 1992 at the ST-ECF, ESO, Garching as Senior Archive Scientist: responsible for the project, development, maintenance and management of the European Archive for the Hubble Space Telescope. Participation in the development of the ULDA/USSP archive of IUE low resolution data. Responsible of the design and implementation of the Archives at the TNG Italian national telescope. Chairman of the Astronomical Databases Working Group of the ESA/ESIS project and member of the ESIS Steering Committee. Member of two ESA evaluation panels.

Name:	**Christopher R. Butler**
Task:	LFI Project Manager
Affiliation:	Agenzia Spaziale Italiana
Address:	Viale Regina Margherita 202 I-00198 Roma Italy
	Tel: 39 6 8567 1 Fax: 39 6 85370772
e-mail:	-
Experience:	Ph. D and B. Sc. Physics from University of Southampton. Many years of experience in construction and operation of instruments in the area of X-ray astronomy. During his recent carrier at the Agenzia Spaziale Italiana (ASI) he has held the posts of Payload Manager of the satellite SAX and Project Manager of the entire satellite during its final integration and test, tacking also responsibility for its launch campaign. Currently he is Mission Director for ASI of the very successful Beppo-SAX mission.

CO - INVESTIGATORS

Name:	**Kevin Bennett**
Affiliation:	Space Science Department,Astrophysics Division
Address:	P.O.Box 299 NL-2200 AG Noordwijk The Netherlands
	Tel: 31 71 565 3559 Fax: 31 71 565 4690
e-mail:	kbennett@astro.estec.esa.nl
Experience:	Staff member of ESA since 1975, Proj Sci. of COS-B. Study Scientist for ESA X-ray and gamma-ray missions. Co-PI of COMPTEL on GRO. Local experiment manager responsible for design, provision and test of the on-board electronics, software, calibration units and GSE. Deputy head of the Astrophysics Division responsible for Data Archives and Analysis.

Name:	**Thierry J.-L. Courvoisier**
Affiliation:	INTEGRAL Science Data Center
Address:	Chemin d'Ecogia 16 CH-1290 VERSOIX Switzerland
	Tel: 41 22 950 91 01 Fax: 41 22 950 91 33
e-mail:	Thierry.Courvoisier@obs.unige.ch
Experience:	P.I. INTEGRAL Science Data Centre. Participation in the EXOSAT mission as Duty Scientist: development of analysis software, participation in the orbit operations (1980-1984). Member of the ST-ECF: participation in the development of analysis software and simulations (1984-1988). Astronomy professor (prof. adjoint) at the Geneva University (now). Co-I on the XMM-RGS. Former chairman of the ESIS steering committee and member of the AWG. Research in the physics of active galactic nuclei. Teaching courses on general astronomy, physical basis of astrophysics and high energy astrophysiscs. Since 1996 leader of the INTEGRAL Science Data Centre. Decisions will be taken on a time frame that is adapted to the Planck mission development.

Name:	**Luigi Danese**
Affiliation:	Scuola Internazionale Superiore di Studi Avanzati (SISSA)
Address:	via Beirut 2-4 I-34013 Trieste Italy
	Tel: 39 40 3787476 Fax: 39 40 3787528
e-mail:	danese@sissa.it
Experience:	Born on 18 November 1946. Since 1974 until 1982 he has been astronomer at Padua Observatory. Since 1982 he has been Associate Professor at Padua University for 10 years and then he moved to SISSA in Trieste as full professor. He has been associate scientist of ISOCAM and member of the AGN panel of the Observing Time Allocation Committee of ISO. He is responsible of the italian pole of the ELAIS network funded by European Community. He served since 1994 to 1997 as scientist in the Astronomy Working Group of ESA. Presently he is a member of the Scientific Committee of the Italian Space Agency (ASI).
Name:	**Rodney D. Davies**
Affiliation:	Nuffield Radio Astronomy Laboratories University of Manchester Jodrell Bank
Address:	Macclesfield Cheshire SK11 9DL United Kingdom
	Tel: 44 1477 571321 Fax: 44 1477 571618
e-mail:	rdd@jb.man.ac.uk
Experience:	Prof. Rodney D. Davies BSc, MSc (Adelaide), PhD, DSc (Manchester) Emeritus Professor of Radio Astronomy. Director NRAL (1988-97). Fellow of the Royal Society, President of the Royal Astronomical Society (1987-89), CBE awarded for services to Astronomy. Founder and leader of the Jodrell Bank CMB research team (1985-97) Over 200 scientific publications on solar radio emission, structure of galactic magnetic fields, neutral hydrogen in galaxies, the Hubble flow in the nearby Universe, structure in the CMB. Technical publications on techniques for observations of fluctuations in the CMB.
Name:	**Richard J. Davis**
Affiliation:	Nuffield Radio Astronomy Laboratories University of Manchester Jodrell Bank
Address:	Macclesfield Cheshire SK11 9DL United Kingdom
	Tel: 44 1477 571321 Fax: 44 1477 571618
e-mail:	rjd@jb.man.ac.uk
Experience:	BA (Cambridge), PhD (Manchester). Senior Lecturer in Radio Astronomy. Development Scientist for MERLIN L-Band link system (1975-79), design and development of CMB interferometer systems (1986-date), Project Scientist for 4.8M GBP MERLIN Phase 2 Project (1987-1992), Project Scientist for the Lovell Telescope Upgrade Project (1992-97) and the CMB VSA Project (1995-date). Over 100 scientific publications on astrometry, stellar radio emission, supernova remnants, the polarization and structure of radio galaxies and quasars, and fluctuations in the CMB. Technical publications on the development of broadband and radio linked interferometers, telescope design and performance.

Name:	**Gianfranco De Zotti**
Affiliation:	Osservatorio Astronomico di Padova
Address:	vicolo dell'Osservatorio 5 I-35122 Padova Italy
	Tel: 39 49 8293444 Fax: 39 49 8759840
e-mail:	dezotti@pd.astro.it
Experience:	Born on 7 July 1947. Degree (Laurea) in Physics (1970) and Advanced studies degree (Diploma di perfezionamento) in Physics (1975) at the University of Padua. Since 1986 he is Senior astronomer (Astronomo ordinario), a position equivalent to a University Full Professor, at the Astronomical Observatory of Padua. Since 1991 he is the Director of the Astronomical Observatory of Padua and he had, among other things, the responsibility of the management of the optical telescopes located in Asiago-Cima Ekar, the largest optical observational station operating in Italy; he had also the responsibility of the administrative management of the "Galileo" Italian National Telescope, a 3.5 m telescope, built in La Palma, Canary Islands.

Name:	**Todd Gaier**
Affiliation:	Jet Propulsion Laboratory
Address:	4800 Oak Grove Drive Pasadena CA 91109 USA
	Tel: 1 818 354 4402 Fax: 1 818 354 8895
e-mail:	gaier@merlin.jpl.nasa.gov
Experience:	Ph.D. 1993 (UCSB) has 10 years experience in observations of CMB anisotropy. He has designed, fabricated and operated experiments for measuring CMB anisotropy from the South Pole and White Mountain Research Station, pioneering the use of receivers based on HEMT amplifiers for CMB measurements. He currently leads a technology program at JPL to develop HEMT receivers for frequencies as high as 200 GHz, including cryogenic receivers to 120 GHz.

Name:	**Krzysztof M. Gorski**
Affiliation:	Theoretical Astrophysics Center
Address:	Juliane Maries Vej 30 2100 Copenhagen 0 Denmark
	Tel: 45 35 325898 Fax: 45 35 325910
e-mail:	gorski@tac.dk
Experience:	Senior cosmologist with extensive research experience in the areas of large scale structure in the universe and cosmic microwave background and an expert in analysis and interpretation of the CMB data. He was a member of the COBE team at NASA/GSFC before moving to Copenhagen in 1997, and played critical role in definitive interpretation of the COBE-DMR results. His current research is focused on Planck related issues. He has recently introduced a new high resolution full sky pixelization which permits fast computations and simulations of the CMB sky. Presently he develops new methods for analysis of very large CMB data sets to be produced by satellite missions, and coordinates the simulation activities in the LFI consortium.

Name:	**Erik Kollberg**
Affiliation:	Microwave Technology Chalmers University of Technology
Address:	S-41296 Göteborg Sweden
	Tel: 46 31 7721841 Fax: 46 31 164513
e-mail:	kollberg@ep.chalmers.se
Experience:	Professor at School of Electrical and Computer Engineering since 1980, and was the acting Dean of Electrical and Computer Engineering 1987-1990. A major responsibility from 1967 to 1987 has been the development of radio astronomy receivers working from a few GHz up to 250 GHz for the Onsala Space Observatory telescopes in Sweden and in Chile. From 1963 to 1976 he performed research on low noise masers amplifiers used for radio astronomy observations. He is the inventor of the heterostructure barrier varactor diode. In the fields mentioned above, about 190 scientific papers have been published. He became member of the Royal Swedish Academy of the Engineering Sciences 1992.

Name:	**Philip M. Lubin**
Affiliation:	Physics Dept. University of California Santa Barbara
Address:	Santa Barbara CA 93106 USA
	Tel: 1 805 893 8432 Fax: 1 805 893 8597
e-mail:	lubin@cfi.ucsb.edu
Experience:	Ph.D. 1980 (UC Berkeley) has flown 15 balloon-borne and fielded 6 ground-based experiments in the last 18 years. He was a member of the COBE Science Working Group, and has designed and built a number of measurement systems in cryogenic millimeter-wave and microwave systems. He is currently involved in several degree-scale studies of the CMB anisotropy, including BEAST, a long-duration balloon effort.

Name:	**Enrique Martinez-Gonzalez**
Affiliation:	Instituto de Fisica, Facultad de Ciencias, Universidad de Cantabria
Address:	Avda. de Los Castros s/n SP-39005 Santander Spain
	Tel: 34 42 201468 Fax: 34 42 201459
e-mail:	martinez@ifca.unican.es
Experience:	Born at Reinosa, Cantabria, Spain on October 12, 1960. Degree in Physics (1982) and PhD in Physics (1986) by Universidad de Cantabria. Doctorate studies in NORDITA, Copenhagen, September 1983-September 1986. Postdoc fellow in Universidad de Cantabria, October 1986-October 1988. Teaching Assistant in Universidad de Cantabria, November 1988-March 1990. Member of the International Astronomical Union and Spanish Astronomical Society. 46 papers in refereed journals (about 20 on the CMB) and more than 30 publications of proceedings. Projects: participation in 3 international projects and 18 national projects. Coordinator of a HCM european network on the CMB with 6 participating groups from 4 european countries.

Name:	**Hans Ulrik Nørgaard-Nielsen**
Affiliation:	Danish Space Researh Institute
Address:	Juliane Maries Vej 30 DK-2100 Copenhagen Denmark
	Tel: 45 35 325728 Fax: 45 35 362475
e-mail:	hunn@dsri.dk
Experience:	Born on March 24 1948. Master degree in Astronomy (1976) and Ph.D. in Astronomy (1981) at the Copenhagen University Observatory. Since 1987 position held as research physicist at Danish Space Research Institute (DSRI). From 1987 to 1990 member of the IUE Allocation Committee. Project scientist on the XSPECT/SODART mirror system (1988-1994). From 1992 to 1996 member of the Danish Board for Astronomical Research. From 1993 to 1996 member of the ESA Astronomy Working Group. Acting Director of DSRI (1994-1995). Since 1994 member of the ESA PLANCK (former COBRAS/SAMBA) Science Team. Since 1996 member of the board of the Instrument Center for Danish Ground-based Astronomy (IJAF). In 1997-1998 member of the ESA PLANCK/FIRST Tiger Team.

Name:	**Rafael Rebolo**
Affiliation:	Instituto de Astrofisica de Canarias
Address:	c/o via Lactea La Laguna, Tenerife, Spain
	Tel: 34 22 605262 Fax: 34 22 605210
e-mail:	rrl@ll.iac.es
Experience:	Degree in Physics at Granada University (1984), Ph.D. in Astrophysics from the University of La Laguna (1987). Rafael Rebolo is currently Research Professor with the Spanish Higher Council for Scientific Research, and works at the Instituto de Astrofisica de Canarias as Head of the Research Division (over 120 researchers). Principal Investigator of 7 projects in the field of Anisotropy of the Cosmic Microwave Background (CMB), 7 in Origin and distribution of Light Elements and 7 in Brown Dwarfs search and characterization. He has published more than 70 refereed papers and 100 contributions to International Conferences. He has led the spanish participation in several experiments on Anisotropy of the CMB (the Tenerife Experiment, the 33GHz-Interferometer, the IAC-Bartol millimetric experiment).

Name:	**George Smoot**
Affiliation:	University of California, Berkeley
Address:	MS 50205 LNBL Cyclotron Rd. Berkeley CA 94720 USA
	Tel: 1 510 486 5505 Fax: 1 510 486 7149
e-mail:	smoot@celest.lbl.gov
Experience:	Ph.D. 1970 (MIT), has been active in CMB experiments for over 20 years. He was PI of the COBE DMR and is currently involved in the BOOMERANG/MAXIMA CMB anisotropy balloon program.

Name:	**Jan Erik Solheim**
Affiliation:	Department of Physics University of Trømso
Address:	N-9037 Tromsø Norway
	Tel: 47 77 64 51 91 Fax: 47 77 64 55 95
e-mail:	janerik@phys.uit.no
Experience:	Responsible for planning, construction and operations of Skibotn Observatory from 1975. Chairman of the Scientific and technical Committee for the Nordic Optical Telescope at La palma (1983-87), during the construction and bulding phase. Host for several CMB experiments in the Tromso region 1978-821. Research fields: Cosmological models, photometry of galaxies and CMB (1965-81). Thereafter Cataclysmic variable stars and interacting white dwarf bibinary systems.

Name:	**Luigi Spinoglio**
Affiliation:	CNR Istituto IFSI
Address:	Via del Fosso del Cavaliere s/n I-00133 Roma Italy
	Tel: 39 649934395 Fax: 39 64993 4383
e-mail:	luigi@ifsi.rm.cnr.it
Experience:	Education: Laurea in Physics at the Torino University (1982). Present position: Research staff at IFSI-CNR (since 1988). (1984-85) Research Fellow at Southampton University (UK), data analysis on multifrequency data on active galaxies, IRAS data analysis. (1986-87) NATO Fellow at University of California at Los Angeles (US), definition of IRAS Galaxies samples. (1988-98) ISO-LWS Astronomer, preparation of the ISO-LWS Core Program, responsible of ISO-LWS AGN Working Group. (1994-97) Member of the Physics Committee and of the Informatics Committee of the National Research Council of Italy. Co-author of more than 35 articles on refereed international journals on the fields of active galaxies and star formation.
Name:	**Gianni Tofani**
Affiliation:	CNR Istituto CAISMI
Address:	Largo E. Fermi 5 I-50125 Firenze Italy
	Tel: 39 55 2752217 Fax: 39 55 2752 287
e-mail:	tofani@arcetri.astro.it
Experience:	Large experience in: - spectroscopy of star formation regions at radio and millimeter wavelenghts; - design of radioreceivers and of microwave components; - Co-I in design and construction management of large radiotelescopes: 32 meter antenna of Medicina and the new 64m Sardinia Radiotelescope.
Name:	**Jussi Tuovinen**
Affiliation:	Millimetre Wave Laboratory of Finland
Address:	Otakaari 7 B Espoo P.O. Box 1202 FIN-02044 VTT Finland
	Tel: 358 9 4566508 Fax: 358 9 4567013
e-mail:	Jussi.Tuovinen@vtt.fi
Experience:	Dr. Tech. 1991, Lic. Tech.1989, Dipl. Eng. 1986. Since 1995 Laboratory Director, MilliLab. Since 1996 Docent, Helsinki University of Technology (HUT). From 1994 to 1995 Project Manager, HUT. Development of 119 GHz front-end and a hologram based antenna test method for Odin-satellite. From 1991 to 1994 Senior Postdoctoral Research Associate, University of Massachusetts, Five College Radio Astronomy Obsersvatory. Development of a solid state source for 1 THz and testing of a 14 m telescope. ESA Fellowship for frequency multiplier work at FCRAO (1993-94). From 1986 to 1991 Research Engineer, HUT. Over 75 scientific publications and two patents.
Name:	**Nicola Vittorio**
Affiliation:	Università di Roma, Tor Vergata
Address:	via della Ricerca Scientifica I-00133 Roma Italy
	Tel: 39 6 72594421 Fax: 39 6 2023507
e-mail:	vittorio@roma2.infn.it
Experience:	Degree of Physics at the University of Rome, La Sapienza, in 1978. Full Professor at the University of Rome, Tor Vergata, since 1994. Experience on theoretical calculation, simulations and data analysis of CMB anisotropy. Presently is Director of the National Group of Astronomy of the National Council of Research.

Name:	**Lawrence A. Wade**
Affiliation:	Jet Propulsion Laboratory
Address:	4800 Oak Grove Drive Pasadena CA 91109 USA
	Tel: 1 818 354 2272 Fax: 1 818 354 4878
e-mail:	lawrence.a.wade@jpl.nasa.gov
Experience:	B.A. 1980 (California State University, Fullerton) has over 19 years experience in developing advanced cryogenic devices, 12 of which have been spent developing sorption cryocoolers. His research has resulted in over 30 refereed publications. He was the cognizant engineer responsible for the BESTCE sorbent beds flown on STS-77. He has led or participated in the mission design and development of over 10 flight astrophysics missions (e.g., ExNPS) and earth observing instruments (e.g., TES). Currently he is Principle Investigator for the Vibration-Free Cryocooler Program which is developing flight coolers for operation between 20 and 1.5 K.
Name:	**Simon White**
Affiliation:	Max-Planck-Institut für Astrophysik
Address:	Karl-Schwarzschild-Str. 1 D-85740 Garching bei Germany
	Tel: 49 89 3299 3211 Fax: 49 89 3299 3235
e-mail:	swhite@mpa-garching.mpg.de
Experience:	Simon White is a senior cosmologist who has played a major role in establishing the current standard paradigm for the evolution of structure in the Universe. He has managed the Max-Planck-Institut für Astrophysik for the last four years. His current research involves supercomputer simulations of structure formation carried out as part of an international consortium. The current generation of simulations being carried out on the Garching Cray T3E typically each produce about a Terabyte of output and thus present Data Processing Problems of similar magnitude to the Planck Surveyor pipeline.

The list of the LFI associates, together with their position and affiliation, is given in Appendix B at the end of this volume.

Similarly, the list of the LFI key personnel with their tasks and affiliation, is also given in Appendix B

Chapter 8

Organisation and Management of the LFI Consortium

8.1 Introduction

The LFI will be implemented by the LFI Consortium, which is based on the coordinated effort of scientific institutes, individual investigators, and industries from many countries. Some provide scientific support only; others in addition provide deliverable items or have functional responsibilities.

To enable successful implementation of the LFI, we have defined: 1) clear lines of responsibility and authority; 2) a detailed Work Breakdown Structure (WBS) with clear work-package and interface definitions; and 3) detailed schedules of the deliverables and receivables, with thier own critical path elements.

At the same time, a challenging mission like Planck requires a clear scientific vision to reach its maximum potential. For this reason the Project Organisation reflects the key roles played by the Co-I's and Associates.

8.1.1 Project Organisation

Figure 8.1 shows the overall Project Organisation. The main features are:

- The PI has overall responsibility for the LFI, and interacts between the LFI Consortium and the Planck ESA Project.
- A Project Office will be settled in order to support the PI for the General Management, the Instrument Manager and the DPC Manager for the management of their activities. The Head of the Project Office is hereafter called the LFI Project Manager.
- The Survey Scientist (SS) provides scientific and technical support to the Consortium and to the Science Team (ST). He reports directly to the PI.
- The Instrument and DPC Managers, in their managerial roles, report to the PI.
- The Funding Committee (FC) consists of the PI, one Co-I from each country with a substantial financial commitment to the LFI, and of a representative of ESA/SSD (see the Funding Proposal). FC members will ensure that institutes, groups and industries from their respective countries keep organisational committments and make funding and manpower available as required. The Instrument and DPC Managers, as well as the Project Manager, will attend meetings of the FC when requested by the PI.
- The Co-I's are senior scientists and managers of major WBS elements who take responsibility for substantive contributions to the LFI, either scientific or technical. The Co-Is form a scientific and technical advisory Co-I Group, chaired by the PI, which plays an important role in experiment definition, in design and implementation of the instrument, and in ensuring that the mission meets the science objectives. The Co-I Group meets regularly and whenever the PI deems it necessary.
- The scientific and technical activities of the Consortium are organised through a number of Working Groups. Each is chaired by a co-I and is supported by a number of Associates who provide significant expertise but are not expected to take functional responsibilities. A list of Working Groups is given in Table 1.1. Working Group Chairs are appointed by the PI and report on Working Group activity, as determined by the PI, either to the PI himself, to the Instrument Manager, to the DPC Manager, or to the Project Manager.

Given their crucial role within the Project, the final list of Co-I's will be established as firm committments to the LFI are agreed. The list of Associates will be reviewed each year on the basis of individual contributions to the Project.

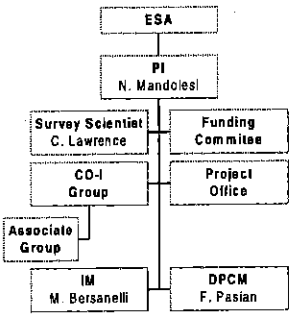

Figure 8.1: LFI organisation.

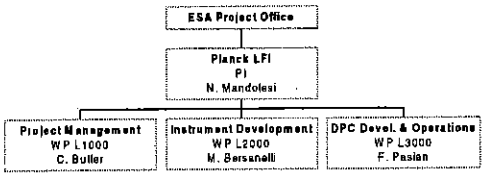

Figure 8.2: LFI Work Breakdown Structure: top levels

TABLE 8.1

WORKING GROUPS AND CHAIRPERSONS

	Working Groups	Chairperson
	Radiometer	Richard Davis – Jodrell Bank
	Electronics	Jose Miguel Herreros – IAC
C	Thermal	Lawrence A. Wade – JPL
C	Telescope	Hans Ulrik Norgaard-Nielsen – DSRI
C	AIV	TBD
	Theory	Nicola Vittorio – Univ. di Roma "Tor Vergata"
	Foregrounds	Gianfranco De Zotti – Oss. Astron. di Padova
	Simulations	Krzysztof M. Gorski – TAC

The mark C implies agreed commonalities with the HFI and/or the TP.

8.1.2 Work Breakdown Structure

The upper levels of the Work Breakdown Structure (WBS) are shown in Figure 8.2. Each of the Level 1 branches—Project Management, Instrument Development, and DPC Development & Operations—is broken down further into Work Packages (WP), as shown in Figures 8.3, 8.4, and 8.5. The WBS is a product-based structuring of tasks within the LFI Project and serves to define work assignments and associated interfaces. This provides a basis for specific work commitments by team members, and states management control by clarifying lines of responsibility and accountability.

Responsibilities within each of the three first level WP (1000, 2000 and 3000) are clearly identified according to the deliverable item to be provided or to the packages to be managed. Preliminary summary tables of the main lower level WPs are shown in the draft of the Science Implementation Plan (SIP). Each WP includes a description of the tasks to be performed, deliverables, and schedule, and gives the name of the WP Manager. This manager is responsible for ensuring timely completion of the WP, either through resources entirely under his control or through further subWPs agreed with other Consortium members.

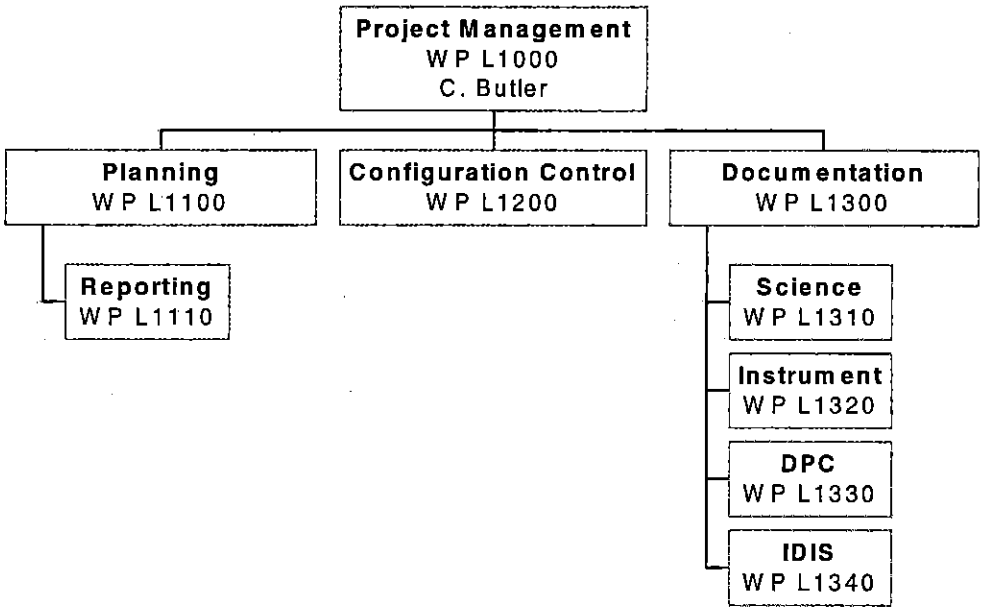

Figure 8.3: General management WBS

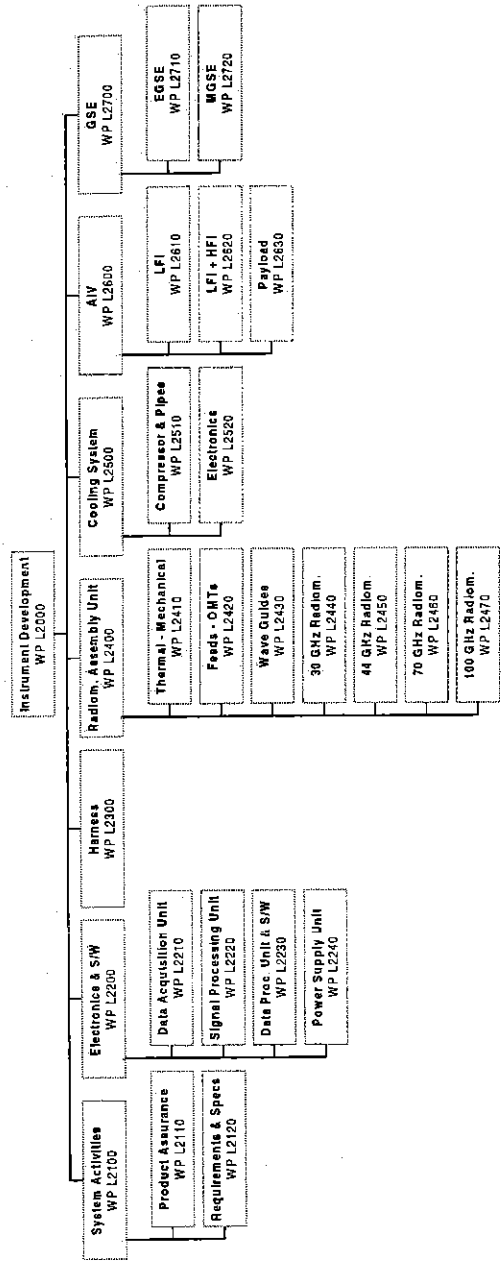

Figure 8.4: Instrument developemnt WBS

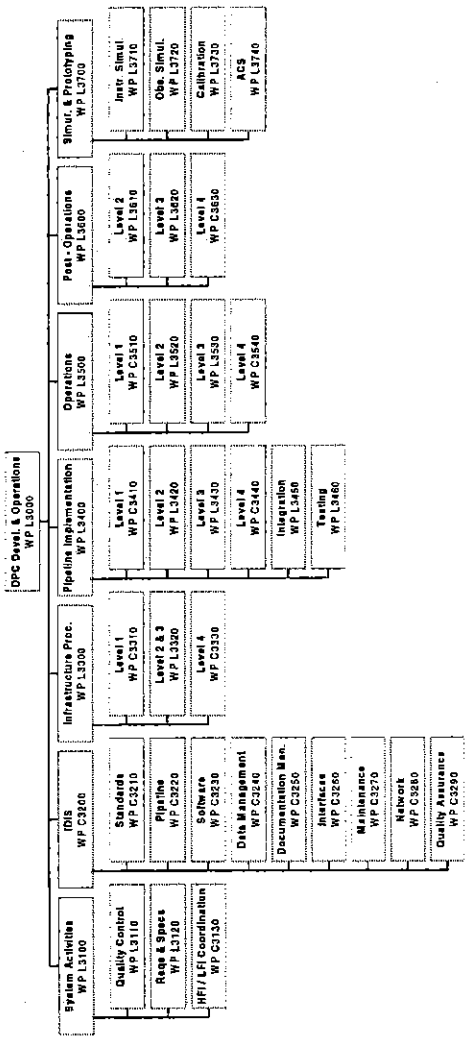

Figure 8.5: DPC developemnt and operations WBS

8.2 LFI external relationships

The relationships between the LFI Consortium and the outside world are shown schematically in Figure 8.6.

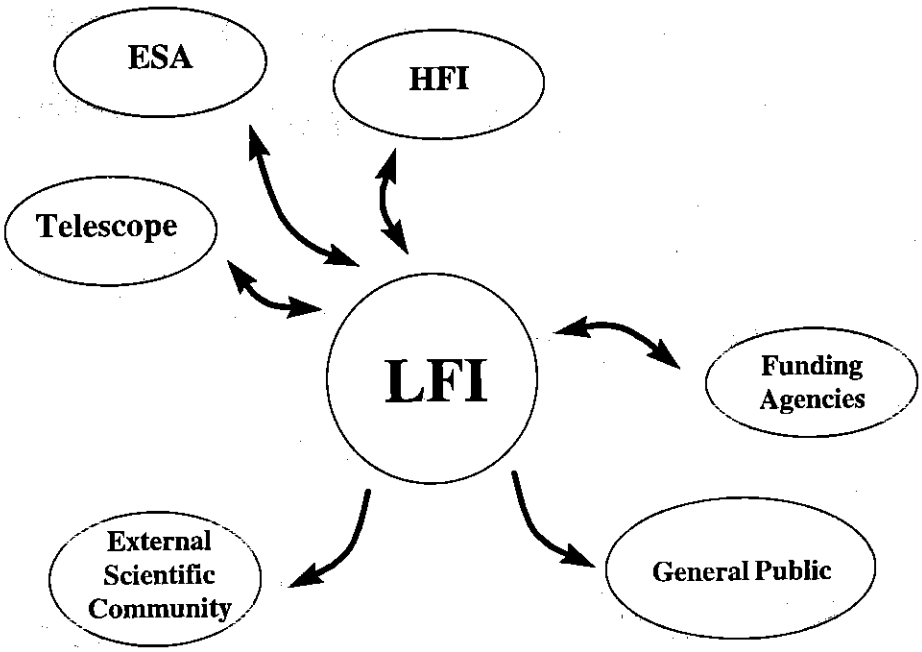

Figure 8.6: LFI external relationships

8.2.1 Relationship with ESA

There are two formal lines of communication between the ESA Planck Project Office and the Planck LFI Consortium. One is through the PI, the other through the ESA Planck Science Team, where the LFI is represented by the PI, the Instrument Manager, the DPC Manager, and the Survey Scientist. Other contacts, mainly during the design phase, occur via various Working Groups which include ESA and HFI experts as needed.

8.2.2 Relationships with the HFI and TP teams

Some of the deliverable items will be developed in common with the HFI Consortium, e.g., the two 20 K coolers and their control electronics; IDIS; the Level 1 and Level 4 processing pipelines and the AIV plan. Effective working relationships have been established with the HFI team in all these areas. In addition the LFI team is strongly commited to providing ESA with an integrated Payload (LFI and HFI and Telescope) with the goal of developing an integrated scientific programme. The LFI, the HFI and the Telescope Provider (TP) have already established or will soon establish integrated teams to address all common areas. For the scientific programme it is the intention of the three teams to set up a "Common Scientific Committee", composed of a number (TBD) of Co-I's chosen to give a balanced representation

of the teams as well as of the various national contributions to the Planck Project. This Committee will be chaired alternately by the PI's of the two instruments or their designated substitutes.

8.2.3 Relationships with funding agencies

One Co-I from each country (plus a representative of ESA/SSD) is responsible for the contribution to the project from that country, including funds, personnel, and deliverable items. These Co-Is plus the PI form the LFI Funding Committee (FC), chaired by the PI (see Funding Proposal). The FC meets at least once per year.

8.2.4 Relationships with the external scientific community

The majority of the CMB scientific community is already significantly involved in the Planck Project. The interface with the larger astrophysical community refers mainly to the "secondary" goals of the mission, e.g. those connected to galactic and extragalactic foregrounds. Participation from external scientists is encouraged and welcome in any phase of the project.

Planck data can be accessed by the external scientific community in the following modes:

- The LFI Consortium will consider proposals for Associateship from those scientists willing to contribute significantly to the scientific and/or technical aspects of the Project. Associates can participate in the "data exploitation by Planck scientists", as defined in the Planck Science Management Plan (SMP).
- External scientists wishing to access Planck data before its public availability may submit research proposals according to the Planck SMP.
- Planck data will be made available to the scientific community at large at the end of the Instrument Teams' proprietary period. The LFI Team is committed to provide support to the community for accessing and exploiting the Planck archive.

8.2.5 Relationship to the wider external community

The Planck mission, and in particular its cosmological goals. are already generating substantial public interest. The LFI Consortium is strongly committed to promoting public awareness of the mission as it proceeds, and intends to make full use of ESA support in such activities as detailed in ESA's recent document, "Publicity Agreement for Scientists involved in ESA Science Projects".

8.3 Schedule

A schedule for the main items of the instrument and the DPC development is shown in Figure 8.7. More detailed schedules are included in the IID-B document. Several points are worth noting:

- The LFI "elegant" breadboard, which is not a deliverable, will be a simplified version of the critical parts of the instrument. It will contain one complete radiometer at each of the four LFI frequencies, including feed horns and passive components, mounted on a support plate. It is crucial to the project because it will demonstrate that the instrument specifications can be met. It will be completed in mid-2000.
- The EM and the QM are developed in parallel, the former to be delivered to ESA, the latter (together with the GSE) to an external contractor (TBD) who will be responsible for LFI and HFI integration. The FPU will be delivered in mid-2001.
- The sorption cooler EM will be delivered to TESRE in mid-2000 for integration in the "elegant breadboard". Once it has been refurbished, it will be delivered for QM and FS.

- The FM will be delivered in mid 2003 to an external contractor (TBD) for integration with the HFI in the Focal Plane Unit (FPU), which in turn will be delivered to ESA at the end of 2003.
- A preliminary version of the RTA/QLA software will be developed to support internal testing of the EM, QM, and FM.
- The complete LFI data processing pipeline will be delivered to the DPC when the latter starts operations (one year prior to launch).

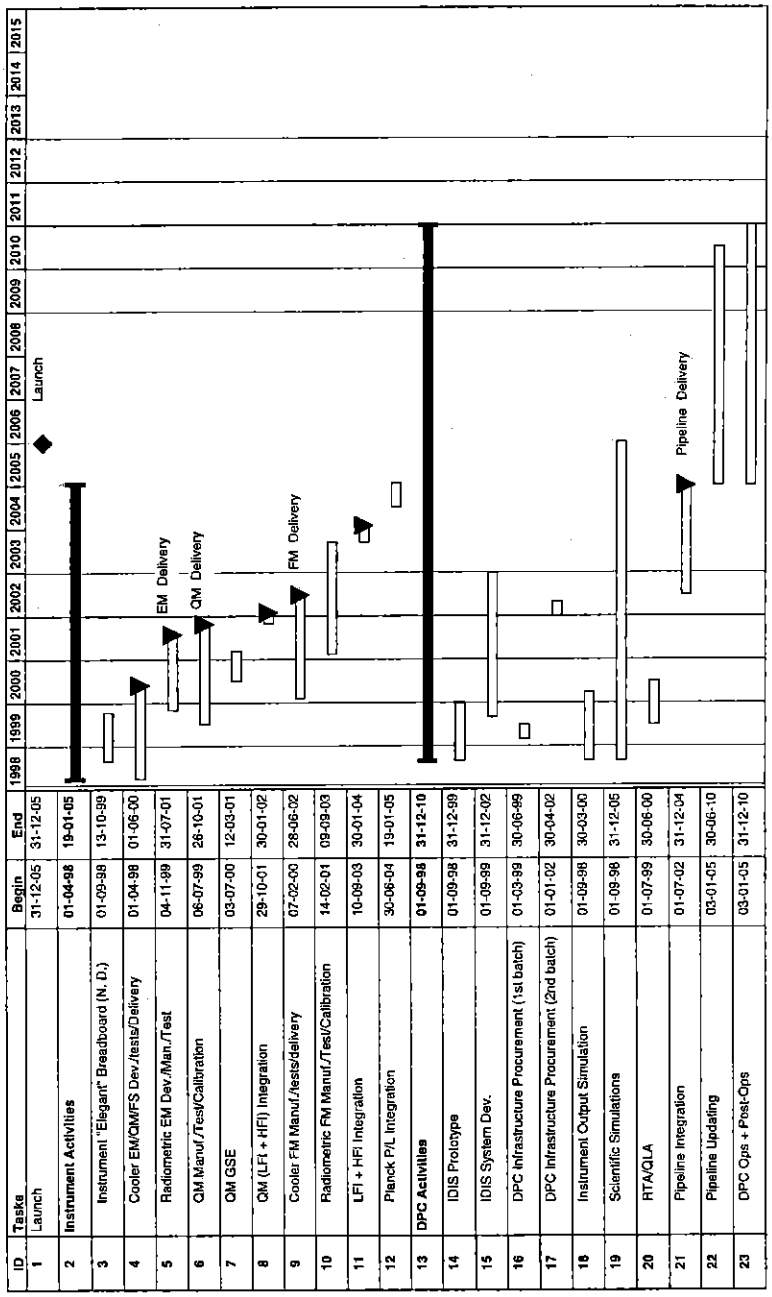

Figure 8.7: Top level LFI schedule.

References

Abbott, L.F., Wise, M.B., 1984, ApJ, 282, L47

Bard, S., et al, 1993, 7th International Cryocooler Conference Proceedings, PL-CP93-1001, 1107-1119

Bard, S., et al, 1997, Cryocoolers 9, pp. 567-576, R. G. Ross, Jr. ed., Plenum Press, New York

Bersanelli, M., et al., 1996, "COBRAS/SAMBA – Report on the phase A Study", ESA Report D/SCI(96)3

Bersanelli M., Muciaccia P.F., Natoli P., Vittorio N., Mandolesi N., 1997, A&ASS, 121, 393.

Birkinshaw, W, M., Hughes, J.P., 1994, ApJ, 420, 33

Bond R.J., Efstathiou G., Tegmark M., 1997, preprint (astro-ph/9702100)

Bouchet F., Gispert R., Puget J.L., 1995, in Proceedings of the 1995 Moriond Meeting on "Clustering in the Universe"

Bouchet F. et al., 1995, Space Sci. Rev. 74, 37

Brandt W.N., Lawrence C.R., Readhead A.C.S., Pakianathan J.N., Fiola T.M., 1994, ApJ, 424, 1

Brown, L.M.J., *et al.*, 1989, ApJ, 340, 129

Burigana C., Maino D., Mandolesi N., Pierpaoli E., Bersanelli M., Danese L., Attolini M.R., 1998, A&ASS, in press.

Burigana C., et al, 1997 MNRAS, 287, 17

Cavaliere, A., Danese, L., De Zotti, G., 1977, ApJ, 217, 6

Cavaliere, A., Danese, L., De Zotti, G., 1979, A&A, 75, 322

De Oliveira-Costa A., Kogut, A., Devlin, M.J., Netterfield, C.B., Page, L.A., Wollack, E.J., 1997, ApJ, 482, L17

Crawford, T., Marr, J., Partridge, R.B., Strauss, M.A., 1996, ApJ, 460, 225

Danese, L., Toffolatti, L., Franceschini, A., Bersanelli, M., Mandolesi, N., 1996, Ap. Lett. Comm., 33, 257

Davies, R.D., Watson, R.A., Gutierrez, C.M., 1996, MNRAS, 278, 925

de Vries, W.H., Barthel, P.D., O'Dea, C.P., 1997, A&A, 321, 105

Di Matteo, T., Fabian, A.C., 1997, MNRAS, 286, L50

Dodelson S., 1997, ApJ, 482, 577

Draine, B.T., Lazarian, A., 1997, astro-ph/9710152

Fabian, A.C., Rees, M.J., 1995, MNRAS, 277, L55

Fanti, C., Fanti, R., Dallacasa, D., Schilizzi, R.T., Spencer, R.E., Stanghellini, C., 1995, A&A, 302, 317

Franceschini, A., Vercellone, S., Fabian, A.C., 1997b, MNRAS, submitted

Gaier T., Seiffert M., Meinhold P., Lubin P., Sholley M., Lai R., Wang H., Allen B., Osgood B., Block T., Liu P.H., Jackson C., Lawrence C.R., 1996 SPIE Proceedings, Millimeter and Sub-millimeter III, 2842, 46

Gaustad, J., McCullough, P., van Buren, D., 1996, PASP, 108, 351

Gautier, T.N., Boulanger, F., Perault, M., Puget, J.-L., 1992, AJ, 103, 1313

Gorski, C.L., *et al.*, 1996, ApJ, 464, 11

Gunn, J.E., 1978, in "Observational Cosmology", eds. Maeder, Tammann

Hancock S., Gutierrez C.M., Davies R.D., Lasenby A.N., Rocha G., Rebolo R., Watson R.A., Tegmark M., 1997, MNRAS, 289, 505

Haslam, C.G.T., Klein, U., Salter, C.J., Stoffel, H., Wilson, W.E., Cleary, M.N., Cooke, D.J., Thomasson, P., 1981, A&A, 100, 209

Haslam, C.G.T., Salter, C.J., Stoffel, H., Wilson, W.E., 1982, A&A Suppl., 47, 1

Hauser, M.G., *et al.*, 1998, preprint

Hu, W., Scott, D., Sugiyama, N., White, M., 1995, Phys. Rev. D, 52, 5498

Hu, W., Sugiyama, N., Silk, J., 1997, Nature, 386, 37

Hu, W., White, M., 1997, ApJ, 479, 568

Kamionkowski M., Kosowski A., Stebbins A., 1997, Phys. Rev. D, 55, 7368

Kawara, K., *et al.*, 1997, in proc. ESA symposium

Knox L., 1995, Phys. Rev. D, 48, 3502

Jonas, J.L., Baart, E.E., Nicolson, G.D., 1998, MNRAS in press

Jungman, G., *et al.*, 1996, Phys. Rev. Lett., 76, 1007

Kaiser, N., 1983, MNRAS, 202, 1169

Kogut, A., et al., 1996, ApJ, 460, 1

Kogut, A., 1996, Proc. XVI Moriond Astrophysics Meeting "Microwave Background Anisotropies", eds. F.R. Bouchet, R. Gispert, B. Guiderdoni, J. Trân Thanh Vân, p. 445

Lai et al., 1997, in InP and Related Materials conference, reprinted in Microwave Journal September 1997

Lasenby, A.N., 1996, Proc. XVI Moriond Astrophysics Meeting "Microwave Background Anisotropies", eds. F.R. Bouchet, R. Gispert, B. Guiderdoni, J. Trân Thanh Vân, p. 453

Lawson, K.D., Mayer, C.J., Osborn, J.L., Parkinson, M.L., 1987, MNRAS 225, 307

Leitch, E., Readhead, A.C.S. , Pearson, T.J., Myers, S.T., 1997, astro-ph/9705241

Melhuish, S.J., et al., 1997, MNRAS, 286, 48

Myers S.T., Baker J.E., Readhead A.C.S., Leitch E.M., Herbig T., 1997, ApJ, 485, 1

Narayan, R., Yi, I., 1995, ApJ, 444, 231

O'Dea, C.P., Baum, S.A., 1997, AJ, 113, 148

Platania P., Bensadoun M., Bersanelli M., De Amici G., Kogut A., Levin S., Maino D., Smoot G.F., 1997, preprint (astro-ph/9707252)

Primack J. 1996, in Critical Dialogues in Cosmology, ed. N. Turok (World Scientific)

Puget, J.-L., *et al.*, 1996, A&A, 308, 5

Readhead, A.C.S., Taylor, G.B., Pearson, T.J., Wilkinson, P.N., 1996, ApJ, 460, 634

Reich, P., Reich, W., 1986, A&A Suppl. 63, 205

Rephaeli, Y., 1995, ARA&A, 33, 541

Reynolds, J., 1992, ApJ, 392, L35

Reynolds, R.J., Cox, D.P., 1992, ApJ.L, 400, 33

Sachs, R.K., Wolfe, A.M., 1967, ApJ, 147, 73

Schlegel, D.J., Finkbeiner, D.P., Davis, M., 1997, preprint astro-ph/9710327

Seiffert M., Burigana C., Mandolesi N., Bersanelli M., Meinhold P., Lubin P., 1998, Rev. Sci. Inst., in press.

Seljak, U., Zaldarriaga, M., 1997, Phys. Rev. Lett., 78, 2054

Silk, J., 1968, ApJ, 151, 459

Smail, I., Ivison, R.J., Blain, A.W., 1997, ApJ, 490, L5

Smoot, G., *et al.*, 1992, ApJ, 396, L1

Snellen, I.A.G., 1997, Ph. D. Thesis, University of Leiden

Sunyaev, R.A., Zel'dovich, Ya.B., 1970, Ap. Space Sci., 7, 3

Sunyaev, R.A., Zeldovich, Ya.B., 1970, Comments Astroph. Sp. Phys., 2, 66

Tegmark, M., Efstathiou, G., 1996, MNRAS, 281, 1297

Tegmark M., 1997, preprint (astro-ph/9712038)

Tegmark M., Taylor A., Heavens A., 1997, ApJ, 480, 22

Tegmark M., 1997, ApJ, 480, L87

Toffolatti, L., Argüeso-Gómez, F., De Zotti, G., Mazzei, P., Franceschini, A., Danese, L., Burigana, C., 1997, MNRAS, in press

van Breugel, W., Miley, G., Heckman, T., 1984, AJ, 89, 5

Van Mal, H.H., and Mijnheer, A., 1971, Proceedings ICEC 4, IPC Science & Technology Press, Guildford, UK, pp. 122-125

Veeraraghavan, S., Davies, R.D., 1997 in Particle Physics and the Early Universe, eds. Bately, R., Jones, M.E., Green, D.A.

Tegmark M., 1997, ApJ, 480, L87

Wade, L. A., 1991, Advances in Cryogenic Engineering, Plenum Press, New York, vol. 37 , pp. 1095-1105.

Wade, L. A., Recent Advances In Cryogenic Engineering-1993, 1993,267 (1993), pp. 57-63, ed. By J.P. Kelley and J. Goodman, American Society of Mechanical Engineers, New York, NY, HTD-Vol.

Wade, L. A., and Levy, A. R., 1997, Cryocoolers 9, pp. 587-596, R. G. Ross, Jr. ed., Plenum Press, New York

Wright E.L., 1996, Paper presented at the IAS CMB Data Analysis Workshop in Princeton on 22 Nov 96

Wright E.L., Hinshaw G., Bennett C.L., 1996, ApJ, 458, 53

Zaldarriaga M., Spergel D., Seljak U., 1997, preprint (astro-ph/9702157)

Acronyms

ADS	Advection Dominated Sources
AO	Announcement of Opportunity
API	Application Program Interface
ASCII	American Standard Code for Information Interchange
BETSCE	Brillant Eyes Ten-Kelvin Sorption Cooler Experiment
BEU	Back End Unit
CBR	Cosmic Background Radiation
CDM	Cold Dark Matter
CDMU	Control and Data Management Unit
CD-R	Compact Disk - Recordable
CD-ROM	Compact Disk - Read Only Memory
CDS	Centre de Donnees Strasbourg
CMB	Cosmic Microwave Background
CMBR	Cosmic Microwave Background Radiation
CNR	Consiglio Nazionale delle Ricerche
COBE	COsmic Background Explorer
COBRAS	COsmic Background Radiation Anisotropy Satellite
CoI	Co-Investigator
COTS	Commercial Off-The-Shelf software
CPAC	Cambridge Planck Analysis Centre
CPU	Central Processing Unit
CSIC	Consejo Superior de Investigaciones Científicas
DAT	Digital Audio Tape
DAU	Data Acquisition Unit
DBMS	DataBase Management System
DDQ	Design Development and Qualification Plan
DLR	Deutsche Luft und Raumfahrt
DMR	Differential Microwave Radiometer (on COBE)
DPC	Data Processing Center
DPCCG	Data Processing Center Coordination Group
DPCM	Data Processing Center Manager
DPU	Data Processing Unit
DRS	Data Reduction Software
DU	Digital Units
DVD	Digital Video Disk
EGSE	Elecriocal Ground Support Equipment
EM	Electrical Model
EQM	Engineering and Qualification Model
ESA	European Space Agency
ESTEC	ESA Science and TEchnology Centre
FDDI	Fiber Digital Data Interconnct
FET	Field Effect Transistor
FEU	Front End Unit
FINDAS	FIRST Integrated Network and Data Archive System
FIRAS	Far Infra-Red Absolute Spectrophotometer (on COBE)
FIRST	Far InfraRed and Submillimetre Telescope
FITS	Flexible Image Transport System

FM	Flight Model
FOV	Field Of View
FPU	Focal Plane Unit
FS	Flight Spares
FSC	FIRST Science Centre
FTE	Full-Time Equivalent
FWHM	Full Width at Half Maximum
GPS	GHz Peaked radio Sources
HEALPIX	Hierarchical Equal Area and Longitude PIXelisation
HEMT	High Electron Mobility Transistor
HFI	High Frequency Instrument
H/K	House-Keeping
HLS	High Level Software
HST	Hubble Space Telescope
H/W	Hardware
IAS	Institute d'Astrophisique Spatiale
ICP	Instrument Control Processor
IDIS	Integrated Data and Information System
IDIS-DT	Integrated Data and Information System Development Team
IDIS-MT	Integrated Data and Information System Management Team
IDR	Intermediate Design Review
IFCTR	Istituto di Fisica Cosmica e Tecnologie Relative
IR	InfraRed
IRAS	InfraRed Astronomical Satellite
ISDC	INTEGRAL Science Data Centre
ISRF	InterStellar Radiation Field
kbps	Kilobits per second
L2	The L2 Lagrangian point of the Earth-Sun system
LAN	Local Area Network
LEOP	Launch and Early Orbital Phase
LFI	Low Frequency Instrument
LLS	Low Level Software
LPAC	London Planck Analysis Centre
MAP	Microwave Anisotropy Probe
MIC	Microwave Integrated Circuit
MMIC	Monolithic Microwave Integrated Circuit
MOC	Mission Operating Center
MPA	Max Planck institute fur Astronomie
MPE	Max Planck institute fur Extraterrestrische physik
NASA	National Aeronautics and Space Administration
NL-NET	NetherLands national NETwork
OAPd	Osservatorio Astronomico di Padova
OAT	Osservatorio Astronomico di Trieste
OBDH	On Board Data Handling
OMT	Ortho Mode Transducer
PA	Product Assurance
PC	Personal Computer
PI	Principal Investigator
P/L	PayLoad
POSDAC	Paris-Orsay-Saclay Data Analysis Centre
PPLM	Planck PayLoad Model
PSU	Power Supply Unit
PV	Performance Verification

RTA	Real-Time Assessment
QA	Quality Assurance
QLA	Quick-Look Analysis
QM	Qualification Model
QSO	Quasi Stellar Object
RAA	Radiometer Array Assembly
RAL	Rutherford-Appleton Laboratories
RBE	Radiometer Back End
RF	Radio Frequency
RFE	Radiometer Front End
REBA	Radiometer Electronics Box Assembly
SAMBA	SAtellite for Measurements of Background Anisotropies
S/C	SpaceCraft
SCE	Sorption Cooler Electronics
SIP	Science Implementation Plan
SIRD	Science Implementation Requirements Document
SISSA	Scuola Internazionale Superiore di Studi Avanzati
SMP	Science Management Plan
SPS	Scientific Pipeline Software
SPU	Signal Processing Unit
SSC	Sorption Cooler Compressor
SSD	Space Science Department (ESTEC Department)
ST	Science Team
S/W	Software
SZ	Sunjaev-Zeldovich
TESRE	Istituto per le TEcnologie e lo Studio delle Radiazioni Extraterrestri (CNR)
TBC	To Be Confirmed
TBD	To Be Defined
TBR	To Be Reviewed
TOD	Time Ordered Data
TP	Telescope Provider
UC	Universidad de Cantabria
URD	Users Requirements Document
VSWR	
WG	Working Group

Appendix A

Proposed Integration Approach

This appendix provides additional details on the integration approach for the Planck Payload Module described in the ESA AO for FIRST and Planck. Integration proceeds as follows:

1. Integration of the LFI Front End Unit (FEU), Back End Unit (BEU), and waveguide assembly to form the LFI Radiometer Array Assembly.
2. Integration of the HFI focus assembly into the LFI Radiometer Array Assembly to form the LFI/HFI Array Assembly.
3. Integration of the LFI/HFI Array Assembly into the telescope assembly.
4. Integration of the Planck Payload Module.

These steps are described below. *The structural designs and overall integration approach are applicable with minor modification to all concepts being considered for both the Merged and Separate Mission options.*

A.1 Steps 1 and 2

The Planck Focal Plane Unit and the LFI BEU, and the structures that support them, must meet several requirements:

- The Focal Plane Unit must be supported precisely and rigidly with respect to the telescope.
- The Focal Plane Unit must be thermally isolated from the Equipment Platform.
- Insertion of the HFI FEU into the surrounding LFI FEU must not require disassembly of the LFI FEU.
- Connections between the Focal Plane Unit and the Equipment Platform must tolerate relative displacements between the two during launch of as much as 3 mm.
- The LFI BEU must be thermally connected to the Equipment Platform.

In addition, it is highly desirable, although not a hard requirement, that the waveguides connecting the LFI FEU with the BEU not be disconnected following the complete performance characterization of the LFI by the LFI team. The reason for this is partly to save the time and expense of connecting 112 waveguides and coaxial cables more often than absolutely necessary, and partly because even tiny changes in the relative positioning of waveguide joints can change standing wave patterns inside the waveguides, and hence the eveness of the response across the band. Every disassembly and reassembly of the waveguide connections requires an additional performance check of every channel, to ensure that no significant changes have occurred.

The trickiest problem to solve is how to allow 3 mm of motion between the Focal Plane Unit and the Equipment Platform while maintaining good thermal contact between the LFI BEU and the Equipment Platform, given that 92 waveguides connect the LFI FEU and BEU. Several solutions have been considered, including the use of flexible, dielectric waveguides to connect the LFI FEU to the BEU, and a BEU design that allows individual amplifier chains to be supported by metal waveguides with only flexible electrical and thermal connections to the Backend Unit box. While it is possible that such an "internally compliant" design might be developed, significant work would be required to establish and validate the performance and long term stability of such a solution. Fortunately, a more straightforward solution exists. Described below, it is proposed as the baseline design the LFI Radiometer Assembly Array, with compliant designs held as backups.

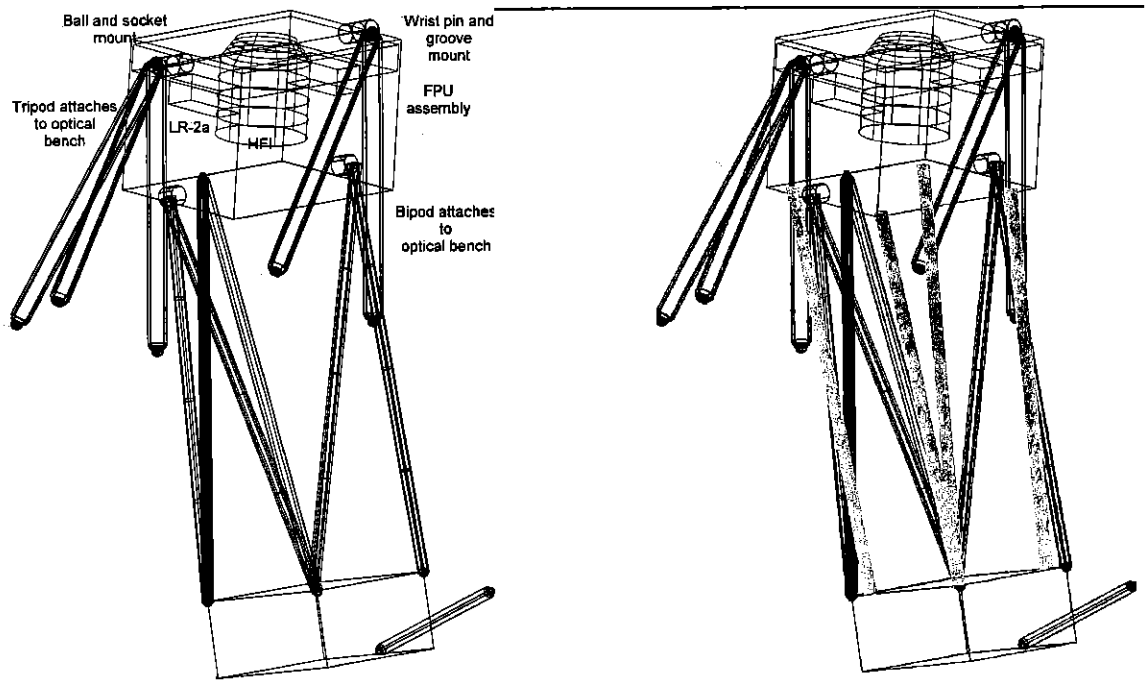

Figure A.1: Perspective drawing of the LFI Radiometer Array Assembly with and without waveguides, showing the position of the HFI within the LFI Front End Unit.

Figures A.1, A.2, and A.3 sketch this proposed baseline approach. A structure rigid except for one degree of freedom supports the Focal Plane Unit from the Optical Bench. The LFI BEU is then supported rigidly from the Focal Plane Unit by a structure designed to constrain the relative motion of the LFI FEU and BEU to a level acceptable for the waveguides. This is a substantial structural design challenge, especially if redundant structures are employed (e.g., where the Frontend Unit is attached to an optical bench supported by struts to the mid-adapter, and the Backend Unit is attached to the equipment platform supported by struts to the mid-adapter).

The proposed solution to this problem is a "Stewart platform" arrangement, with five struts supporting the Focal Plane Unit off the Optical bench, and six struts arranged as three bipods rigidly supporting the LFI BEU off the Focal Plane Unit. The three bipods are arranged so that the side of the Radiometer Array Assembly nearest to the edge of the optical bench is open (strut free). These struts have as high a resonant frequency as possible consistent with requirements on thermal isolation of the Focal Plane Unit to minimize the relative motion of the waveguide ends during launch ($\sim$200 Hz). In comparison, with this structure, the waveguide bundles are soft and carry little load. The CTE of the struts will be matched to that of the waveguide bundles in the conventional manner through appropriate selection of strut materials. The clear opening on one side enables insertion of the HFI into the LFI FEU. This arrangement neatly handles the problems of maintaining LFI alignment, simplifying the insertion and bolt-up operations, and providing high strength against launch loads.

The four waveguide bundles are arranged so that they connect near the corners of the LFI BEU as seen in Figure A.1. The arrangement of struts and waveguide bundles ensures that the center of the assembly is open to enable integration of the HFI Frontend Unit, the coolers, and the cables with the LFI Radiometer Assembly Array.

Three of the five struts that support the FPU assemblies from the optical bench of the telescope mate with the LFI/HFI assembly via a ball and socket joint. The other two mate via a wrist pin and plain bearing mount. In combination these remove five degrees of freedom but leave the assembly free to move

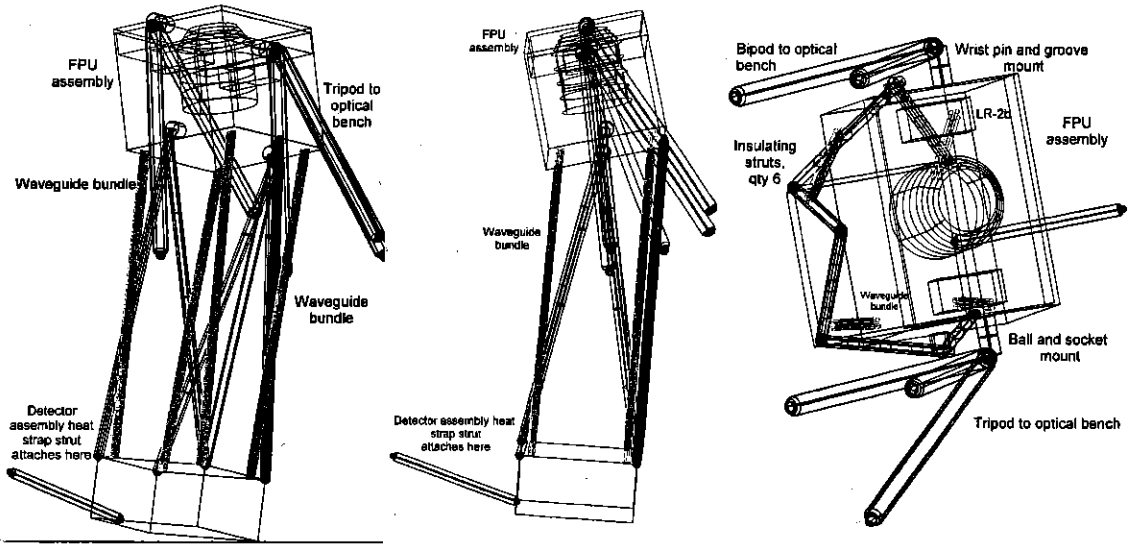

Figure A.2: Views of the LFI/HFI Array Assembly.

rotationally in one axis. The sixth degree of freedom—rotation about the hinge axis between the tripod and bipod—is removed with a single strut at the BEU end of the sub-assembly, which is tied to the Equipment Platform. The sixth strut is made of a high conductance material to transfer heat produced by the LFI BEU into the Equipment Platform. Since no redundant structures are present in either the payload assembly or more specifically in the instruments, there is no interference of load paths in any of the structures described above or the spacecraft structure.

A.2 LFI/HFI frontend integration procedure

The HFI and LFI FEUs are integrated prior to integration of the FPU with the telescope. First the primary 4 K load for the LFI is mounted on the front of the HFI FEU. Then the HFI FEU is inserted into the surrounding LFI FEU from the rear. This is possible because the middle of the LFI Radiometer Assembly Array is open on one side. The coolers are not attached at this time. The HFI incorporates a thick aluminum mounting ring with through holes. To attach the HFI FEU to the main structural plate of the LFI FEU, self-locking fasteners are inserted from the rear and tightened. The sides and bottom of the FPU, which radiatively shield the FPU but have no structural role, are not attached until near the end of integration. The assembly is therefore open with easy access as new components need to be attached.

After the HFI FEU is mounted, the LFI 4 K load assembly for the second row of horns is mechanically and thermally connected to the HFI, and a test for crosstalk between the LFI and HFI is performed using a helium-cooled load in front of the integrated assembly. Following this test, the complete LFI/HFI Array Assembly is integrated with the Planck telescope and payload module.

A.3 Example Planck Payload Module Assembly Procedure

Integration of the Planck Payload Module Assembly is illustrated in Figures A.4, A.5, and A.6. Figure A.4 shows three side views of an exploded strawman design. Figures A.5 and A.6 show several views of the fully assembled strawman design. The design comprises a thermally shielded telescope assembly, two radiation shields, the warm payload Equipment Platform, and the LFI/HFI Array Assembly. It incorporates a Tilt-Bench configuration similar to the configuration adopted by one of the industrial contractors studying

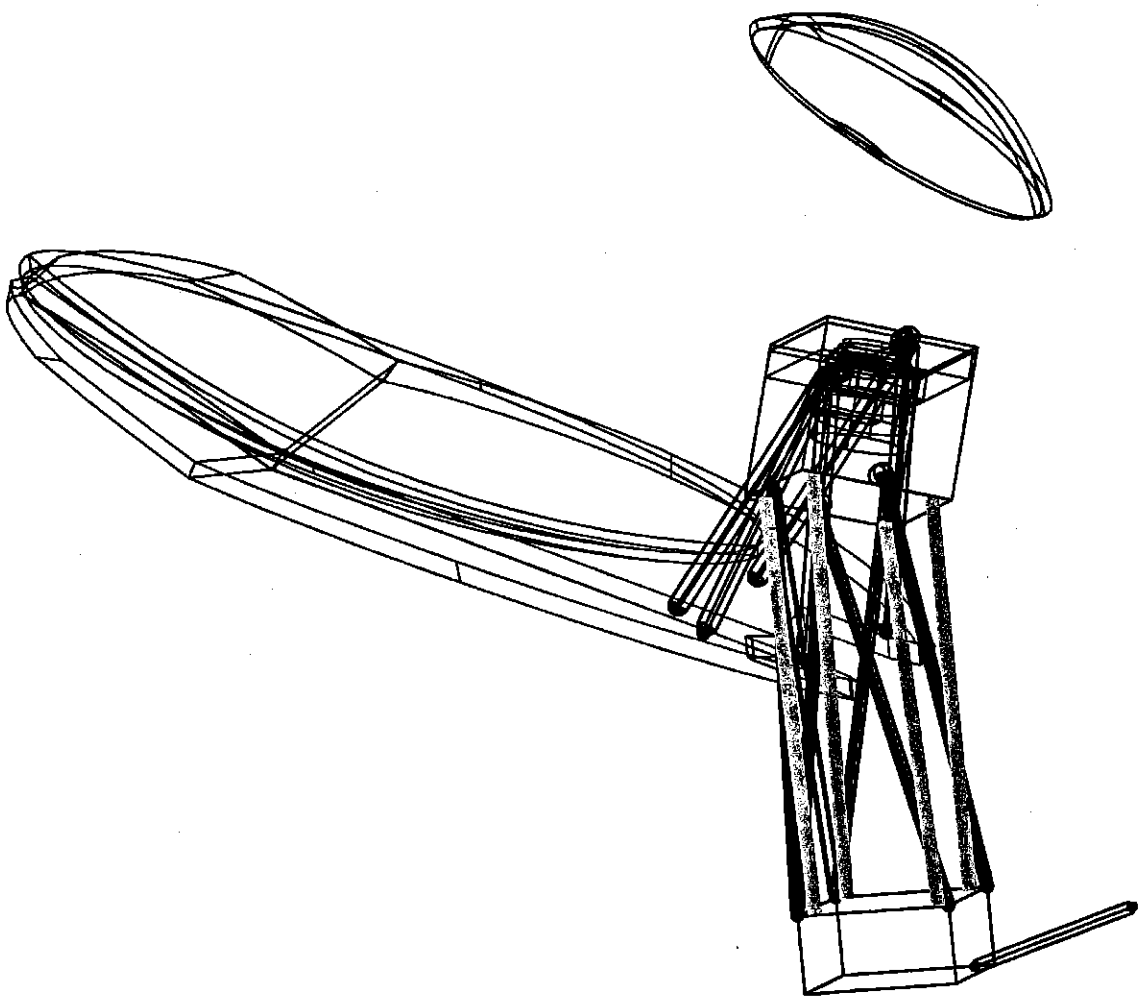

Figure A.3: LFI/HFI Array Assembly orientation relative to the telescope mirrors and the Optical Bench.

the merged mission.

Integration of the LFI/HFI Array Assembly with the telescope is done after the telescope has been characterized and aligned warm and verified while cold. Ideally an alignment tool would be built which is a non-functioning, mechanically identical model of the detector-focal plane assembly. This high fidelity mock-up would provide an opportunity for the insertion team to proof their tooling and verify the position of the final inserted assembly well before installation of the Array Assembly into the Payload Module.

Three assembly procedures have been considered. The first is to draw the LFI/HFI Array Assembly into the partially assembled Payload Module (including the telescope assembly, thermal shields, struts, and Equipment Platform) from the warm equipment side. The second (for those of stronger constitution!) is to drop the Array Assembly into the partially assembled Payload Module from the top, past the telescope mirrors. The third and probably the best method is to integrate the Array Assembly into the telescope assembly first, and then build up the rest of the Payload Module. This last approach is the one described in more detail below.

In the preferred approach, the LFI/HFI Array Assembly is mounted in the telescope assembly by pulling it up with a crane through a port in the Optical Bench (see Figure A.4 for the geometry, but note that the radiation shields are installed later). If the telescope assembly is tilted away from vertical there

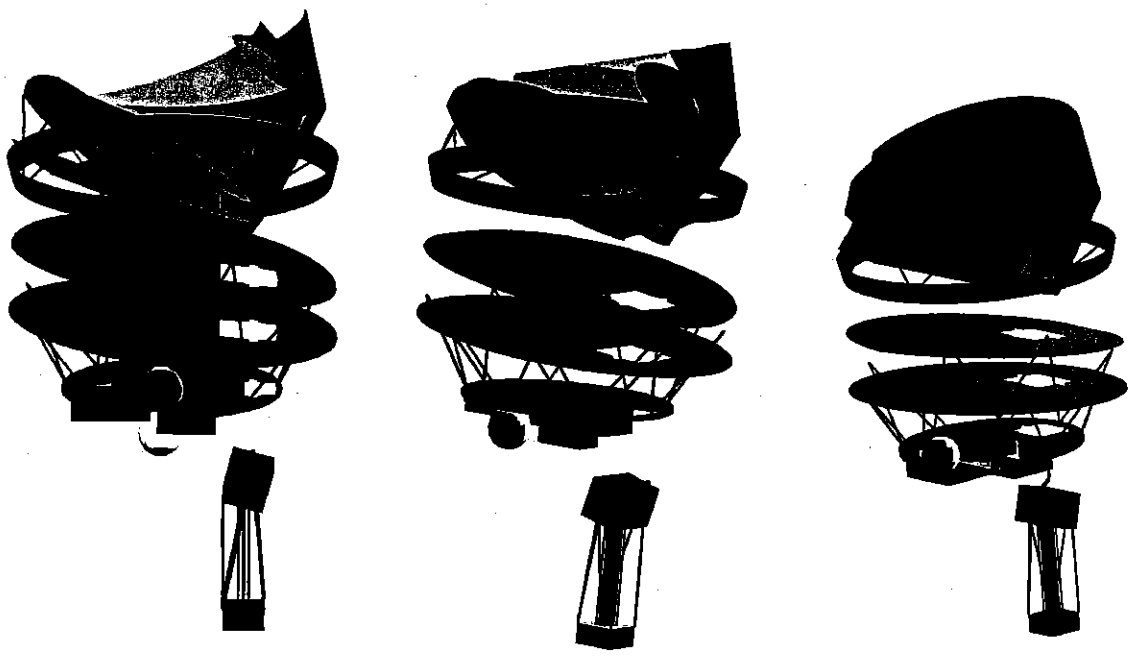

Figure A.4: Exploded views from three directions of a strawman "tilt-bench" design, showing, from top to bottom, the telescope assembly mounted to the Mid-Adapter, two radiation shields, the Equipment Platform, and the LFI/HFI Radiometer Array Assembly.

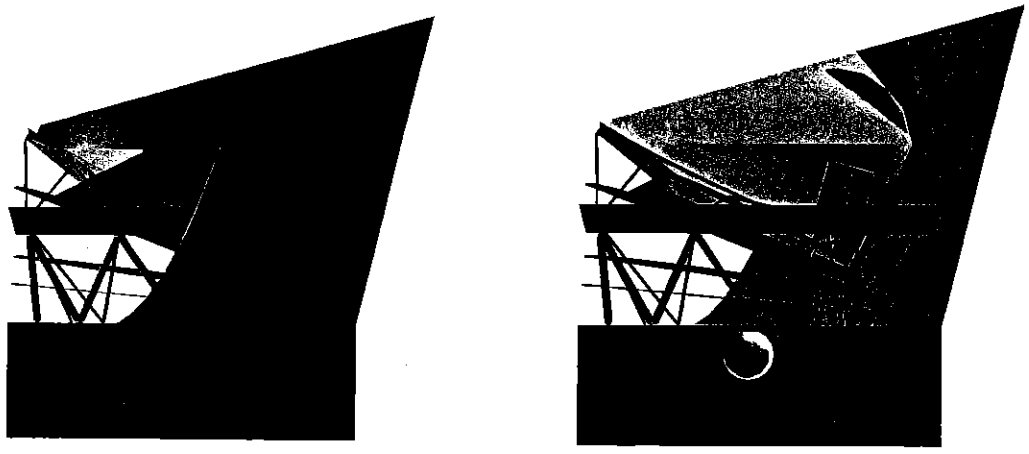

Figure A.5: *Left*—Exterior view of the integrated strawman concept.
Right—Section through the telescope enclosure and thermal shields.

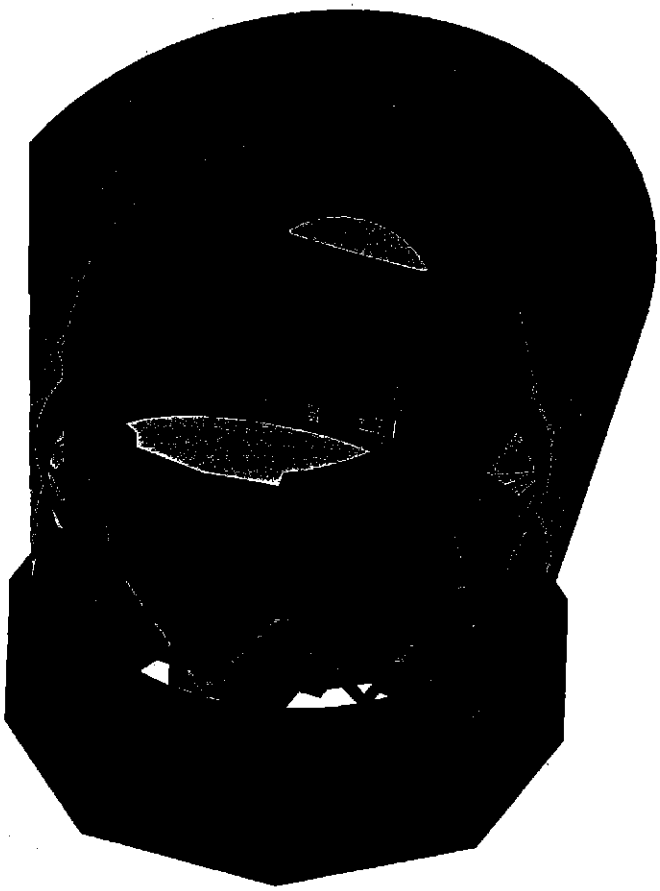

Figure A.6: Perspective view of the integrated strawman concept, showing the Focal Plane Unit and associated struts.

is clear access for the crane. The Array Assembly is then attached to the five supporting struts from the optical bench, which have already been alignment to tens of microns in a previous operation at the ball/socket and wrist pin/grove joints. These joints provide security under the assemblies' own weight during assembly, and are then bolted shut to withstand launch loads. The strut between the Equipment Platform and the LFI BEU is not installed until later.

From the standpoint of the assembler, mounting components with such ball/socket and pin/groove joints is cosidered easy when a crane or other load bearing structure is employed to provide suspension from the top. The highly desirable feature of such joints is that the mating elements simply rest together and are self-retaining prior to bolt-up. This permits the insertion and alignment tasks to be done at separate times.

Independently of the previous integration of the Array Assembly with the telescope and Optical Bench, the warm electronics (other than the LFI BEU) and coolers of the two instruments are mounted to the payload equipment platform. The heat exchangers of the two sorption coolers, the 4 K cooler, and the dilution cooler are coupled together and supported by several GSE struts. This assembly is then attached to the Mid-Adapter via 16 struts arranged as 8 bipods. The 50 K precooler for the sorption coolers is attached to the optical bench and the cold tips are attached to the FPU. The GSE struts are then removed. Figures A.7 and A.8 show details of the interfaces within the Focal Plane Unit and the overall thermal interfaces with the coolers, respectively.

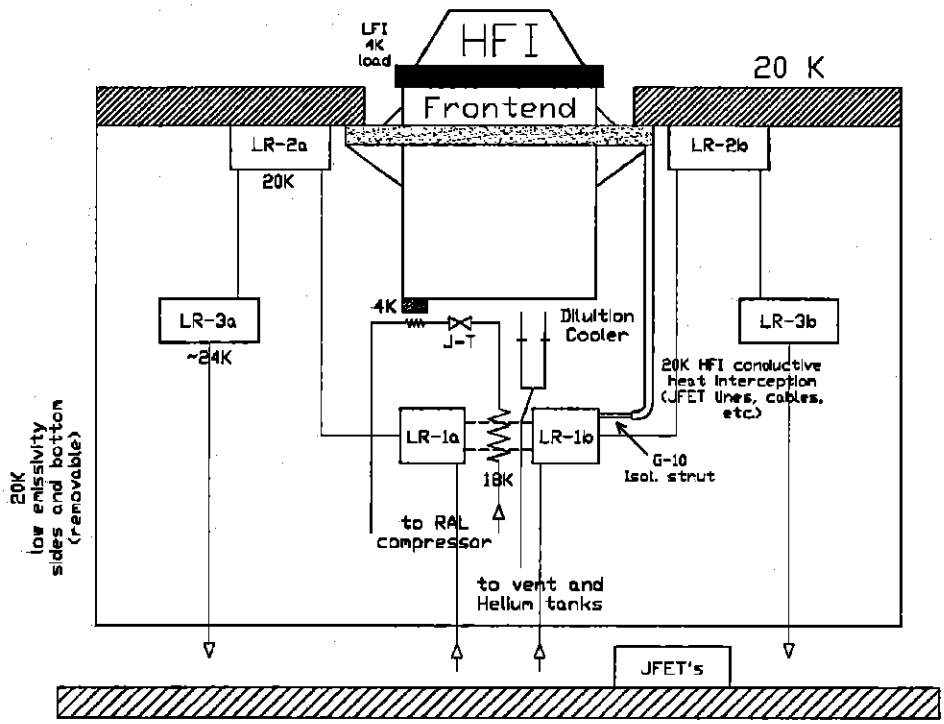

Figure A.7: Detailed schematic of the thermal interfaces in the Focal Plane Unit.

The two thermal shields are sectioned in six pieces:

- A center piece whose diameter corresponds to the outer diameter of the struts connecting the Planck Equipment Platform to the Mid-Adapter. A U-shaped cut in in this shield enables the waveguide bundles, cooler tubing, and supporting struts to pass easily.
- A U-shaped assembly to fill in the U-shaped cutout in the central piece.
- Four outer pieces that include through-holes for the struts that later connect the Mid-Adapter to the SVM.

After the coolers are fully integrated, 12 of the 16 struts that connect the Mid-Adapter and the Equipment Platform are removed to allow the center pieces of the two radiation shields to be inserted. The Equipment Platform is supported from below and the telescope assembly is supported by crane lines attached to the Mid-Adapter during this process. The struts removed are those furthest from the Focal Plane Unit. The shields are inserted U-shaped-cutout-first, and attached to the remaining four struts. The other 12 struts are then reinstalled. The final strut connecting the LFI Backend Unit to the Payload Equipment Module is connected.

The four struts between the Mid-Adapter and the Equipment Platform that were left in place during installation of the radiation shields are then removed. Along with the U-shaped cutouts in the thermal shields and telescope enclosure shields, and the fact that the four outer pieces of the thermal shields are not yet installed, the sparse nature of the radiometer structure enables easy and convenient access to the LFI/HFI Array Assembly and associated boxes on the Equipment Platform. As a result all elements of the two instruments are accessible for integration and any future modifications or repairs that might be required.

The remaining precooling interfaces for the coolers are attached. Cables between the backend electronics on the Equipment Platform and the Focal Plane Unit are attached and mounted. Temperature sensors are mounted and connected as appropriate. The HFI JFET assembly is thermally connected to

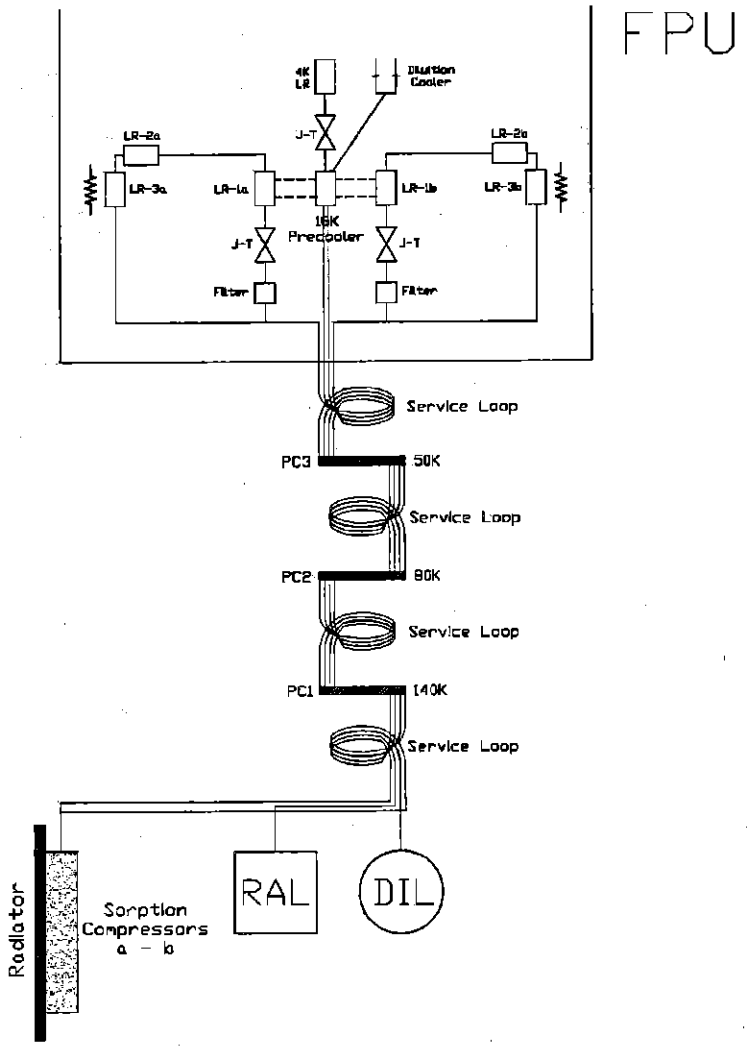

Figure A.8: Schematic of the thermal interfaces to the sorption coolers, the 4 K cooler, and the dilution cooler.

the optical bench. When instrument integration is complete the four sides and bottom plates for the frontend of the Focal Plane Unit are attached. Then the optical bench and shield cutouts are mounted. Final optical alignment is checked and adjusted.

At this point the Planck payload is fully integrated. For thermal tests the outer four pieces of each shield can be temporarily attached. Final integration of the outer four pieces of each shield occurs when the Planck payload is integrated with the SVM.

Appendix B

LFI Associates and Key Personnel

Associates

Roberto Ambrosini
Research Staff
IRA - CNR, Bologna

Bo Andersen
Director
Space Science and Infrastructure,
Norwegian Space Centre

Amedeo Balbi
Ph.D. Student
Universita' di Roma, Tor Vergata

Andrea Balestra
Astronomer
Osservatorio Astronomico di Trieste

Anthony Banday
Staff Scientist
Max-Planck-Institut für Astrophysik

Matthias Bartelmann
Staff Scientist
Max-Planck-Institut für Astrophysik

James G. Bartlett
Adjoint Astronomer
Cosmology Group/CDS, Obs. de Strasbourg

Carlo Burigana
Research Staff
Istituto TESRE - CNR Bologna

Sergio Colafrancesco
Astronomer
Osservatorio Astronomico di Roma

Mike Cruise
Professor
Astrophysics and Space Research Group,
University of Birmingham

Giorgio Dall'Oglio
Associate Professor
Dip. di Fisica, Universitá di Roma Tre

Giancarlo de Gasperis
Ph.D. Student
Universita' di Roma, Tor Vergata

Ruth Durrer
Staff Member
INTEGRAL Science Data Centre,
Switzerland

Kari Enqvist
Senior Researcher
Physics Department and
Helsinki Institute of Physics

Alberto Franceschini
Associate Professor
Osservatorio Astronomico di Padova

Enrique Gaztañaga
Postdoc Contract
Consejo Superior de Investigaciones
Cientificas, España

Gianluigi Granato
Astronomer
Osservatorio Astronomico di Padova

Carlos Gutierrez
Scientist
Instituto de astrofisica de Canarias

Eric Hivon
Postdoctoral Researcher
Theoretical Astrophysics Center - Copenhagen

Michael A. Janssen
Lead Scientist Astrophysics Element
Jet Propulsion Laboratory

Steve M. Levin
Research Scientist
Jet Propulsion Laboratory

Marco Malaspina
Software Engineer
Istituto TESRE - CNR Bologna

Michele Maris
Software Engineer
Osservatorio Astronomico di Trieste

Kalevi Mattila
Professor
Department of Astronomy,
University of Helsinki

Peter Meinhold
Assistant Research Physicist
Univ. of California Santa Barbara

Gianluca Morgante
Research Staff
Istituto TESRE - CNR Bologna

Paolo Natoli
Ph.D. Student
Universita' di Roma, Tor Vergata

Daniel Pfenniger
Staff Member
INTEGRAL Science Data Centre,
Switzerland

Paola Platania
Postdoc
IFCTR-CNR, Milano

Paolo Salucci
Researcher
SISSA Trieste

Jose Luis Sanz
Full Professor
Universidad de Cantabria

Michael D. Seiffert
Research Scientist
Jet Propulsion Laboratory

Joseph Silk
Full Professor
Univ. of California, Berkeley

Per Lilje
Professor
Institute of Theoretical Astrophysics,
University of Oslo

Wojciech Marczewski
Staff Researcher
Space Research Center,
Polish Academy of Science

Antonio Masiero
Full Professor
SISSA

Pasquale Mazzotta
Ph.D. Student
Universita' di Roma, Tor Vergata

Gabriele Morigi
Senior Research Staff
Istituto TESRE - CNR Bologna

Vincenzo Natale
Research Staff
Istituto CAISMI - CNR Firenze

Bruce R. Partridge
Professor of Astronomy
Haverford College

Elena Pierpaoli
Ph.D. Student
SISSA

Lucia Popa
Senior Researcher
Institute of Space Sciences, Bucarest-Magurele

Diego Saez
Lecturer
Facultad de Fisica, Universidad de Valencia

Douglas Scott
Assistant Professor
Univ. of California, Berkeley

Uros Seljak
Research Staff
Max-Planck-Institut für Astrophysik

Laura Silva
Ph.D. Student
SISSA Trieste

Alessandro Simonetto
Research Staff
Istituto di Fisica del Plasma - CNR Milano

Naoshi Sugiyama
Professor
Max-Planck-Institut für Astrophysik

Jan Tauber
Staff Member
ESA/SSD

Seppo Urpo
Professor
Metshovi Radio Research Station, Finland

Esko Valtaoja
Professor
Tuorla Observatory, Finland

Mario Vigotti
Senior Researcher
IRA - CNR, Bologna

Fabrizio Villa
Research Staff
Istituto TESRE - CNR Bologna

Martin White
Assistant Professor
Univ. of Illinois, Urbana-Champaign

Herbert Zirath
Professor
Chalmers University of Technology, Sweden

Riccardo Smareglia
Software Engineer
Osservatorio Astronomico di Trieste

Rashid Sunyaev
Director
Max-Planck-Institut für Astrophysik

Luigi Toffolatti
Teaching Assistant
Universidad de Oviedo

Luca Valenziano
Research Staff
Istituto TESRE - CNR Bologna

Giulio Ventura
Senior Research Staff
Istituto TESRE - CNR Bologna

Osmi Vilhu
Docent
Department of Astronomy,
University of Helsinki

Roland Walter
ISDC Project Manager
INTEGRAL Science Data Centre,
Switzerland

Althea Wilkinson
Daphne Jackson Research Fellow
NRAL University of Manchester, Jodrell Bank

Key personnel

DENMARK

Institute:
Theoretical Astrophysics Center
Juliane Maries Vej 30 2100 Copenhagen 0 Denmark

Personnel:

Name:	**Krzysztof M. Gorski**
Position:	Associate Professor
Task:	Simulation Coordinator

Institute:
Danish Space Research Institute
Juliane Maries Vej 30 DK-2100 Copenhagen Denmark

Personnel:

Name:	**Hans Ulrik Nørgaard-Nielsen**
Position:	Research Physicist
Task:	IDIS Participation

ESA/SSD

Institute:
Space Science Department, Astrophysics Division
P.O.Box 299 NL-2200 AG Noordwijk The Netherlands

Personnel:

Name:	**Kevin Bennett**
Position:	ESA Staff Member
Task:	IDIS

FINLAND

Institute:
Millimetre Wave Laboratory of Finland
Otakaari 7 B Espoo P.O. Box 1202 FIN-02044 VTT Finland

Personnel:

Name:	**Jussi Tuovinen**
Position:	Laboratory Director
Task:	Radiometer Procurement

Institute:
Ylinen Electronics Co.
Teollisuustie 9 A
FIN-02700 Kauniainen Finland

Personnel:

Name:	**Petri Jukkala**	Name:	**Nicholas Hughes**
Position:	Managing Director	Position:	Business Development Director
Task:	Flight H/W Constructor	Task:	Flight H/W Constructor

GERMANY

Institute:
Max-Planck-Institut für Astrophysik
Karl-Schwarzschild-Str. 1 D-85740 Garching bei München Germany

Personnel:

Name:	**Simon White**	Name:	**Matthias Bartelmann**
Position:	Managing Director	Position:	Staff
Task:	DPC level 4 Coordinator	Task:	Data Center Manager

ITALY

Institute:
TeSRE - CNR
Istituto per le Tecnologie e lo Studio delle Radiazioni Extraterrestri
via P. Gobetti 101 I-40129 Bologna Italy

Personnel:

Name:	**Nazzareno Mandolesi**	Name:	**Christopher R. Butler**
Position:	Director	Position:	Effective from September 1998
Task:	Principal Investigator	Task:	LFI Project Manager
Name:	**Carlo Burigana**	Name:	**Luca Valenziano**
Position:	Research Staff	Position:	Research Staff
Task:	Simulations	Task:	Optical and Cryogenics Design
Name:	**Fabrizio Villa**	Name:	**Gianluca Morgante**
Position:	Research Staff	Position:	Research Staff
Task:	Optical Antenna Design	Task:	Thermal Mechanical
Name:	**Giulio Ventura**	Name:	**Marco Malaspina**
Position:	Senior Research Staff	Position:	Software Engineer
Task:	Electronic, EGSE	Task:	Onboard Software
Name:	**Gabriele Morigi**		
Position:	Senior Research Staff		
Task:	Microwave Testing		

Institute:
Istituto di Fisica Cosmica e Tecnologie Relative (IFCTR) - CNR
via Bassini 15 I-20133 Milano Italy

Personnel:

Name:	**Marco Bersanelli**	Name:	**Alessandro Simonetto**
Position:	Senior Researcher	Position:	Research Staff
Task:	Instrument Manager	Task:	Microwave Testing

Institute:
Istituto CAISMI - CNR
Largo E. Fermi 5 I-50125 Firenze Italy

Personnel:

Name:	**Gianni Tofani**	Name:	**Vincenzo Natale**
Position:	Director	Position:	Research Staff
Task:	Passive Components Procurement	Task:	Passive Components Design and Testing

Institute:
Istituto di Fisica dello Spazio Interplanetario (IFSI) - CNR
Via del Fosso del Cavaliere snc I-00133 Roma Italy

Personnel:

Name:	**Renato Orfei**	Name:	**Pasquale Cerulli-Irelli**
Position:	Research staff	Position:	Research staff
Task:	EGSE	Task:	EGSE

Institute:
Osservatorio Astronomico di Padova
Vicolo dell'Osservatorio 5 I-35122 Padova Italy

Personnel:

Name:	**Gianfranco De Zotti**	Name:	**Luigi Toffolatti**
Position:	Senior Astronomer	Position:	Associate Professor
Task:	Foregrounds and Simulations	Task:	Foregrounds

Institute:
Osservatorio Astronomico di Trieste
Via G.B.Tiepolo 11 I-34131 Trieste Italy

Personnel:

Name:	**Fabio Pasian**	Name:	**Claudio Vuerli**
Position:	Associate Astronomer	Position:	Astronomer
Task:	DPCenter Manager	Task:	Pipeline Integration Manager

Institute:
Scuola Internazionale Superiore di Studi Avanzati (SISSA)
via Beirut 2-4 I-34013 Trieste Italy

Personnel:

Name:	**Luigi Danese**	Name:	**Davide Maino**
Position:	Full Professor	Position:	Ph.D. Student
Task:	Foregrounds and Scientific Analysis	Task:	Simulations

Institute:
Universitá di Firenze, Dipartimento di Ingegneria Elettronica
Via Lombroso 6/17 I-50100 Firenze Italy

Personnel:

Name:	**Pelosi Giuseppe**	Name:	**Selleri Stefano**
Position:	Associate Professor	Position:	Postdoctoral Researcher
Task:	Feed Horn Design	Task:	Feed Horn Design

Institute:
Universitá di Roma, Tor Vergata
Via della Ricerca Scientifica I-00133 Roma Italy

Personnel:

Name: **Nicola Vittorio**
Position: Full Professor
Task: Science Coordinator

Institute:
LABEN S.p.A.
Strada Padana Superiore 290 I-20090 Vimodrone (Milano) Italy

Personnel:
Name: **Patrizio Tua**
Position: Staff
Task: System Engineering

NORWAY

Institute:
Department of Physics University of Tromsø
N-9037 Tromsø Norway

Personnel:
Name: **Jan Erik Solheim**
Position: Professor
Task: EGSE

SPAIN

Institute:
Instituto de Astrofisica de Canarias (IAC)
c/o Via Lactea 38200 La Laguna Tenerife Spain

Personnel:
Name: **Rafael Rebolo**
Position: Research Division Director
Task: Electronics Procurement

Name: **Jose Miguel Herreros**
Position: P. M. for Space Payloads
Task: LFI Electronic Manager

Name: **Roger Hoyland**
Position: Microwave Engineer
Task: Research Engineer

Institute:
Universidad de Cantabria
Avda. Los Castros s/n E-39005 Santander Spain

Personnel:
Name: **Enrique Martinez-Gonzalez**
Position: Researcher
Task: Back End Procurement

Name: **Eduardo Artal**
Position: Full Professor
Task: Local Technical Manager

Name: **Joaquin Portilla**
Position: Postdoc Contract
Task: Research Engineer

Institute:
Universidad Politecnica de Cataluña
Sor Eulalia d'Anzizu s/n E-08034 Barcelona Spain

Personnel:

Name:	**Lluis Pradell**
Position:	Lecturer
Task:	Research Engineer

SWEDEN

Institute:

Microwave Electronics Laboratory, Chalmers University of Technology
S-412 96 Göteborg Sweden

Personnel:

Name:	**Erik Kollberg**	Name:	**Iltcho Angelov**
Position:	Professor	Position:	Research Staff
Task:	MMIC Design and Prototyping	Task:	MMIC Design and Testing
Name:	**Muhammad Nawaz**	Name:	**Magnus Persson**
Position:	Research Staff	Position:	Research Staff
Task:	MMIC Design and Testing	Task:	MMIC Design and Testing

SWITZERLAND

Institute:

INTEGRAL Science Data Center (ISDC)
Chemin d'cogia 16 CH-1290 Versoix Switzerland

Personnel:

Name:	**Thierry J.-L. Courvoisier**	Name:	**Roland Walter**
Position:	INTEGRAL PI	Position:	ISDC Project Manager
Task:	Level 1 DPC Manager	Task:	Level 1 DPC Manager

UK

Institute:

Nuffield Radio Astronomy Laboratories
University of Manchester Jodrell Bank Macclesfield Cheshire

Personnel:

Name:	**Rodney D. Davies**	Name:	**Richard J. Davis**
Position:	Emeritus Professor	Position:	Senior Lecturer
Task:	Foregrounds	Task:	Radiometer Procurement
Name:	**Althea Wilkinson**	Name:	**Neil Roddis**
Position:	Research Fellow	Position:	Engineer (Receivers)
Task:	Local Project Manager	Task:	Project Engineer

Institute:

Rutherford Appleton Laboratory (RAL) - Space Science Dept.
Chilton DIDCOT Oxon United Kingdom OX11 0QX

Personnel:

Name: **Brian Maddison**
Position: Staff
Task: AIV Manager

USA

Institute:
Jet Propulsion Laboratory
4800 Oak Grove Drive Pasadena CA 91109 USA

Personnel:

Name:	**Charles R. Lawrence**	Name:	**Lawrence A. Wade**
Position:	Research Scientist	Position:	Member of Technical Staff
Task:	Survey Scientist	Task:	Soprtion Cooler Design and Procurement
Name:	**Todd Gaier**	Name:	**Michael D. Seiffert**
Position:	Member of Technical Staff	Position:	Research Scientist
Task:	Radiometer Designing and Prototyping	Task:	Radiometer Stability
Name:	**Michael A. Janssen**	Name:	**Steve M. Levin**
Position:	Lead Scientist	Position:	Research Scientist
Task:	Astrophysics Element Observing Strategy	Task:	Foreground Expert

Institute:
Haverford College
Haverford PA 19041 USA

Personnel:
Name: **Partridge R. Bruce**
Position: Professor of Astronomy
Task: Foreground Expert

Institute:
Physics Dept. University of California Santa Barbara
Santa Barbara CA 93106 USA

Personnel:

Name:	**Philip M. Lubin**	Name:	**Meinhold Peter**
Position:	Professor of Physics	Position:	Assistant Research Physicist
Task:	Radiometer Prototyping	Task:	Post Detection Electronics

Institute:
University of California, Berkeley
MS 50205 LNBL Cyclotron Rd. Berkeley CA 94720 USA

Personnel:

Name:	**George Smoot**	Name:	**Douglas Scott**
Position:	Professor of Physics	Position:	Assistant Professor
Task:	Instrument Operation	Task:	Theoretical Simulations

Institute:

Five College Radio Astronomy Observatory
LGRC-617 University of Massachusetts Amherst MA 01003

Personnel:
Name: **Sander Weinreb**
Position: Professor
Task: MMIC Design

Institute:
TRW
1 Space Park M5/1017E Redondo Beach CA 90278 USA

Personnel:

Name:	**Barry Allen**	Name:	**Robert Haas**
Position:	Staff	Position:	Staff
Task:	MMIC Design	Task:	TRW Coordinator